Atmospheric ice accretion on sea structures

by Lasse Makkonen

CORRIGENDA

Contents, chapt. 5, the word ON is missing.

p.7, line 4, symbol π is missing (ratio π of...)

p.9, line 13, "(chapter 3.3.)" should be removed.

p.16, Eq (17), symbols ρ and μ are missing from the first term. should read $I = k_a (v \rho_a / D \mu_a)$....

p.19, second line from below, $\sim$ is missing. Should read $c_w \Delta t / E_a L_f \sim 10^{-2}$.....

p.21, before Eq. (22) the reference should be Stallabrass, 1978a (not 1982).

p.30, Eq. (29), symbol $\sim$ is missing. Should read $-L \sim 3.2$....

p.31, capter 4.1.4., line 8 should read (see Fig. 22, p. 88) Next line: Should read (see Fig. 23, p. 89).

p.34, line 1, symbol ρ is missing. Should read density ρ of...

p.43, line 9, should read $t_a - t_s$ (not $t_s - t_a$).

p.45, line 6 from below, the reference should be Stallabrass, 1978b (not 1978).

p.54, second chapter, line 9, the reference should read Hanamoto et al., 1980.

p.63, the reference Drannevič should read Dranevič.

p.64, the reference Hanamoto, H.G., Gagnon, J.J. & Pratt, B, 1980: Deicing a satellite communication antenna. CRREL Special Rept., 80-18, ADA 085397. is missing.

p.70, two references are missing: Smirnov, V.I., 1974: Conditions of ship icing and means of combatting it. CRREL Draft Transl., 411, 178-182. and
Stallabrass, 1978b: An apprisal of the single rotating cylinder method of liquid water content measurement. National Res. Council, Canada, Rep., LTR-LT-92, Ottawa. Reference Stallabrass, 1978 should read 1978a.

p.71, reference is missing: Wasserman, S.E. & Monte, D.J., 1972: A relationship between snow accumulation and snow- intensity as determined from visibility. J. Appl. Meteor., 11, 385-388.

p.83, Fig. 12, legend: should read $d = 30 \mu m$.

p.88, Fig. 22, legend: should read ...fog over the sea surface with salinity of 35 ‰ .....

p.97, "(continued)" should be removed.

Appendix 2, legend, t_d should read T_d.

A T M O S P H E R I C I C I N G

O N S E A S T R U C T U R E S

by

Lasse Makkonen

Prepared for U.S. Army Cold Regions Research & Engineering Laboratory (CRREL), Hanover, New Hampshire, 03755, U.S.A.

CONTENTS

(continued)

1. INTRODUCTION

Icing on structures in the marine environment is a hazard to navigation and other offshore activities in the regions where freezing temperatures exist over the sea. Several ships are lost due to ship icing each year and icing on tower structures, buoys, automatic meteorological instruments, helicopter platforms etc. causes many risks to human safety and other inconveniences.

Ship icing has been regognized as an serious problem for a long time and has been discussed in the scientific literature for more than hundred years (see Anon, 1881). Ship icing is primarily caused by sea spray and therefore little attention has been paid to atmospheric ice accretion at sea, i.e. icing due to fog and precipitation particles. However, during the past decade the need for deeper understanding of atmospheric icing in the marine environment has considerably increased as human activities, such as offshore oil drilling, have been intensified in the arctic and sub-arctic waters. The assessment of safety criteria, structural design etc. requires knowledge of the hazards caused by the arctic environment and atmospheric icing is one of the potential dangers especially to stationary structures at sea.

The purpose of this report is to give an up-to-date presentation of the different aspects of atmospheric icing on stationary sructures with a special emhasis on the marine environment. The probabilities of encountering atmospheric icing, the expectable hazards caused by it and the means of combatting it are analyzed using theoretical calculations, connections with icing and other atmospheric conditions, climatological considerations and the available icing data. Simultaneously the report is aimed to serve as a literature review on atmospheric icing on sea structures. Both spray icing and atmospheric icing in continental regions are dealt with, but only when they are connected with the main topic. No complete review is attempted here of either ship icing or atmospheric icing in general However, the theoretical aspects (chapters 3 and 5) are discussed in such detail that in this respect the report may be used as a review of atmospheric icing physics. Also, the part of the report dealing with anti-icing and de-icing methods (chapters 8 and 9) may be seen as a review of these aspects regarding both icing of ships and of

stationary structures. The reader interested in all aspects of atmospheric icing in continental regions, too, is suggested to see the references Dranevič (1971), Minsk (1980) and the following collections: Symposium Nebelfrost und Glatteisablagerungen, Abhandl. Meteor. Dienst, DDR, 107 (1973) and Proceedings of the First International Workshop on Atmospheric Icing of Structures, published by the Cold Regions Res. and Eng. Laboratory (CRREL), USA in 1982. The most generic references considering spray icing on ships are Panov (1976) and Aksiutin (1979) and the most complete reviews on ship icing published in English are those by Shellard (1974), Minsk (1977), Stallabrass (1980) and the translation of the Russian collection "Investigation of the physical nature of ship icing", CCREL Draft Translation 411 (1974). Parts of this report have been published earlier in Finnish by Makkonen (1979).

2. ICING PROCESSES AND THEIR RELATIVE IMPORTANCE

2.1. Ship icing

Ice on sea structures is either of the origin of sea water (spray icing) or the atmospheric fresh water (atmospheric icing). Atmospheric ice accretions can further be classified according to the source of the ice; glaze and rime are formed from supercooled water droplets in air, hoarfrost from water vapour and wet snow from snow flakes. Dry snow does not accrete in substantial amounts on vertical surfaces which are of primary concern regarding icing of structures.

The outlook and internal structure of ice accretions from supercooled water droplets vary considerably. Therefore, this type of ice is generally divided into three groups the main criteria being the density of ice. These are

- glaze, which is hard, almost bubble-free and clear homogeneous ice of density close to that of pure ice (0.92 g cm^{-3})
- hard rime, which is rather hard, granular, white or translucent ice of the density of 0.6 - 0.9 g cm^{-3}
- soft rime, which is white and opaque fragile ice with a loosely bonded structure and the density of less than 0.6 g cm^{-3}

For the purposes of theoretical treatment (chapter 3) it is convenient to make the division between glaze and rime according to the thermal conditions prevailing during ice formation: glaze is forming in the wet growth conditions with surface temperature of $0^{o}C$ and

rime in the dry growth conditions with surface temperature below 0°C (see chapter 3.1). It should be noted that the division into the three ice types is subjective and that slightly different criteria regarding e.g. ice density have been used by different authors (e.g., Dranevič, 1971, Glukhov, 1972, Minsk, 1977). Moreover, a mixture of the different ice types is not uncommon, because the atmospheric conditions during icing storm are changing. Also, it will be shown in chapter 3. that ice density and ice type may vary even in constant enironmental conditions, so that the type of ice is different in different layers in the ice deposit.

Sea spray is a major source of ship icing as can be seen in Table 1 According to the data of more than 2000 ship reports from the world ocean spray alone causes ship icing in 89.8 % of all cases, spray combined with rain or fog in 6.4 %, spray combined with snow in 1.1 %, and atmospheric icing alone in 2.7 % (Borisenkov and Panov, 1974). In the Arctic sea areas the cause of ship icing is spray alone in 50 %, spray combined with atmospheric icing in 41 %, fog in 3 % and precipitation in 6 % of all cases. Hoarfrost is never reported as a cause of ship icing.

As spray icing and atmospheric icing are often observed simultaneously on ships, it would be interesting to know in which way the relative importance of these two phenomena changes with height from the sea surface, but this has not been documented. It is only known that spray icing is restricted to lower levels, to such structures as decks, derricks and handrails and that superstructure icing on ships due to sea spray does not usually reach levels higher than about 16 m from the sea surface (Anon, 1962). This indicates that the relative importance of atmospheric icing is generally at its maximum on the upper parts of the ship (masts, antennas etc.). It therefore seems that if rapid icing is observed due to atmospheric ice accretion it may be more dangerous to the ship's stability than spray icing of the same intensity. It should, however, be pointed out that the relative intensity of spray icing and atmospheric icing on a ship depends on the speed of the vessel and of the wave heading and roughness of the sea. Spray icing has been observed on structures at the height of more than 30 m on the Finnish high speed turbine ship "Finnjet".

2.2. Icing of stationary sea structures

Considering stationary sea structures, there is not the mechanical impact caused by the movement of the structure itself as in the case of ship icing. Therefore spray icing is limited to lower levels on stationary structures. On the light-houses in the Baltic Sea, as an example, the upper limit where traces of spray icing are observed is 5-10 m. Spray generated directly from the wave tops without the effect of the impact with the structure is a cause of icing only in the first few meters above sea surface, since only very small droplets are forced upwards by wave action and air turbulence. Droplets of diameter more than 30 μm rise above 7 m only when the wind speed v is more than 12 m s^{-1} and 100 μm droplets only when v is more than 25 m s^{-1} (Preobrazhenskii, 1973). The data of Preobrazhenskii (1973) on the vertical distribution of liguid water content in air due to sea spray is given in Fig. 1. From these data, which are from field observations, it can be concluded (see chapter 3.2.1) that only very slight icing can be caused by spray directly from waves on stationary sructures above 4 m level in wind speeds less than 25 m s^{-1}. The liquid water content w at 4 m height in Fig. 1 is 1-2 orders of magnitude smaller than the typical maximum values of w during atmospheric icing (see Appendix 1).

Since wave impact on stationary structures seldom creates large amounts of sea spray and since this amount can rather easily be restricted by structural design, it seems that atmospheric icing is the major potential source of ice accretions especially on high sea structures. The relative importance of the different sources of atmospheric icing is not well known except what can be seen in Fig. 1, i.e., that icing from both supercooled fog and precipitation has been observed on ships and that the formation of hoarfrost is negligible. According to the statistics wet snow seems also to be less important.

In continental regions the total amount of ice usually increases with height in such a way that the portion of hard rime and glaze increases with height and the role of soft rime decreases as shown in Fig. 2. It is not known whether the relationship between different ice types resembles that of Fig. 2 in the marine environment, but there may be substantial differences due to different boundary layer structures over land and over sea (see chapter 4). The measurements by McLeod (1981) indicate that the mean monthly and seasonal values

of the total ice deposition increase with height in the marine environment as well, but these measurements are made over land surface on small islands. More representative data from real offshore conditions are needed to confirm these results.

3. THEORY

3.1. Freezing process

Freezing of supercooled water drops when they hit a surface of a structure when falling or moving with wind is a rather complicated phenomenon affected by various properties of the air flow, of the icing object and of the impinging water drops. The amount of the affecting parameters is so large that only a part of them in a limited range of variation can be handled in any practical experiment of ice accretion. Therefore, theoretical approach in explaining the basic characteristics of the icing process is needed. A proper understanding of the icing mechanics is essential in order to estimate the icing intensity and to develop successful means of reducing the hazards and inconveniences caused by atmospheric icing on structures.

Water drops in air may remain in liquid state down to air temperatures as low as about $-40^{\circ}C$ before a spontaneous freezing will occur. Turning of the droplets into ice at higher air temperatures is caused by mechanical impact or the precence of a freezing nucleus. Particles acting as freezing nucleus are different kinds of inpurities in air such as NaCl particles. The mechanical impact may be a collision of the droplet with another droplet, with ground or with a surface of a structure.

When a supercooled droplet hits a solid obstacle it spreads and turns to ice. The freezing process can be divided into two phases: First a part of the supercooled water in the droplet freezes rapidly releasing the latent heat of fusion and therefore warming the temperature of the remaining water to $0^{\circ}C$. In the subsequent freezing phase this remaining part turns to ice, since the droplet gives heat to its environment by convection, evaporative cooling and conduction. The intensity of these processes determines the time τ_f required by the subsequent phase of freezing. The duration of the initial phase is 1-2 orders of magnitude shorter than the duration of the subsequent phase (Macklin and Payne, 1968, Murray and List, 1972). The time

required for the complete spreading of the droplet to take place in different conditions is not well known, but it obviously depends on the impact speed and droplet size. The spreading probably occurs while the major part of the droplet is in liquid state (Brownscombe and Hallet, 1967).

The time τ_f of the droplet freezing can as a first approximation be estimated by the heat balance of the individual droplet, since the rate at which the latent heat released in the freezing is transferred to the environment determines τ_f. Based on this idea Macklin and Payne (1968) have made calculations of τ_f for unventilated drops which remain hemispherical during freezing and whose surface is in liquid state until complete freezing has taken place. These calculations resulted to the values of τ_f of about 10^{-2} s for 10μm droplets in the temperature conditions typical to atmospheric icing. The wind speed in natural environment may, however, increase the heat transfer from the droplet considerably, resulting to smaller values of τ_f. On the other hand, if the freezing in the droplet advances inwards the droplet is covered by ice and the heat transfer problem is somewhat more complicated (see Johnson and Hallett, 1968), giving shorter freezing times.

The time required for the droplet to freeze is an important parameter, since it affects the properties of the ice formed and the way in which the problem of theoretical estimation of icing intensity must be treated (see chapters 3.2.1. and 3.2.2.). If $\Delta\tau$ denotes the time interval of impingement of droplets to the same spot on the surface (in a sense of the surface area covered by one spreading droplet), then the type of the ice formed may be determined as follows:

$\tau_f \ll \Delta\tau$,soft rime

$\tau_f < \Delta\tau$,hard rime

$\tau_f \geq \Delta\tau$,glaze

The time interval τ for droplets of a fixed size depends on droplet velocity (i.e., on wind speed) and on the amount of droplets in air. The time of freezing τ_f depends on the factors involved with the heat transfer from the droplet, such as droplet size, air temperature and wind speed. Qualitatively, high wind speed, high air temperature and large droplets favour the situation where $\tau_f > \Delta\tau$. The time of droplet spreading may be important, too, regarding the type of the ice,

since even if $\tau_f < \Delta\tau$ the ice may be quite compact and glaze-like if the droplets spread efficiently and form spots of water film before they turn to ice. This may be the case during light freezing rain, for example. The ratio of the time which the icing surface spends in liquid phase to the time it spends in solid phase is

$$\Pi = \frac{\tau_f}{\Delta\tau} \qquad (1)$$

In the growth conditions, where $\tau_f << \Delta\tau$ the ratio $\Pi \to 0$ and the process is called "dry growth". When $\tau_f \cong \Delta\tau$ then $\Pi \to 1$ and hard rime or glaze is formed, but the process is still called dry growth. Only when $\tau_f \geq \Delta\tau$ the process is called "wet growth". In a sense it would be more logical to make the division between dry growth and wet growth at $\Pi = 0.5$, but the criterium $\Pi = 1$ when there is a uniform water film on the icing surface is generally used. One reason for using $\Pi = 1$ as the criterium is that the existence of the uniform water film is more easy to define than any specific value of Π, because in real nature there are droplets of different size and because the impinging of droplets is a stochastic process, so that the time interval $\Delta\tau$ is not constant. There is also a practical reason for using $\Pi = 1$ as the deviding condition, since only when $\Pi > 1$ the mean surface temperature of the icing surface is $0^{\circ}C$ and there is run-off of unfrozen water from the surface. This run-off water is an important factor regarding the intensity of ice accretion as will be shown in chapter 3.2.2.

3.2. Estimation of icing intensity

3.2.1. Rime

In the dry growth conditions all the impinging water droplets freeze completely and rime is formed. Hence, when calculating the rate of rime formation it is only necessary to determine the amount of impinging water per unit time and unit surface area. Consequently the icing intensity I (in g $cm^{-2}h^{-1}$, for example) of rime formation on a vertical surface can be formulated as

$$I = E\, v\, w \quad , \qquad (2)$$

where v is the wind speed (terminal velocity of the small droplets

causing rime formation is small enough to be neglected), w is the liquid water content in air and E is the collection efficiency, i.e., the ratio of the mass flow of water droplets striking the surface to the mass flow that would be experienced by the surface if the droplets had not been deflected in the air stream (see Fig. 3). Droplet deflection is due to the viscous drag forces making the droplets follow air stream lines around the icing object. However, the inertia of the droplets causes the droplet trajectories to deviate from air stream lines, so that part of them srike the surface giving a non-zero value of E. It is possible to determine E by calculating the droplet trajectories, which are controlled by the balance between droplet inertia and drag forces.

In the conditions prevailing during atmospheric icing the potential flow is a good approximation upstream from the boundary layer separation point, where practically all the droplets that contribute to E are collected by a typical icing object. The potential flow satisfies the Laplace equation whose solution yields the stream function ψ for the potential flow.

$$\nabla\psi^2 = 0 \qquad (3)$$

The components U_a and V_a of the two dimensional velocity vector $\bar{V}_a$ are the partial derivatives of the stream function

$$U_a = \frac{\partial\psi}{\partial y} \quad , \quad V_a = -\frac{\partial\psi}{\partial x} \qquad (4)$$

The stream function and the velocity components at each point around the object can be solved analytically for simple objects such as a circle and ellipse if the free stream velocity v is known. For more complex objects numerical methods must be used.

A typical shape of an icing object is a cylinder. The dimensionless equation of motion for spherical droplets around a cylinder (the balance between inertial and viscous forces) is according to Langmuir and Blodgett (1946)

$$K\frac{d\bar{V}_d'}{dt} = \frac{c_d Re_d}{24}\left(\bar{V}_a' - \bar{V}_d'\right) \quad , \qquad (5)$$

where K is the inertial parameter analogous to mass in dimensionless

form ($K = d^2 \rho_w v / 9 \mu D$), c_d is the drag coefficient, Re_d the droplet Reynolds number ($Re_d = d \rho_a v / \mu$), $\bar{V}_a'$ the dimensionless air velocity vector ($\bar{V}_a' = \bar{V}_a / v$) and $\bar{V}_d'$ the dimensionless droplet velocity ($\bar{V}_d' = \bar{V}_d / v$). Here d is the droplet diameter, ρ_w the water density, μ the absolute viscosity of air, D the cylinder diameter and ρ_a the air density. The drag coefficient c_d is a function of the droplet Reynolds number Re_d. Empirical expressions based on laboratory measurements in steady motion have been given by Langmuir and Blodgett (1946) and Beard and Pruppacher (1969). The deceleration of the droplets may have some influence on c_d (Temkin and Mehta, 1982) but this is obviously of minor importance considering the solution for $\bar{V}_d$ from Eqs. (3)-(5), since verification of theoretical values for E have been convincing (chapter 3.3.) even though this effect is neglected.

The calculation of droplet trajectories requires an iterative numerical method of solution, which involves considerable computation time, but the solution of E for a circular cylinder can be presented conveniently as a function of two dimensionless parameters, namely K and ϕ, where $\phi = 18 \rho_a^2 D v / \mu \rho_w$, either in the form of analytical expressions (Cansdale and McNaughtan, 1977) or of curves as shown in Fig. 4. Qualitatively the dependence of the collection efficiency E on the atmospheric parameters is such that E increases with increasing wind speed and droplet size and with decreasing cylinder dimensions (see Fig. 12 on p. 82). Regarding practical applications it is unfortunate that in typical atmospheric icng conditions E is very sensitive to the droplet diameter which is difficult to measure and to estimate. Air temperature t_a has an effect on E due to dependence of ρ_a and μ on t_a, but this effect is negligibly small regarding practical applications.

The local collection efficiency β at different angle θ from the stagnation line varies and has its maximum value at the stagnation line. When the conditions turn to such that E decreases close to zero then icing will occur near the stagnation line only. At some conditions E = 0 and no icing will occur. It has been shown by Langmuir and Blodgett (1946) that this happens when K = 1/8. Hence, it is possible to calculate the combinations of wind speed, droplet size and cylinder diameter for which icing does theoretically not occu Results of such calculations are presented in Fig. 5. It must be stressed, however, that the curves in Fig. 5 may not be fully applicable

to the real nature, since the air flow is turbulent and the droplets are not of uniform diameter. It is also interesting to notice that since E is so critical to the object dimensions, ice may sometimes accrete on small roughness elements on the icing object forming rime feathers, although E = 0 for the object as a whole. These feathers usually grow from the side of the object.

The problem that there is a rather wide size distribution of droplets in natural clouds in calculating E and β can be solved by determining these parameters differently for each size category. Then the effective E (or β) is the sum of the values for each size times the fraction of the total liquid water content represented by that size. Since this procedure is more laborious E and β are often calculated for the droplets that have the medium volume diameter of the droplet distribution. This method gives fairly accurate results for the typical size distributions in icing fogs and clouds (Cansdale and McNaughtan, 1977).

As an ice deposit grows during ice accretion its dimensions change continuously and therefore both the collection efficiency and the collecting surface area also change. This can be taken into account in the theoretical considerations by time-dependent numerical modelling. Such models have been recently developed for simulation of icing under dry growth conditions particulary on airfoils (McComber and Touzot, 1981, Oleskiw, 1982, Oleskiw and Lozowski, 1982). These models are cabable of determining E and β and hence the theoretical icing intensity for each time-step on the ice profile obtained after the preceeding time-step, and are therefore not limited to purely cylindrical surfaces. The models have given some promising results, but there are restrictions to their use since the present models are stable only for about five time-steps. They also use constant ice density which may deteriorate the results (Bain and Gayet, 1982). Ackley and Templeton (1979) have constructed a stable model for simulating elliptical long-term ice growth and Makkonen (1982) a time-dependent model for cylindrical ice growth on wires. These models simulate also ice density variation, but are restricted to modelling accretions of pre-defined shape. For overall estimates of the ice loads the non-time-dependent solution of E for cylindrical surface applied in Eq. (2) should generally give useful results, since the width of the ice deposit does not usually increase very much in dry growth process and since E is not very sensitive to the relatively even form of the rime deposit (see McComber and Touzot, 1981).

As to practical application of Eq. (2) and the models based on it, the determination of E is not the only problem, because estimation and prediction of the liquid water content w is also difficult. These difficulties originally result from our unability to measure w and the droplet diameter d in clouds and fogs except using expensive and laborious methods, so that there is little data on these variables and on their correlations with other more easily measurable parameters. It is interesting to consider the possibility that there would be a usefully strong relationship between w and wind speed v or between w and air temperature t_a, for example. By estimating w using these relationships it might be possible to calculate also E more accurately relating medium volume diameter d with w. The relationship between d and w for different kinds of fogs is presently poorly known quantitavely but for freezing rain the Marshall-Palmer distribution may be used (see Pruppacher and Klett, 1978). Qualitatively, of course, d increases with increasing w, except possibly in evaporation fogs (see Saunders, 1964).

An attempt to relate liquid water content in icing fogs with v and t_a using available continental data is shown in Fig. 6. The correlation is weak but slight decrease in w seems to be followed by a decrease in t_a and increase in v. In the marine environment the situation may be somewhat different, especially concerning evaporation fogs for which w increases with decreasing t_a as shown in Fig. 7. Visibility λ is one potential indicator of w, since a reduction in λ is often associated with fog or precipitation. Even on high structures, the upper parts of which sometimes reach the cloud base, the horizontal visibility λ may be used as an indicator of icing events since λ and the height of the lower cloud boundary are statistically correlated, at least on continental locations (Milyutin and Yaremenko, 1981). Stanew (1976), for example, has demonstrated that there exists a correlation between w and λ and has used this fact in ice load calculations. However, it is suggested by the Mie theory and by observations that the relationship between w and λ is not a simple one, but is considerably affected by the droplet size distribution. This is demonstrated in Fig. 8, where observations and theoretical relationships for two types of fog with different duration and mean droplet diameter are given. In Fig. 8 it can be seen that value of w can vary by a factor of 3 for the same value of λ. Waibel (1956) has

studied experimentally the correlation between the icing intensity and liquid water content w, and found"only an incidental relation", which is not encouraging either. Hence, it seems that visibility only is not presently a very useful parameter for icing intensity estimation, since reliable prediction of the droplet size spectrum of fogs is mostly beyond our abilities. If, however, the mean droplet diameter d_m can be estimated then a better indicator for w can be found: the results of Kumai (1971, Fig.8) indicate a relationship $w = 1.3\ d_m/\lambda$ for arctic fogs. The scatter of the data in Fig. 8 is quite large and there is no data for the whole possible range of conditions. Therefore, more measurements should be made to establish more quantitative relationship between w and λ to be used in icing intensity estimations.

3.2.2. Glaze

In the wet-growth process, which involves the loss of unfrozen water, the intensity of ice accretion can be formulated as

$$I = E_a E v w \qquad (6)$$

where E_a is the accretion efficiency, i.e., the ratio of the icing intensity to the mass flow of the impinging water. In Eq.(6), E_a is assumed to be determined by the heat balance of the water film on the icing surface only. Eg. (6) can also be expressed in terms of the icing efficiency $E_i = E_a E$. Accordingly E_i is the ratio of the icing intensity to the mass flow of droplets that would have struck the surface if they had not been deflected in the airstream, and must also be a function of the factors controlling the heat balance of the icing surface.

The heat balance equation for the water film on the stagnation line of the icing surface in the wet growth process is

$$q_f + q_v + q_k = q_c + q_e + q_w + q_r + q_s + q_i \ , \qquad (7)$$

where q_f = latent heat released during freezing
q_v = frictional heating of air
q_k = kinetic energy of the impinging water
q_c = loss of sensible heat to air
q_e = evaporative heat loss
q_w = heat loss in warming to 0 ^{o}C the mass of water that does freeze
q_r = heat loss in warming the run-off water to the temperature it has when leaving the area of the surface under consideration
q_s = heat loss due to radiation
q_i = heat loss to the substrate due to conduction

The terms in (7) can be parameterized as follows:

$$q_v = h\ r\ v^2 / 2 c_p \ , \qquad (8)$$

where h is the heat transfer coefficient, r is the recovery factor

for viscous heating (r = 0.9), v is the wind velocity and c_p is the specific heat of air at constant pressure.

The kinetic energy of the droplets q_k can safely be neglected on stationary objects under natural atmospheric conditions

$$q_c = h\ (0\ ^{\circ}C - t_a)\ , \qquad (9)$$

where t_a is the air temperature (in $^{\circ}C$).

$$q_e = h\ k\ L_e\ (\ e_0 - e_a\ )\ /\ c_p\ p_a\ , \qquad (10)$$

where k = 0.62, L_e is the latent heat of evaporation, e_0 and e_a are the saturation vapour pressures over water at 0 $^{\circ}C$ and at t_a, respectively, and p_a is the free atmospheric pressure.

The temperature of the droplets in the free stream is very nearly the same as that of air. Hence

$$q_w = I\ c_w\ (0\ ^{\circ}C - t_a)\ , \qquad (11)$$

where c_w is the specific heat of water.

The temperature of the run-off water leaving the deposit has a considerable effect on the ice accretion, and its determination has been seen as a difficulty in estimating the accretion intensity in the wet growth process (e.g. List, 1977). The problem is much simplified, however, if we consider the stagnation area only, because the water is lost within the water film and its temperature is therefore that of the surface. viz. 0 $^{\circ}C$, unless bouncing of the impinging droplets occurs. No evidence of noticeable bouncing has been reported near the stagnation line in the conditions corresponding to atmospheric icing on stationary objects. Hence

$$q_r = c_w\ (\ E\ v\ W - I\ )\ (\ 0\ ^{\circ}C - t_a\ ) \qquad (12)$$

The radiation budget at the surface can be estimated, as a first approximation, by neglecting the short wave radiation in fog conditions, and assuming that the emissivity of the fog in the horizontal direction approaches unity (see Herman, 1980). Linearizing the equation for the difference in the emitted radiation of the icing

surface and the fog we obtain

$$q_s = \sigma n \ (0\ ^{o}C - t_a) \ , \qquad (13)$$

where σ is the Boltzmann constant and $n = 4 \cdot (273K)^3$.

According to experimental results (see e.g. Schlichting, 1979) the Nusselt number Nu ($=hD/k_a$) and the Reynolds number Re ($= vD\rho_a/\mu_a$) in a flow around a cylinder are related at the stagnation point by

$$Nu = Re^{\frac{1}{2}} \qquad (14)$$

Using this result the local heat exchange coefficient h in Eqs. (8) - (10) can be expressed as

$$h = k_a \ (v \rho_a / D \mu_a)^{\frac{1}{2}} \ . \qquad (15)$$

Here k_a is the molecular thermal conductivity, ρ_a the air density, μ_a the molecular viscosity of air and D the diameter of the cylinder examined. It has been shown both experimentally (e.g., Seban, 1960) and theoretically (Sundén, 1979) that the Nusselt number depends on turbulent intensity and scale, but this effect is not very pronounced during icing in real atmosphere since it is brought up by turbulent eddies much smaller than the icing object and the intensity of turbulence of this scale in free stream is not very high. The situation may be different near the ground or sea surface and close to other structures which produce small scale turbulence as shown by Kowalski and Mitchell (1976) who studie heat transfer from a sphere in the natural environment. They found that the ratio Nu_t/Nu_0 of the Nusselt number measured in the natural environment (Nu_t) to the one measured in a low intensity wind tunnel (Nu_0) varied from 1.1 at the height of 2 m from the ground to 1.8 at the ground surface.

Another factor which may considerably influence the heat transfer coefficient h is the surface roughness. Increasing surface rougness moves the transition point from laminar to turbulent flow upstream leading to increased heat transfer. Fortunately, at the Reynolds numbers relevant to atmospheric icing this effect is rathe small (see Achenbach, 1977). However, the experimental data is limited to smaller magnitudes of roughness than expected on ice accretions formed in the wet growth conditions. Therefore,

Lozowski et al. (1979) have made an attempt to take the effect of roughness on h into account by applying the data of Achenbach (1977) for the roughest cylinder tested (ratio of the height of the roughness elements to the cylinder diameter $9 \cdot 10^{-3}$). This resulted to

$$Nu = Re^{\frac{1}{2}} \left(2.4 + 1.2 \sin\left(3.6 (\theta - 25^{o}) \right) \right) , \qquad (16)$$

which gives $Nu = 1.2\ Re^{\frac{1}{2}}$ for the stagnation point. Eq. (16) is valid for $Re \leq 2.6 \cdot 10^{5}$ only and for more precise estimates of Nu a formula corresponding to (16) should be constructed for the whole range of Re relevant to atmospheric icing cases.

The conductive term q_i is difficult to parameterize, since it depends on the thermodynamical properties of the object undergoing icing. The treatment is here limited to the cases, where the conductivity of the structure is low, or to the cases where icing has been going on for a sufficient time for an ice deposit several centimeters thick to develop. A qualitative view of the nature of factors affecting q_i can be obtained from Fig. 9, which shows that there are considerable temperature gradients within the ice and the structure if the icing object is made of material with high heat conductivity.

The relative magnitude of the heat balance terms is largely dependent on the environmental conditions. In general, it can be established that the term q_f is the major gain of heat and that q_c and q_e are usually the dominating heat loss terms - q_w becoming, however, more important with increasing liquid water content, and q_s with decreasing wind speed. The term q_v can be neglected except when the wind speed is very high and the air temperature close to 0 ^{o}C.

Using the parameterizations in (3) and neglecting q_k and q_i an analytical expression for the intensity I is found:

$$I = k_a (v_a / D_a)^{\frac{1}{2}} L_f^{-1} \left[-t_a + \frac{k L_e}{c_p p_a} (e_0 - e_a) - \frac{r v^2}{2 c_p} \right]$$

$$- L_f^{-1} (E v w c_w + \delta n)\ t_a \qquad (17)$$

The values of k_a, ρ_a, μ_a, c_p and e_a in (17) are dependent on the air temperature and can be found from tables or expressed in analytical form in computer simulations. L_f, L_e, c_w, e_0, p_a, σ, n and r can be considered constants. With information on the droplet size spectrum and cylinder diameter, the collection efficiency E can be found as indicated in chapter 3.2.1. Using Eq. (17) the intensity of accretion in the wet growth process on the stagnation line of a cylinder of an arbitrary diameter can thus be estimated as a function of air temperature t_a, wind speed v, liquid water content w and droplet diameter d.

The conditions under which the ice accretion process changes from wet growth to dry growth or vice versa can be found by equalizing the intensities in (3) and (17). By doing so and taking into account that at the boundary between dry and wet growth $q_r = 0$, we obtain the following expression for the critical liquid water content w_c:

$$w_c = \frac{k_a}{E}\left(\frac{\rho_a}{v D \mu_a}\right)^{\frac{1}{2}} \frac{-t_a + \frac{kL_e}{c_p p_a}(e_0 - e_a) - \frac{r v^2}{2 c_p}}{L_f + c_w t_a} - \frac{\sigma n t_a}{E v (L_f + c_w t_a)} \qquad (18)$$

In a similar manner other critical parameters such as $t_{a,c}$ or v_c can be solved - although not analytically - for given fixed values of other parameters. In Fig. 10 the critical line is presented for different wind speed values in t_a, w coordinates.

Having established the estimation formula for the icing intensity for dry growth (3), wet growth (17) and critical conditions (18), it is possible to make estimates for the whole range of atmospheric conditions. This is done in Fig.11 by presenting the icing intensity as a function of the air temperature for different wind-speed values, using the value 0.3 g m^{-3} for the liquid water content in air. An example of the dependence of the accretion intensity on the wind speed, with fixed values of other parameters, is given in Fig.12 in terms of the icing efficiency E_i. In Fig.12 the icing efficiency E_i increases with increasing wind due to an increase in the collection efficiency E ($E_a = 1$ in dry growth) up to the wind speed value (4 m s^{-1} in Fig.12) where the

change to the wet-growth process occurs, and then decreases due to the decreasing accretion efficiency.

It has been shown by Makkonen (1981) that the effect of the runoff term q_r is small during atmospheric ice accretion in the conditions near the ground or sea surface. For liquid content values less than 0.5 g m^{-3}, relevant to atmospheric icing at sea (see appendix 1), the error in icing intensity I caused by neglecting q_r is less than 10% with all combinations of the other relevant parameters. This is of great practical importance since it allows the formulation of wet growth accretion, which is independent of the liquid water content w and the collection efficiency E. Neglecting q_r Eq. (17) becomes

$$I = \frac{h\left[-t_a + \frac{k L_e}{c_p p_a}(e_0 - e_a) - \frac{r v^2}{2 c_p}\right] - 6nt_a}{L_f + c_w t_a} \qquad (19)$$

The advantage of (19) is that properties of the fog - which are usually not known, and are difficult to forecast - need not to be considered, apart from the fact that the existence of sufficient quantity of supercooled droplets is necessary for wet growth icing to occur. Because the maximum intensity of wet growth accretion at fixed values of v and t_a is reached in the wet growth process, it is concluded that Eq. (19) can be used for estimating maximum intensity of droplet icing at sea. Since w seldom exceeds 0.3 g m^{-3}, during atmospheric icing at sea, curves in Fig. 11 can be used as a first approximation of maximum glaze intensity on objects with diameter more than 5 cm for each combination of v and t_a.

There are two possible mechanisms affecting on I that were not considered when deriving Eqs. (17) and (19). Firstly, it has been found in hailstone growth simulations that the excess water - instead of being shed - may be incorporated into the ice structure, giving a spongy ice deposit (see Macklin, 1961, Roos and Plum, 1974). Observations of unfrozen water in glaze deposits on stationary structures under natural conditions have, however, not been reported, which is probably because the values of atmospheric parameters in near-ground conditions are quite different from those prevailing during hailstone growth. It has been shown by

Lesins et al. (1980) that the liquid water fraction of ice on slowly rotating cylinders (0.5 Hz) depends strongly on liquid water content in air in such a way that with the smallest value of w in the tests ($w = 2\ gm^{-3}$) spongy ice was not formed in the conditions $-4^{o}C \geq t_a \geq -16^{o}C$ and $v = 18\ ms^{-1}$, which also indicates that spongy ice is not likely in the case of atmospheric icing at sea ($w << 2\ gm^{-3}$). Secondly ice crystals mixed with supercooled water droplets may affect I. Mixed conditions do not seem to lead to greatly enhanced icing rates, however (Ashwort and Knight, 1978, Lozowski et al., 1979). Furthermore, the occurence of ice crystals in liquid water clouds is unlikely in the air temperatures typical to glaze formation (Mason, 1971).

In the case of freezing rain and drizzle there are some special aspects in the theoretical treatment of the icing intensity that should be considered. Air temperature is close to $0^{o}C$ during freezing precipitation, so that it is not likely that dry growth conditions would prevail, except when liquid water content w is very small. In this case w can be approximated according to Eq. (20) by Best (1950)

$$w = 0.072\ R^{0.88} \quad , \qquad (20)$$

where R is precipitation rate in $mm\ h^{-1}$. Since the maximum value of R during freezing precipitation is about $4.8\ mm\ h^{-1}$ according to Stallabrass (1982), it can be seen from Eq. (20) that w should not exceed about $0.3\ gm^{-3}$ in freezing rain and drizzle. Hence, the use of Eq. (19) instead of (17) seems to be justified in the case of freezing precipitation too. However, it should be pointed out that the droplets in freezing rain are large and may therefor not be in a complete thermal balance with their environment, as supposed in Eqs. (17) and (19). This means that the terms q_w and q_r in Eq. (7) may not be estimated using w and t_a only, Large rain droplets may also bounce from the surface, in which case the temperature they have, when leaving the surface, is not known (see List et al., 1976). Fortunately the contribution of the terms q_w and q_r to the total heat balance is large only when the icing intensity I is amall, so that these problems are overcom when estimating maximum intensities. This is because $q_w+q_r/q_f = c_w E v w \Delta t/IL_f = c_w \Delta t/E_a L_f \quad 10^{-2} \Delta t/E_a$, where Δt is the difference in the droplet temperature before impact and after bouncing

or shedding. Since Δt can hardly be above $5^{o}C$, it can be seen that q_w+q_r/q_f is large only if E_a is small, but then the icing intensity I is also small (see Eq. (6) and far from its maximum value.

As pointed out earlier the maximum intensity of ice accretion for fixed values of t_a and v is reached in the wet growth process, and is therefore limited by t_a and v (see Fig.11). Hence, it is interesting to notice that these parameters do not reach their extreme values during freezing precipitation. For the freezing precipitation cases the mean value of t_a was -0.4 ^{o}C (minimum -6.5 ^{o}C) and the mean value for v was 5.9 $m\,s^{-1}$ (maximum 14.9 $m\,s^{-1}$) in the 10-year period at Toronto airport according to Stallabrass (1982). Even at coastal regions v seldom reaches high values during freezing precipitation (Austin and Hensel, 1956). According to Stallabrass (1982) 98.5 % of the hourly wind readings during freezing precipitation are contained within the velocity/ temperature envelope by the relation

$$v = 1.5\ t_a + 18 \quad , \qquad (21)$$

where v is in ms^{-1} and t_a in ^{o}C. Eq. (21) may be used together with Eq. (19) in estimating the maximum icing intensity during freezing precipitation. This is demonstrated in Fig.13 , where the icing intensity I is presented as a function of t_a and v_a as calculated from (19) as well as the line representing Eq. (21).

The ice deposit diameter D is involved with the calculation of the icing intensity (see Eq. (17)), and the surface area for the heat exchange between the deposit and air to take place depends on D as well. Therefore - similarly to dry growth simulation - time-dependent models have been developed in order to calculate ice loads after some time of accretion (e.g, Lozowski et al., 1979). An example of the results from a time-dependent model, which simulates icing on wires in both dry and wet growth is presented in Fig. 14.

3.2.3. Wet snow

Wet snow accretes on a structure when snow flakes covered by a thin water film strike the structure surface and adhere to it. Snow particles become wet falling through a layer where the air temperature is above $0^{o}C$. This layer must not be too thick since otherwise the snow flakes would melt completely and therefore t_a at the surface layer where the snow accretion on structures occurs is usually close to $0^{o}C$.

Snow accretion on structures is frequently observed in air temperatures somewhat above the freezing point of water and in humid air, which reveals that no external cooling of the snow deposit is required in order to the deposit to grow (Makkonen, 1981, Colbeck and Ackley, 1982). It has, in fact, been demonstrated by Wakahama and Kuroiwa (1977) that free-water content of the deposit increases during the accretion process. Also, the observations that snow accretions on wires are often not attached to them but form a loose fitting cylinder around the wire (Bauer, 1973) indicate melting in the deposit. That the density and strength of the snow deposit increase and that it turns hard and often nearly transparent in spite of the melting in the deposit can be explained by the deformation process in the deposit caused by the impact force of the snow particles and by wind drag. These forces create a packing stress on the snow which therefore becomes denser and experiences a deformation process in which large snow particlaes grow at the expence of smaller particles (see Colbeck, 1979, Colbeck and Ackley, 1982). This process is comparable to what happens when squeezing a snow ball.

Since freezing of the snow deposit on average is not necessary for the accretions to grow, it is apparent that the heat exchange with the environment does not substantially control the growth rate I_s of wet snow deposits. Therefore, the theoretical approach used for rime, i.e., Eq. (2) is more appropriate in estimating I_s than heat balance considerations. The amount of snow flakes in air w_s can be used in Eq. (2) similarly to w in the case of rime formation. The snow content w_s may be obtained from visibility data, for example (Wassermar 1972, Stallabrass, 1982). According to Stallabrass (1982) w_s and visibility λ (in meters) are related by Eq. (22):

$$w_s = 2100\,\lambda^{-1.29} \qquad (22)$$

It has been shown by Wakahama and Kuroiwa (1977) that the collection

efficiency E in Eq. (2) is close to unity for wet snow flakes around objects of the size of power line conductors in moderate wind speeds, so that that applying (2) to the snow problem would be easy in this respect, too. Unfortunately, there are some additional problems that arise when using (2) in the snow accretion calculations. Firstly, although all the snow particles would strike the icing surface so that E = 1, they are not eventually collected since they tend to rebound from the surface. The "final collection efficiency" may be as low as 0.2 due to rebouncing (Wakahama and Kuroiwa, 1977), and the problem is that for the present the factors controlling the portion of rebouncing particles are not known. Secondly, the excess of free water in the wet snow deposit is partly removed from the lee side of the deposit reducing its weight. Consequently, our present abilities in estimating the growth rate of wet snow deposits are very limited and more experimental data are needed. Laboratory experiment are presently being made to clarify the problem (e.g., Wakahama, 1979, Wakahama et al., 1979).

One possibility in obtaining estimates on wet snow accretion rate is simply to relate it with the measured precipitation rate during icing conditions (Shoda, 1953), but large errors are probable when using this method due to unknown factors controlling snow deposit growth on structures and due to inaccuracy of precipitation measurements during snow fall, especially in high wind speeds.

When a wet snow accretion is formed on a wire suchas an electrical conductor or a guy rope, twisting of the wire or sliding of the snow deposit along the wire surfaces seem to be elemental for heavy snow deposits to grow, since these processes allow a cylindrical deposit which envelopes the wire efficiently (see Wakahama, 1979). On fixed objects or if sliding to the lee side of the deposit is prevented the deposit is more easily broken or blown away by the wind. Therefore, it is to be expected that vertically situated objects and objects of large dimensions experience less severe wet snow accretion than e.g. horisontally elongated wires and small-size structures.

3.2.4. Hoarfrost

According to the eddy diffusion theory the mass growth rate I of hoarfrost formed by condensation of water vapour pressure in air e_a, water vapour pressure at the icing surface e_i and by wind speed v according to Eq. (23) (compare with (10))

$$I = k\, C_e\, \rho_a\, v\, (e_a - e_i) / p_a \quad , \tag{23}$$

where C_e is an empirical transfer coefficient for water vapour, which depends on surface roughness and thermal stability of the boundary layer. It is interesting to note here that although I is controlled by Eq. (23), the growth rate of the thickness of frost seems to be independent of the ambient conditions of mass transfer (Schneider, 1978). It follows from Eq. (23) that frost growth is possible if the surface is sufficiently cold compared to air, but that it is also possible in the case where the surface temperature and air temperature are the same providing that the relative humidity in air is close to 100%. This is seldom the case in the natural boundary layer, and therefore cooling of the surface is usually required for hoarfrost to form in the natural environment. Cooling in the surface lowers e_i and therefore controls the intensity of frost formation I according to (23). From this it follows that it is possible to estimate the maximum growth rate I_m by examining the heat balance of the icing surface since this balance controls the surface temperature and hence the saturation water vapour pressure e_i at the ice surface. For practical purposes this is a more simple method for estimation of I_m than Eq. (23) due to the difficulties in estimating e_i and the transfer coefficient C_e.

The heat balance equation (3) in the absence of supercooled water droplets becomes

$$q_f - q_e = q_v + q_c + q_s + q_i \quad , \tag{24}$$

where $q_f - q_e = q_{cond}$ is the latent heat released in the condensation process. Also,

$$q_{cond} = I\, L_c \quad , \tag{25}$$

where L_c is the latent heat of condensation. As we wish to estimate

the maximum intensity I_m we can neglect the terms q_c and q_v which in the situation examined give heat to the surface and tend to reduce icing intensity. Furthermore, for objects which are not internally cooled, the surface temperature is colder than the temperature inside the ice or in the structure, so that the conductive term q_i also tends to warm the surface and can be neglected for the present purpose By neglecting q_c, q_v and q_i Eq. (24) yelds

$$q_{cond} = q_s \qquad (26)$$

and taking (25) into account we get

$$I_m = q_s / L_c \quad , \qquad (27)$$

which gives the theoretical maximum intensity of hoarfrost formation. According to (27) the rate of frost growth is controlled by radiation from the surface in such a way that the radiative heat loss is balanced by the latent heat released by condensing water vapour. Using the value $q_s = 100\ Wm^{-2}$ for the maximum radiative loss on a horisontal surface (Gavrilova, 1966) we obtain $I_m = 0.013\ g\ cm^{-2}h^{-1}$ ($= 0.3\ g\ cm^{-2}d^{-1}$). Largest observed condensation rates are of order of $0.1\ g\ cm^{-2}d^{-1}$ (Nyberg, 1966). These estimates clearly show that the formation of hoarfrost is negligibly small compared to the typica growth rates of glaze, rime and wet snow (see chapters 3.2.1-3.2.3.).

4. METEOROLOGICAL CONDITIONS DURING ICING EVENTS

4.1. Boundary layer conditions

4.1.2. Air temperature and wind

In order to be able to make forecasts of icing and statistical risk analysis based on meteorological data it is important to know the atmospheric conditions in which the occurence of atmospheric ice accretion is likely. The meteorological conditions that prevail during ship icing have been studied widely (see e.g., Shektman, 1968, Tabata, 1968, Borisenkov and Pchelko, 1972, Smirnov, 1974, Lundqvist and Udin, 1977, Stallabrass, 1980). In the data of these studies atmospheric icing events are rare and have in most cases not been distinquished from spray icing events. Therefore, ship icing data are not very useful regarding calculation of the conditions where atmospheric icing occurs, and theoretical considerations and observations from continental locations must be used.

Roughly speaking rime or glaze may form when there is liquid water in air, air temperature t_a is below $0^{\circ}C$ and there is air movement with respect to the object considered. However, there are some deviations from this general rule. For example, ice accretion is possible when $t_a > 0^{\circ}C$ if the icing surface is at a temperature below $0^{\circ}C$ due to radiative cooling or evaporation. Icing does not occur in low air temperatures if the surface temperature is warmer than $0^{\circ}C$ due to internal heat transfer in the structure or due to solar radiation.

The practical upper limit for t_a during ice accretion by water droplets seems to be about $2^{\circ}C$ for vertical surfaces (Sadowski, 1965, Volobueva, 1975) and about $3^{\circ}C$ for horizontal surfaces (see Lenhard, 1955, McKay and Thompson, 1969). The difference is obviously due to more intensive outgoing radiation to horizontal direction. The upper limit for wet snow accretion is about $1.5\ ^{\circ}C$ (Shoda, 1953, Sadowski, 1965) in real nature, but in laboratory simulations wet snow accretions have been grown at air temperatures as high as $2.0^{\circ}C$ (Wakahama and Kuroiwa, 1977).

There seems to be no lower limit for t_a during droplet accretion in the range of t_a values expectable over the sea. The lower limit for t_a observed in different studies varies according to local conditions, but icing is not rare at air temperatures below $-20\ ^{\circ}C$ (Dranevič, 1971, Volobueva, 1975, Makkonen and Ahti, 1982).

The theoretical lower limit for t_a is determined by the temperature in which crystallization of the supercooled water droplets occurs. According to Bashkirova and Krasikov (1958) this temperature is about -20 °C over the sea. The limiting values of t_a for the different ice types is discussed in more detail in chapter 5. In this connection it is only mentioned that the lowest air temperatures reported during wet snow accretion are -4 °C (Sadowski, 1965).

In addition to the maximum and minimum air temperatures during icing it is interesting to know the frequency of icing in different temperature intervals since this kind of data can be used in estimation of icing probabilities. Data of the distribution of icing events with air temperature are available in many continental regions but they are apparently not representative to the marine environment due to different statistical features of the boundary layers over the ground and over the sea. It seems reasonable, however, to assume that since atmospheric icing in continental data is concentrated close to 0°C (see Fig.16 on p. 85), this will be the case at sea as well. According to the data by McLeod (1981) for the Gulf of Alaska t_a is in the range -3 to 0 °C for the reported icing events. It should not, however, be forgotten in this connection that evaporation fogs, which are a potential source of icing at sea, are formed only at low air temperatures (see chapter 4.1.3.). Hence, it is possible that atmospheric icing probability distribution according to air temperature has a two-peak structure. More data from actual offshore conditions is necessary to clarify this aspect. Some conclusions of the frquency of atmospheric icing in different temperatures may also been drawn from ship icing results in Fig. 15, although these data include mostly spray icing.

There is very limited amount of data on the occurence of atmospheric icing over sea with wind speed. Some indications may be found in Fig. 15, but the higher intensity of spraying in high wind speeds in the data must be kept in mind when interpreting these data. If one wishes to make conclusions based on continental data, distribution of icing events according to wind speed in one location can be seen in Fig. 16 and frequency of icing with wind shear in the boundary layer in Fig. 17.

Distribution of icing cases according to wind direction is usuall quite uneven in continental regions. This is probaly so at sea as well. Generally winds from the north are more likely to be associat

with icing on the open sea than winds from the other quarters (in the northern hemisphere). An example of this can be seen in Fig.18 . Local differences in this respect are ,however, probably large depending on the synoptic conditions typical for the location and on the direction to the nearest coast.

4.1.2. Precipitation and humidity

It is well known that supercooled precipitation may cause serious damages in continental regions. However, the views regarding the contribution of precipitation events to the total ice loads, i.e., its relative importance compared to icing due to fogs (in-cloud icing) are contradictonary. Some authors have seen precipitation even as a necessary condition for atmospheric icing (e.g., Lenhard, 1955, McLeod, 1981) and some others have used precipitation as the main parameter in icing forecating models (e.g., McKay and Thompson, 1969, Chaîné, 1974). On the other hand, it has been shown by Waibel (1956) and Ahti and Makkonen (1982) that icing intensity has no correlation with the measured precipitation amounts, and by e.g., Rink (1938) and Sadowski (1965) that the majority of icing events are observed in days with no precipitation. These discrepancies can partly be explained by the fact that the frequency of precipitation during icing on continental regions is clearly dependent on locality - mostly due to orographic effects (see Lomilina, 1977).

The question of the importance of supercooled precipitation is even more troublesome over the sea, since experimental data is lacking. Ship reports do not give much data for this problem because liquid precipitation has usually not been distinquished from fog or snow in these observations. Coastal data and data from islands may not be representative either, since the temperature inversion necessary for the falling water droplets to supercool (see the solid curve in Fig. 19) mostly develops due to radiative or advective cooling of the air in the surface layer, and this cooling is much less pronounced over water due to mixing and large heat capacity of water which prevent the surface temperature from decreasing rapidly. Moreover, it is impossible for the surface layer

in air to cool much below 0°C, to -2°C at the most, and hence the formation of surface inversion at freezing temperatures is unlikely over the sea. This is a situation similiar to the one discussed in chapter 4.1.3. in the connection of advection fogs (see Fig. 22 on p.88 For these reasons it seems that generally speaking the occurence of freezing precipitation at sea far from the coasts is not to be expected. However, a suecundary temperature inversion - such as shown by the dotted curve in Fig. 19 - is possible near the coast-line during offshore winds. This kind of surface layer is unstable and does not extend very far from the coast.

The humidity conditions during atmospheric icing vary within a rather large interval. One might expect that during in fog or precipitation the relative humidity R would be quite close to 100%, but this seems not to be the case as shown by Fig. 20 . Regarding icing in a fog this is probably due to inhomogeneity of air humidity produced by turbulence and entrainment, and due to the fact that droplet formation from water vapour is possible in values of R slightly below 100% (Woodcock, 1978). Also, it must be remembered that supersaturation in air with respect to ice surface is reached before it is reached with respect to water when R is increasing. During freezing precipitation R may be as low as 70%. According to the data from Toronto R<90% was experienced during 20% of the time with freezing precipitation (Stallabrass, 1982). Continental data for the dew-point spread during glaze formation in different air temperatures are given in Fig 21 According to Dranevič (1971) the dew-point spread is slightly smaller during rime formation than during glaze formation at the same air temperature.

4.1.3. Fogs

For severe atmospheric ice accretion to occur it is necessary to have supercooled water droplets in air. In most cases this means that fog is observed in the atmospheric boundary layer. Since other conditions that are conditional to severe ice accretion (freezing temperatures, strong winds) are quite common in arctic waters, it is obvious that that the existence of fogs in air temperatures below 0°C is the key factor determining e.g., the frequency of atmospheric ice accretion in the different sea areas. For this reaso the conditions favourable for the formation of supercooled fogs in

the marine environment are discussed in more detail in the following.

Fogs are generally classified into three main categories: radiation fogs which develop due to air cooling as a result of radiative cooling of the underlying surface, advection fogs which form when warm air is cooled when brought over a cold surface and evaporation fogs which result from evaporation from water surface as the moist air is mixed with the colder air resulting to condensation and droplet formation. As to marine conditions, radiative fogs can be excluded since the rate of cooling of the sea surface is too slow for producing radiative fogs.

Advection fogs, on the contrary, are quite common over the sea the fogs in the English Channel being the best-known example. However, when restricting our interest to fogs which are supercooled, it can be concluded that this kind of icing fogs are rare because cooling of surface air to temperatures below $0^{o}C$ is possible only if the surface temperature of the sea t_s is below $0^{o}C$. Therefore, supercooled advection fogs may occur only over oceans with saline water and with $t_s < 0^{o}C$. It is also obvious that supercooled advection fogs formed over land can prevail when brought over the sea only in the above mentioned conditions, the surface layer being otherwise unstable. As to the importance of advection fogs it should be pointed out that the other limiting condition, in addition to the condition $t_s < 0^{o}C$, namely, that air temperature is above the surface temperature, is significant considering the intensity of icing during advection fogs: the maximum icing intensity is limited by air temperature as shown in chapter 3.2.2. and therefore extreme icing rates are not possible in advection fogs whose temperature must be above $-2\ ^{o}C$. This is demonstrated in Fig.22 ,which shows the temperature conditions under the occurence of supecooled advection fog.

Evaporation fog (sea smoke) occurs typically in low air temperatures and is therefore a possible source of severe icing providing that its liquid water content is high and that strong winds prevail (see Lee, 1958, Shannon and Everett, 1978). Several criteria have been suggested for the occurence of evaporation fog. Jacobs (1954) suggested that sea-air temperature difference must be above $9\ ^{o}C$ for the onset of evaporation fog. According to Church (1945) vapour pressure difference between water surface and air must be above 0.5 kPa for evaporation fog to develop. Vapour pressure in air e_a correlates strongly with air temperature t_a and these determine the relative humidity R. On the other hand, water vapour at water

surface e_s is a function of the water temperature t_s. Therefore, the criteria by Church (1945) can also been formulated by means of t_a, t_s and air humidity. This has been done by Currier et al. (1974) giving the index $i = (t_s - t_a)/(e_{as} - e_a)$, where e_{as} is the saturation water vapour pressure in air ($e_{as} = f(t_a)$). In the data of Currier et al. (1974) the probability of the occurence of evaporation fog varied from 0.04 for i = 10 to 1.00 for i > 90. Saunders (1964) has derived a theoretical criterium which also includes t_a, t_s and R. His results are presented in Fig. 23. Utaaker (1979) has verified the theoretica criteria and found a satisfying agreement with observations of steaming and no steaming. Wind speed has not been found to have any effect on whether fog will or will not be formed (e.g., Hicks, 1977).

When considering icing on marine structures, the onset of supercooled fog is not always the thresold condition, because these fogs are often limited to the height of only a few meters above the sea surface. The vertical extent z_f of evaporation is therefore important. The regime of possible value of z_f is from 0 to at least 100 m, where it can reach (or form) a stratus cloud (Church, 1945). Observations by Utaaker (1979) show that z_f is clearly dependent on sea-air temperature difference, i.e., on the difference between t_s and the thresold value of t_a based on Fig. 23. These observations are shown in Fig. 24, from which it can be seen that the scatter of z_f values at the same temperature difference is quite large indicating that there are additional factors affecting the variance of z_f. One possible factor of this kind is the wind speed v ; it has been suggested on theoretical basis by Wessels (1979) that z_f can be determined according to Eq. (28)

$$z_f = 0.003\ P_f^{-3.05}\ (-L) \quad , \qquad (28)$$

where P_f is the critical rate of mixing which depends on temperature and humidity conditions only (see Wessels, 1979) and L is the Monin-Obukhov length characterizing the stability conditions in the atmospheric surface layer. According to Wessels (1979) for moderate wind speeds and water surfaces about 15°C warmer than air, the definition for L can be simplified to

$$-L \quad 3.2\ v^2 / (\theta_s - \theta_a) \quad , \qquad (29)$$

where v is the wind speed at the height of 10 m, and θ_s and θ_a are the

potential temperatures of water and in air at 10 m height, respectively. Now, if z_f is roughly proportional to -L as indicated by Eq. (28), then it follows from Eq. (29) that z_f is strongly affected by the wind speed v - other conditions being fixed - in such a way that z_f increases with increasing v. This is important regarding icing on high structures, since high wind speeds are, for other reasons too (chapter 3), associated with the most serious icing conditions. The model of Wessels is also cabable in simulating the properties of evaporation fog - such as z_f or w - as a function of the downwind distance from the shore (see table 6 , on p. 75). These simulations show that z_f decreases downwind, and this decrease is dependent on the height of the inversion layer in the original air mass. These aspects dealing with the horizontal extent of icing risk from the shore are discussed in more detail in chapter 6.

4.1.4. Sea surface temperature and salinity

Sea surface temperature has, naturally, no direct effect on atmospheric icing - as in the case of spray icing, but it has an indirect influence. Firstly, the modification of cold air flowing from the continent over the sea is controlled by the sea surface temperature t_s along the air trajectory. Air temperature, above all, but also wind speed and fog and precipitation characteristics are affected by surface layer stability which is partly determined by t_s. Secondly, the occurence of advection fogs (see Fig.22 ,p.80) and evaporation fogs (see Fig. 7 ,p. 88) is controlled by t_s.

In Fig. 23 it can also be seen that the salinity of sea water affects the onset of evaporation fogs in such a way that fogs develop at smaller sea-air temperature differeces and larger relative humidities over fresh water than over saline water. The air-temperature range for the possible occurence of supercooled advection fogs is more limited when water salinity is small as can be seen in Fig. 22 ,p. . Over fresh water surface supercooled advection fogs obviously can not prevail , over long distances.

4.2. Synoptic weather conditions

In chapter 4.1. the meteorological conditions in the boundary layer that are favourable for atmospheric ice accretion at sea were discussed. Forecasting of meteorological variables in the boundary layer is generally based largely on synoptic weather maps and numerical prognosis for synoptic scale phenomena. Therefore, one possibility to forecast or to examine statistics of icing at sea is to relate surface icing conditions directly to the synoptic weather conditions. There are, however, many difficulties in doing this, especially at coastal regions where the role of mesoscale phenomena in determining the surface conditions is very important due to changes in surface roughness and temperature over the coastline. For example, situations which look similar on a synoptic weather map may be associated with quite different surface conditions in different seasons - or even at the same date in different years - due to differences in sea surface temperature and ice edge location. Also, the variety of synoptic weather conditions is so large that when looking for typical weather conditions where icing occurs, the classification is necessarily very rough.

In spite of these difficulties synoptic weather conditions have been used as a preliminary indicator of local surface icing (e.g., Orlicz and Orliczowa, 1954, Dranevič, 1971, Bugajev and Peskov, 1972), but general rules which would be valid regardless of location are not easily found. This can be seen in Table 2, which shows the distribution of ship icing occurence according to the position in relation to the low pressure area. More exact description of synoptic conditions during ship icing in various sea areas is given e.g., in Borisenkov and Pchelko (1972). Ship icing data is obviously to some extent useful in examining the synoptic conditions during atmospheric icing since spray icing and atmospheric icing on ships often take place simultaneously (see Table 1 ,p 72). Most commonly ship icing is encountered in the rear of low-pressure areas with cold air outbreak from north or northwest (Vasilieva, 1967, Sawada, 1970, see also Table 2). If the horizontal temperature gradient in air is large, icing may occur in the forward part of a low (Kaplina and Chukanin, 1971). Air temperature below -18 ^{o}C at the 85 kPa surface is an index of severe ship icing risk according to Borisenkov and Pchelko (1972).

As to the synoptic conditions favourable for the formation of supercooled fogs (see chapter 4.1.3.) it can be seen from Table 3 that fogs during winter months are mostly associated with occlusion fronts, although all types of fogs seem to be extremely rare this time of year. It is not certain that there are any supercooled fogs in the data of Table 3. Evaporation fogs are obviously most probable when a cold air outbreak is from the direction of the coast. Regarding supercooled advection fogs and freezing precipitation it may be noted that the necessary temperature inversion such as the one drawn by solid line in Fig. 19, p. 87 can be expected near the coast-line when a warm front is moving from the continent over the sea.

5. EFFECT OF METEOROLOGICAL CONDITIONS ON THE PROPERTIES OF ICE FORMED

5.1. Density

The density of ice is important regarding the estimation of the hazards possesses by icing for the following reasons:

- icing reports are often given in terms of ice thickness and it is therefore necessary to know ρ for determining the ice load
- adhesive strength and mechanical properties of accreted ice are correlated with ρ.
- modelling of the profile of ice deposits requires estimation of ρ (see Bain and Gayet, 1982).
- the critical ice deposit diameter above which icing does not occur theoretically (see chapter 3.2.1.) is reached at different ice loads depending on ice density, and therefore modelling of the growth of ice loads on structures requires modelling of ρ (Makkonen, 1982).

As pointed out in chapter 3.1. the structure and density of the accreted ice depends mainly on the heat balance on the icing surface and on spreading of the impinging droplets (see also Appendix 2). Basic principles in estimation of the density of ice formed by droplet accretion have been presented by Macklin (1962), who resulted to Eq. (30) based on laboratory experiments on cylinders

$$\rho = 0.11 \left(- \frac{d\, v_0}{2\, t_s} \right)^{0.76} , \qquad (30)$$

where ρ is in $g\,cm^{-3}$, d is the droplet diameter in μm, v_0 is the droplet impact speed in $m\,s^{-1}$ at the stagnation line of the cylinder and t_s is the mean temperature of the riming surface in ^{o}C.
The impact speed v_0 can be calculated according to the theory described in chapter 3.2.1. and the surface temperature t_s from the heat balance equation of the riming surface (see chapter 3.2.2.). Eq. (30) has later been verified by Buser and Aufdermaur (1972), Pflaum and Pruppacher (1979) and Bain and Gayet (1982) with good results, although small modification have been made. As a compilatic of these modifications, Makkonen (1982) has used Eq. (31) in his wire icing model;

$$\rho = 0.1 \qquad \text{for } a < 1$$

$$\rho = 0.11\, a^{0.76} \qquad \text{for } 1 \leq a < 10$$

$$\rho = a / (a + 5.61) \qquad \text{for } 10 \leq a < 60 \qquad (31)$$

$$\rho = 0.92 \qquad \text{for } a \geq 60$$

In Eq. (31) a is the Macklin's density parameter ($-dv_0/2t_s$).

From Eqs. (30) and (31) it can be seen that generally speaking ice density ρ decreases with decreasing impact speed (and wind speed) decreasing droplet size and decreasing air temperature t_a (t_s decreases when t_a decreases). Decreasing liqud water content will result to lower surface temperature t_s and will therefore cause a decrease in ρ as well. It should also be noted that v_0 depends not only on wind speed and droplet size, but also on the dimensions of the icing object, from which it follows that in the same atmospheric conditions ρ is higher on small structure than on large structures. Furthermore, ρ is continuously decreasing during the ice accretion process since the deposit size increases (see Makkonen, 1982). Also, ρ is different at different points on the icing object in dry growth conditions (Bain and Gayet, 1982). These factors make it difficult to simply relate the ice density measured after an icing storm to the conditions that prevailed. If this would not be the case one could calculate e.g., the droplet size - which is difficult to measure - from Eq. (31) by means of density measurements. Some indications may be obtained this way; for example the density values in Fig. 2 ,p. 76 suggest that the average wind speed and droplet size during these ice accretion cases have been quite small ($d v_o \approx 12$).

The quantitative relationship between the density of wet snow accretions and the growth conditions is not known, but obviously wind speed has the most prononced effect on ρ since wind stress is the primary cause of the deformation process which leads to dense and strongly adhered deposits (see chapter 3.2.3.). Wet snow accretions formed in low wind speed are typically of the density 0.2 g cm^{-3}, whereas those formed in strong winds may have density as high as 0.9 g cm^{-3} (Shoda, 1953, Wakahama and Kuroiwa, 1977). Air temperature and duration of strong winds after the snow storm may have an influence as well, but this has not been quantified.

Regarding high structures it may in some cases be important to know the expectable change of ice density with height. The data of Glukhov (1972, Fig. 2 p.76) from a continental location shows an increase in ρ with height, which is predicted by theoretical considerations too, since wind speed in the surface layer usually increases with height and the time spent by the higher part of the structure above the cloud base (where liquid water content is high) is expected to be longer. Whether this is the situation at sea is uncertain and requires experimental evidence. It may even be reversed since air temperature in icing conditions over the sea decreases rapidly with height and since evaporation fogs are usually limited to lower heights, so that liquid water content may decrease with height.

5.2. Ice type

Different types of ice are discussed in chapters 2 and 3 as well as the theoretical distinquishing between wet growth and dry growth processes (see Fig.10,p.82). Here some empirical results are discussed.

As can be seen in Figs. 10,p.82 and 25 ,p. 90 wind speed affects on ice type in such a way that glaze - and in general more compact ice - is favoured instead of porous rime when wind speed is high. Also, when liquid water content is high and droplets are large, glaze is more likely as well as when air temperature is close to 0°C. Ice type seems to be more critical to changes in the air temperature than to changes in the wind speed as shown in Figs. 10 and 25. The extreme air temperature limits are approximately from +2 to -9 °C for glaze, from 0 to -15 °C for hard rime, below -1 °C for soft rime and from +2 to -4 °C for wet snow (Gaponov, 1939, Sadowski 1965, Volobüeva, 1975, Makkonen and Ahti, 1982).

Similarly to ice density, ice type is dependent on the dimension of the icing object and may vary along the object surface and with time. Ice is often more glaze-like in the interior of the deposit and more porous in the surface layer.

Examples of the distribution of different kinds of ice deposits according to air temperature and wind speed are shown in Fig. 16 , which is, however, only indicative for marine conditions, since liqu water content and droplet size may systematically be different from the condtions in continental locations where the data originates fr

The predominating ice type varies with height. According to Glukhov (1972) glaze is more common in upper parts of high structure which is also shown by an increase in ice density with height (see Fig. 2). Again, the situation in the marine environment may be considerably different. McLeod (1981) has suggested that the relationships of the different ice types by Glukhov (1972) will hold true regardless of location. This is, however, somewhat questionable, since the boundary layer structure and the sources of icing are quite different on land and at sea (chapter 4).

5.3 Crystal structure

Close to the object surface, i.e., in the initial state of the icing process, the crystal size is largely determined by the properties of the substrate (Golubev, 1974, Mizuno, 1981). At some distance (5-20 mm) from the substrate the effect of the substrate is very small, and crystal structure is determined by the growth conditions only. In practice this means that the mean crystal size increases with distance above the surface as can be seen in Fig. 26. Fig. 26 also shows that crystal size decreases with decreasing air temperature t_a. This relationship is nearly exponential when the other conditions are fixed (Levi and Prodi, 1978). Droplet size, impact speed and liquid water content seem to have only a very small effect on the crystal size (Rye and Macklin, 1975, Laforte et al., 1982b). When analyzing the specimens from full scale ship icing tests (saline ice) Golubev (1972) found that crystal size depends on the inclination of the substrate in such a way that larger crystals are formed on horizontal than on vertical surfaces. It has not been verified if this is the case for glaze ice from atmospheric icing.

In the case of freezing rain the droplets will be solidified into a single crystal (monocrystallization) in air temperatures typical to this phenomenon. Polycrystallization is also possible, but in lower air temperatures (Hallet, 1964, Mizuno, 1981), in which case the number of the crystals nucleated from one droplet increases with decreasing air temperature.

Crystal size in wet snow deposits is smaller than that of glaze, and is probably related to the dimensions of the ice crystals of the original snow flakes.

5.4. Adhesive strength

It might be expected that the adhesive strength would be closely related to ice density and that the methods presented in chapter 5.1. could therefore be used as an index of adhesion strength. This seems, however, not to be the case as can be seen in Fig. 27 . There is generally speaking a trend towards low adhesion strength with decreasing ice density ρ , but especially for high density ice the adhesion strength may be considerably different for ice deposits of the same density. There are three apparent reasons for this: Firstly, the detachement of ice occurs usually as pure adhesive break-out for glaze and hard rime, so that the cohesive strength of the ice deposit is important only for soft rime. Secondly, since the break-out of ice is mostly adhesive, only a very thin ice layer near the substrate is relevant to ice removal, and this initial ice layer is often formed closer to the wet growth limit than the major part of the deposit (chapter 3.2.2.). The differences in ρ in this thin layer may vary less than ρ in the major part of the ice. Finally, the adhesive bonding for pure ice is dependent on temperature conditions during the icing process. That the effect of ρ on adhesio is small is demonstrated by the fact that the adhesive strength of hard rime and glaze are not principally different from each other (Phan et al., 1978, see Table 4 , p. 74).

The dependence of adhesion strength on air temperature for hard rime and glaze is shown in Fig. 28 . Ice adhesion increases when air temperature decreases down to approximately -10 - -15°C and then slightly decreases similarly to the adhesion of ice formed by spray icing (Kamenitskiy et al., 1971).

An increase in wind speed (or impact velocity of the droplets) seems to increase the adhesive strength of ice formed by droplet accretion (see Table 4 , p. 74), probably because of sronger mechanical bonding when the droplets penetrate to surface irregularities more effectively. The effect of wind speed is less pronounced in air temperatures close to 0°C as can be seen in Fig. 28. Liquid water content has only a small effect on adhesion according to Laforte et. al. (1982a).

When interpreting the results presented in this chapter, it shou be kept in mind that they are applicable mainly for high density ice grown close to - or at - the wet growth limit. If the

combination of the atmospheric parameters is such that rime formation is favoured, then the situation regarding the relationship between adhesion strength and growth conditions may be changed. For example, when air temperature decreases below -10°C soft rime is typically formed, and its porosity increases with decreasing t_a in which case the force required for ice removal probably also decreases with t_a, to the contrary to what is seen in Fig. 28 .

5.5. Shape

The shape of the ice deposit formed by droplet accretion varies considerably depending on the atmospheric conditions. This is important regarding icing on sea structures because the intensity of icing at a specified moment is related to ice deposit dimensions at that moment, and because the difficulties encountered in ice removal may depend on the ice profile, i.e., on the surface area in contact with the substrate. Also, ice shape on a structure affects the sail area and wind drag, which are often the critical factors considering the possible failure of high structures in icing conditions.

The basic parameters affecting the shape of an ice accretion are the same as those determining the density of ice, i.e., air temperature t_a, wind speed v, liquid water content w and droplet size d. Qualitatively, the role of these parameters in determining the ice profile has been well-known for long, based on both observations and theoretical considerations (e.g., Melcher, 1951, Dickey, 1952, Imai, 1953, Ono, 1964). Some basic typical ice profiles observed in near constant atmospheric conditions are shown in Fig. 29 . With high wind speed, air temperature, liquid water content and large droplets ice profile resembles A and B in Fig. 29 , the growth conditons being wet and some runoff taking place. When v, t_a, w and d decrease, the icing process turns to dry growth and the ice profile resembles C and D in Fig. 29 . With very small droplets and low values of w only rime feathers as in profile F are formed.

There is generally not much difference in ice profiles on vertical and horizontal objects, except in very wet conditions (case A) where runoff water may produce icicles on horizontally oriented surfaces.

Also, on structures with the same vertical and horizontal extent ice profile appears to be quite similar both vertically and horizontally in the conditions of atmospheric icing in nature (see Fig. 30).

It has been argued by Dickey (1953) that there are three basic ice deposit shapes that are stable, i.e., into which all other shapes are gradually changed in constant atmospheric conditions. This would mean that the shape of the collecting object has no effect on the ultimate shape of the ice deposit. There is, however, no direct proof that this kind of ice shape stability exists. This problem might be examined using the recent finite element model of McComber and Touzot (1981), which is able to predict the local collection efficiency on irregular surfaces.

Much attention has been paid to theoretical modelling of ice shapes on cylindrical and aerofoil surfaces due to the importance of this problem on icing effects on aircrafts and helicopters. On helicopter rotor blade, for example, ice profile may considerabely affect the aerodynamic lift. The recent models are cabable in predicting the shape of ice fairly well, especially in the low speed conditions corresponding to atmospheric icing on stationary structures (Stallabrass and Lozowski, 1978, Lozowski et al., 1979). Application of the results from these models is, however, not easy, as can be seen in Fig. 31. The real observed ice shapes in Fig. 31 demonstrate the effects of air turbulence and variance in the atmospheric conditions - especially in wind direction - during icing on the final ice shape.

6. GEOGRAPHICAL AND SEASONAL DISTRIBUTION OF ICING PROBABILITIES

Icing observations at sea are distributed unevenly both geographically and seasonally. This is because the majority of all the icing reports are from ships using more or less fixed routes or working at certain fishing areas only, and navigating only during a part of the year. Moreover, the cause of icing (spray/atmospheric) is seldom clearly distinquished in the reports. Hence, it is very difficult to make a clear picture of the distribution of the atmospheric icing cases in the different sea areas. Table 5 shows the periods of probable icing for the sea areas where Soviet ship icing reports have been available. These observations include mostly spray icing (chapter 2.). Regions where icing on ships was observed in the Soviet data are plotted on a map in Fig. 34. More data on spray icing probabilities can be found in various atlases published for this purpose (e.g., Anon, 1958, DeAngelis, 1974, Kolosova, 1974, Stallabrass, 1975, see also Kornyushin and Tyurin, 1979), but data on atmospheric ice accretion is rare. Some indications on atmospheric icing frequencies may be found from aircraft icing observations (see Heath and Cantrell, 1972), but these data may be misleadin regarding icing on sea structures because of the rapid change of the parameters involved with icing with height over the sea.

Because of the lack of representative atmospheric icing observations at sea, studying the probabilities of atmospheric icing must partly be based on frequencies of such combinations of generally measured atmospheric parameters that are expected to cause icing on structures. But the amount of these kind of data, too, is small from the open sea, and therefore observations from islands and coastal station must be used. For this reason, the results of these studies should be interpreted with care, the representativeness of observations made over land surface to the real offshore conditions being questionable, since icing phenomena are affected by such factors as latitude, sea surface temperature patterns, proximity of land and its orography.

The combinations of atmospheric parameters used as indicators of atmospheric icing are slightly different in different studies. In the Soviet classification the combination chosen to represent atmospheric icing conditions on ships is $t_a \leq 0^{\circ}C$, $v \leq 7$ ms^{-1} and occurence of precipitation and fog (e.g., Kolosova, 1974). The distribution of the frequency of this combination of t_a and v for

Chukchki Sea is shown in Fig. 33. In Fig. 33 the occurence of fog or precipitation is not, however, taken into account, and therefore the probability of icing is probably much smaller than shown in Fig. 33 . On the other hand, the criterium $v \leq 7$ ms^{-1} for the existance of atmospheric icing is perhaps not well justified, since there seems to be no reason why it should not occur during high wind speeds (see chapter 4.1.3.). Another possible criterium is therefore simply $t_a \leq 0^{\circ}C$ which has been used by Dunbar (1964) in constructing charts for the areas where superstructure icing is probable in different seasons.

The occurence of supercooled fogs is an obvious atmospheric icing criterium. The worldwide occurence of supercooled fogs has been studied by Guttman (1971), whose charts for the Northern Hemisphere are shown in Fig. 32 . The apparent conclusion from Fig. 32 is that supercooled fogs are seldom met at sea, except in ice covered areas and close to the costs or to the ice edge. The same conclusion, i.e., that supercooled fogs occur only in the conditions which prevail in coastal areas was reached in chapter 4.1.3. The downwind extent from the shore has been studied by a theoretical model by Wessels (1979) for evaporation fogs, and he also concluded that evaporation fogs are restricted to costal waters. The model results for one situation are shown in Table 6. Unfortunately these results from the model by Wessels (1979) are quite sensitive to the rate of entrainment with dry air, and therefore more theoretical and experimental work is needed to confirm the limited range of supercooled fogs from the shore. It must be pointed out in this connection that, at least once, evaporation fog has been observed at a distance of 300 km from the coast (Hay, 1953) although it lasted for less than an hour and was not reported to cause any icing. A rather severe case of icing due to evaporation fog has been reported at a distance of approximately 35 km from the ice edge by Lee (1958).

It seems not only that supercooled fogs are restricted to coastal water, but their frequency in these areas is small too, as shown in Figs. 35 and 36 and in Table 3 . According to Fig. 35 the frequency of fogs at the coastal stations of Northern Norway is practically zero during the time of year when the average air temperature is below $0^{\circ}C$ (December-March, according to Anon, 1959). According to Brower et al. (1977) the frequency of fogs in winter months is 0-10 % in the Gulf of Alaska, 10-20 % in the Bering Sea and 10-15 % in the Sea of Chukutsk and in the Beaufort Sea. However, only a small

portion of these fogs occur in air temperatures below 0°C. The distribution of winter fogs at some arctic locations according to air-sea temperature difference is shown in Fig. 36 . Taking into account the mean winter sea surface temperature in these areas it can be concluded from the data of Fig. 36 that supercooled fogs are very infrequent, occuring 1-2 times a month, at most. The onset of evaporation fogs, when the air is much colder than the sea surface (see chapter 4.1.4.), can be seen as a concentration of fog frequency in Fig. 36 when $t_s - t_a \leq -9^{\circ}C$.

In addition to the frequencies of icing it is interesting to consider the duration of icing conditions when they occur. There is not much data of the duration, but some conclusions can be made from storm and visibility statistics. According to Smirnov (1974) storms at freezing temperatures and lasting for more than three days occur three times in a year on average in the arctic sea areas. Poor visibility ($\lambda < 3.7$ km) is observed in the arctic areas in 4-10 % of all observations, and its duration is in 90 % of the cases less than 12 hours and in 1-3 % of the cases more than 24 hours (Anon, 1963). Number of hourly occurence of freezing precipitation for the arctic stations is given in Fig. 37 . Fig. 37 gives some indications of the icing potential, although the cases of non-precipitating supercooled fogs are not included in the data. Charts giving the presentage of hourly weather observations with liquid precipitation and wet snow in different parts of the world have been presented by Bennet (1959, see Fig. 37). These charts include parts of coastal areas, but it should be noted that it is not known what part of the data has, in fact, been associated with structural icing.

It has been suggested by McLeod (1981) that the data such as those in Fig. 2 is representative for the entire sea area (Bering Sea). Also, Brower et al.(1977) claim that the data in Fig. 36 represents the sea area approximately 500 km from the coast. It is the opinion of the author, however, that the representativeness of observations from the coast or from islands to the offshore areas is quite questionable. As explained in chapters 4.1.2. and 4.1.3. the formation and maintainence mechanisms of freezing fog and precipitation are different over the land and over the sea surface. This is the case even if the land area is small - such as an island - and if the observation point is very close to the coastline. It should be pointed out that coastal observation in general represent the atmos-

pheric surface layer over the continent - not over the sea - when wind is blowing from the continent to the sea. This is almost always the case when atmospheric icing at sea takes place as explained in chapter 4.1.1. For example, many - if not most of the cases in which freezing air temperature is reported at a coastal station or on an island are not the cases in which air temperature is below $0^{\circ}C$ over the sea surface at some distance from the observation point, due to the warming effect of the sea. Hence, it seems that in order to make use of the available icing data from coastal locations in estimating icing probabilities at offshore locations, a more complete understanding of the changes over the coastline in the properties of the atmospheric surface layer with respect to the icing potential is needed. This could be acchieved e.g., by making simultaneous measurements at a coastal location and at an offshore platform.

7. METHODS FOR MEASURING ICING SEVERITY

Most of the results on ice loads in the marine environment have been obtained by simple manual ice thickness measurements, weighing the removed ice and by visual estimates. On ships the change in the sailing depth has generally been used as an ice load indicator. These methods are rather inaccurate and are suitable for rough estimates in severe icing conditions. The instruments that are in use in continental measurements must be used, when high accuracy is required. These instruments are mostly cylindrical objects such as steel cylinders and wires. Also metal plates have been used. The most commonly used devices are the combination of horizontal wires used widely in the USSR (see Nikiforov, 1982) and the so-called Grunow net, which is quite commonly used in the Central Europe (see Grunow and Tollner, 1969, Baranowski and Liebersbach, 1977). The Grunow net is a tube of wire netting and is often installed on top of a precipitation gauge. A device quite similiar to the Grunow net has been used in ship icing measurements by Tabata et al.(1967). This instrument is shown in Fig. 39 . Determination of the icing rate on this kind of simple instruments is usually done by manual weighing after melting the ice.

Manual icing rate measurements can be made easily and rapidly (within a few minutes) by the rotating cylinder method (Fraser and Baxter, 1953). This method, generally used in laboratory experiments and cloud microstructure studies, is essentially similar to the above mentioned methods, the difference being only in that the cylindrical icing object is rotating and is very small (diameter $\approx$ 1 mm). Ice amount is determined by weighing the instrument before and after it is exposed to icing. Relation of the results from the rotating cylinder method to the icing of larger structures is not straightforward, but must be determined using the theory (see chapter 4.2.1.) by the value for the liquid water content, which can be determined rather accurately by the rotating cylinder, providing that the growth conditions on the instrument are dry (see Rush and Wardlaw, 1957, Stallabrass, 1978).

Manual icing measurements are difficult and often dangerous to make in the marine environment. Also there is a need of icing data for unmanned marine installations. Therefore, instruments that can measure and record the icing rate automatically are demanded. One possibility is simply to install an icing cylinder or rod to a

weighing machine with electronic data recording. This method, used in remote mountain areas (e.g., Röthig, 1967), has been applied to ship icing measurements by Tabata et al. (1963, Fig. 40). Weighing instruments have proved useful, but there are some problems that restrict their reliability. Firstly, the weighing mechanism is made unoperative by ice unless it is protected by heating (see Fig. 40). Heating, on the other hand may affect on the icing rate on the instrument. Secondly, heavy wind drag - often associated with icing - is felt by the weighing machine and may be mistakenly interpreted as an increased ice load. Finally, the whole instrumentation may be capsulated by ice after some time of ice accretion.

In order to avoid these problems a more sophisticated device whose working principle is entirely different from the previous detectors has been developed by Rosemount Inc., USA. This insrument which is presently available in several versions, is originally meant to be used in aircraft turbomachinery. It has, however, been used successfully in near ground icing conditions, too (Ackley et al., 1973, 1977, Tattelman, 1982), and also in the marine environment (McLeod 1981). The small cylindrical sensing probe of the Roemount detector (see Fig. 41) is forced to vibrate longitudinally, parallel to its axis by an electrical oscillator. This vibration is in its resonant frequency when the icing probe is free of ice, but accretion of ice will cause a shift in resonance corresponding to the increase in mass adhering to the probe. After a thin layer of ice (about 0.5 mm) has accumulated the sensor is de-iced by an internal heater. The heating cycles are then recorded, and from the frequency of the cycles the ice accretion rate can be evaluated with fairly good accuracy, although some scatter is caused by changes in ice density and due to calibration problems (Tattelman, 1982). Rosemount detectors still require more testing in the marine environment, but it seems that they are the most promising practical method to measure icing rate at sea. Especially their ability to operate through long icing periods with minimum human involvement is superior to all other ice detectors presently available.

8. ANTI-ICING METHODS

8.1. Structural design

Methods for alleviation of the hazards and inconveniences of icing can be divided to anti-icing measures, which aim at prevention or reduction of ice accretion, and to de-icing measures aiming at removal of the accreted ice. Some of the methods described in this chapter and in chapter 9. may be classified to either of these categories depending on the application.

Perhaps the most important anti-icing method used rather generally up to now is the minimizing of small structures and replacing them with fewer large objects. The present design of the superstructure of fishing trawlers, as an example, is based on this principle. The reason for the minimizing the amount of small structures is that they have larger icing efficiency than large objects. In the dry growth regime this effect is due to rapid decrease of the collection efficiency E with bigger size, and in the wet growth regime due to a decrease in the heat transfer coefficient with bigger size. These effects should not, however, to be overestimated since the collecting surface area and the area for the heat exchange to take place increase as a function of object size. It has, in fact, been shown theoretically by Makkonen (1982) that the initial size of a cylindrical object has only a very small effect on the ultimate ice load after long-term icing in the cylinder diameter range 1-5 cm in the case where the ice deposit shape remains cylindrical. This indicates that the amount of separate objects on a ship superstructure, as an example, may be more important than their size regarding the formation of ice loads. On the other hand, if the structures are large enough ice may not occur at all, as pointed out in chapter 4.2.1.

The theoretical result that E reduces towards zero for objects large enough (see chapter 4.2.1.) has been applied to the protection of high masts and towers with promising results (Jaakkola et al., 1982). Considerable reductions in ice formation have been achieved by covering the masts with cylindrical plastic coatings of severals meters in diameter. There are, however, some disadvantages which have restricted the use of this method; the large surface area experiences heavy wind drag which may lead to vibrations of the mast structure. Therefore the method requires more testing, but already

it appears to be a promising practical anti-icing measure for towers and masts which have sufficient steadiness against wind forces caused by the increased sail area of the sheltering cylinder.

8.2. Thermal methods

The most obvious method for ice prevention is heating. However, it is far from being the most practical one. This is because of the large amount of latent heat required to melt ice or to prevent its formation. For example, the power required for anti-icing, when a calculated icing rate on a non-heated surface is 3 g cm^{-2} h^{-1}, is about 3 kW m^{-2}. For a medium size trawler this corresponds to the power of about 2-3 MW for the whole vessel.

Heating is not an economical de-icing method either - especially when compared with mechanical measures. Melting of ice at $0^{o}C$ requires the energy W_t;

$$W_t = L \rho V \quad , \tag{32}$$

where ρ is ice density and V the volume of the melted ice. Supposing that removal of ice of the density of 0.9 g cm^{-3} from a vertical surface requires melting of about 1 mm thick ice layer (Ackley et al., 1973) the heat W_t needed for de-icing of a 1 cm^2 surface would be $W_t \approx 30$ J from Eq. (32). Removal of the same amount of ice mechanically would require energy W_m;

$$W_m = F A \delta \quad , \tag{33}$$

where F is the adhesive strength, A is the surface area and δ is the distance removed before displacement of the ice. Supposing that δ is less than 1 cm and taking a typical value 4.7 kg cm^{-2} 9.8 m s^{-1} for F (see Table 7 ,p. 75) we get $W_m < 0.5$ J for a 1 cm^2 surface. Hence the ratio $W_t/W_m > 60$, at least, which demostrates the uneffectiveness of heating compared to mechanical ice removal.

Large energy requirements of thermal methods have restricted their use mostly to small size objects only. In these cases internal heating is usually used, since external heating - such as protecting meteorological instruments with infrared heaters is quite ineffective (Gerger, 1974, Ahti, 1978). As an example, anti-icing of a cup-anemometer requires power of 300-700 W (Ahti, 1978).

One way of solving technically the heating of sea structures is to use a thermosyphon, the principle of which is demonstrated in Fig.4

The workingfluid can be e.g. ammonia or Freon 21. This method can be applied to structures such as masts and handrails, the structures themselfs working as heat pipes. It is also possible to cover flat surfaces with a loop of heat pipes. Both of these techniques were applied when constructing the first practical thermal de-icing system on a Japanese ship (Okihara et al., 1980, Anon, 1981). This thermostat controlled heating system, which can use different heat sources, is schematically shown in Fig. 43 . The heat consumption of the system has been found to be about 1 $kW\,m^{-2}$ in the field tests under typical icing conditions (Okihara et al., 1980). It is in principle possible to use the waste heat from the vessel's engines as the energy source of the system. A heat pipe method has also been used in de-icing navigation buoys (Larkin and Dubuc, 1976).

Current conducting coatings may be used for heating small surface areas, such as bridge windows (King, 1973). This method may be applied to larger surfaces too, if combined with coatings which reduce ice adhesion. Doing this it may be possible to reduce the power consumption to a level realistic for practical applications (see Panyushkin et al., 1974 e).

The use of hot water is rather effective in short-term ice prevention, and is sometimes used as a de-icing method on ships (in 4 % of the cases when combatting icing, Panov, 1978). A disadvantage of this method is - in addition to high heat consumption - that when used for preventing the upper parts of the structures water falling and flowing along the surfaces may increase icing at lower levels. Non-heated sea water may also be used in anti-icing by producing a water film on structure surfaces. This method is, however, not effective if icing is severe (low air temperature, for example) and may lead to increased icing if poorly controlled. A combination of thermal and mechanical methods is the so-called sea water lance, which consists of a high pressure jet of sea water cabable of ice removal due to melting and dynamic pressure.

8.3. Chemical methods

Distribution of different chemicals on an icing surface in order to reduce ice adhesion has been tested with mostly poor success. The anti-icing effect of e.g., silicone oil, vaselin and Kilfrost has been found to be small in these tests (Alexeiev, 1974). Moreover, these chemicals are easily deteriorated by weathering and by the accreting ice (Ackley et al., 1973). Fixed coatings, which are more effective in reducing the adhesion strength are discussed in chapter 9.2.

Another kind of chemical measure in ice prevention is the use of freezing point depressant applied to the surfaces. The major problems when using this method are the optimization of the quantity and the uniform distribution of the chemicals on the surface. If these problems are overcome, it is possible to reduce icing considerably by using e.g., ethyleneglycol (Gerger, 1974, Stallabrass, 1970) and Santomelt 990-CR organic anti-icing fluid (Bates, 1973). Salts such as kalsiumnitrate (Semenova, 1972) have also been tested, and it seems that reduction - but not prevention - of ice load formation can be obtained by these chemicals (Ackley et al., 1973).

Chemical methods can be seen as appropriate in protecting small special objects (bridge windows, automatic meteorological instruments etc.) and objects which require only ice removal for a short period (helicopters before take-off, as an example). They are difficult to apply on large structures for long-term ice prevention since their rapid deterioration makes the method uncertain and expensive. Other disadvantages are the by-effects such as slipperiness of horizontal surfaces and contamination of the catch on trawlers.

8.4. Other methods

Prevention of ice formation on meteorological instrument housings has been achieved by installing a shelter net around them (Gerger, 1974). The same method in a larger scale could be used for anti-icing of ships or stationary sea structures. If a large amount of wires would be elongated as a net in the bow of a ship or around a stationary structure, icing could be reduced on the protected superstructure. Icing of the wire netting could be prevented by e.g., heating, the anti-iced surface area being in this case smaller than the protected object. Another possibility is to construct the net installation in such a way that it is can be lowered into water for melting, and that another net can be elongated for protection while the other one is melting (Lock, 1972). Water temperature must, of course, be above $0^{\circ}C$ when using this method, and regarding spray icing it must be $\approx 0^{\circ}C$, because the accreted ice has smaller salinit than the water where it originates from, so that its melting temperature is higher than the freezing temperature of sea water. More exact estimates should be made for relating the rate of melting of ice in sea water to the rate of ice accretion in order to confirm the usefulness of this method.

Deflecting the supercooled water droplets from their original trajectories by air inflation and thus preventing them from striking the protected object has been suggested by Minsk (1977). This method seems to be suitable particulary in atmospheric icing prevention since the droplet size - and hence droplet inertia - is small compared to spray icing. The method has not been tested so far. Energy requirements may prove problematic.

It has been shown by Melcher (1951) that the density of ice decreases if it grows under an electric field. This has later been demonstrated by Phan and Laforte (1981) who also showed that the adhesive strength of the accreted ice on wires depends on the electri field applied (see Fig. 44). In some applications this phenomenon might be benefited in anti-icing, but no practical tests have been made so far.

Ice accretion due to evaporation fog is usually found only in a narrow zone (some tenths of meters) from the downwind edge of the water body (Mook, 1965, Utaaker, 1979). Therefore it might be possible to reduce icing on sea structures by preventing evaporation in the vicinity of the structures. Surface films of liquids - such

floats constructed of sheets of styrox, for example, might be used. One possibility is simply to build a platform with sufficiently large horizontal dimensions around for protected mast or other object. Floats for preventing evaporation fog would be useful for reducing spray icing as well, because of their role as wave-dampers.

In the case of wire icing, the formation of ice deposits, especially from wet snow, is promoted by rotation of the wire and by sliding of the deposit to the lee side, so that a cylindrical deposit efficiently enveloping the wire is formed. In this case an anti-icing effect is achieved when twisting of the wires is prevented by anti-torsion weights, and the sliding by small rings or a pair of plastic fins attached to the wire (Wakahama and Kuroiwa, 1977).

9. DE-ICING METHODS

9.1. Mechanical methods

Manual de-icing has been practically the only method of combatting ice at sea so far. Ice removal is done by crew members of a ship on deck using mallets, axes, hammers, baseball bats etc. This method is not satisfactory because of its insufficient efficiency, as shown by many ships lost in spite of manual de-icing. Moreover, the conditions on deck during severe icing are hazardous and completely impossible when the de-icing is most necessary. The use of trucks or other mechanical cutters as a tool in ice removal (Curakov et al., 1981) is usually possible only after the icing storm. Manual removal of ice from the upper parts of the structures most critical to ship stability and to the endurance of stationary structures, is seldom possible at any times.

In order to avoid manual ice removal automatic and semi-automatic de-icing methods have been developed. The most effective of these devices seems to be a pneumatic de-icer, which is s series of tubes alone, or built into a kind of rubber mat. When the tubes are inflated with pressurized air they expand and break down the adhesion of ice to the surface. The same principle has previously been used in protecting aircraft wings from icing. Pneumatic de-icers have proved effective on both small cylindrical objects and on large flat surfaces (Anon, 1969, Stallabrass, 1970, Ackley et.

al., 1973, 1977). An example of a pneumatic de-icer is schematically shown in Fig. 45 . Disadvantages of this methos are the costs and the likelihood of damage to the de-icers if used in working areas. Otherwise this method seems to be very suitable, especially in de-icing the upper parts of sea structures. Combined with automatic icing control devices (see chapter 7) pneumatic de-icers might be a solution for protecting unmanned ocean installations.

Economic mechanical de-icing can be obtained by using a flexible coating, which moves due to wind drag forces. This kind of coating has been tested by Hartranft (1972) in sheltering radar antennas, but the results were not completely satisfactory - probably because accreting ice makes the coating partly inflexible. Small scale models of meteorological masts have been covered with flexible coatings fixing the coatings with the aid of the guy ropes (Alexeiev, 1974). Swinging of the mast and the guy ropes is supposed to move the coating sufficiently for ice removal. Also a large amount of small conical plastic shelters, which move in the wind have been tested with some success in small scale tests. Results from full scale tests of these methods have not been reported. A mechanical de-icer based on metal plates and wires moving by means of electromagnetic induction, which is caused by discharge from a condenser through a solenoid situated near the surface of the plates, has also been used inprotection of meteorological instrumentations (Alexeiev, 1974).

For de-icing the guy ropes of high masts, a vibrator attached to the ropes has been succesfully used by Jaakkola et al.(1982). Vibration of ropes with the frequency of 20-30 Hz seems to loosen thick ice from the ropes after 2-3 minutes in action. Vibration of the object does not, however, prevent icing as shown by e.g., anemometers that often are covered by ice. Test instruments vibrating with the frequency of 50 Hz collected the same amount of ice as the stationary ones in the experiment by Klinov (1970).

9.2. Surface materials and coatings

Surface material does not have much influence on the intensity of ice accretion, and therefore coatings, for example, are not an effective anti-icing method. This has been demonstrated in experiments where ice accretion on surfaces of different materials have been compared (e.g., Rink, 1938, Kreuz, 1941, Popolansky and Kružik, 1976). Only in the very initial stage of icing some anti-icing effec has been observed on coatings such as organosilicone epox (Panyushkin et al., 1974e). This effect is probably due to high hydrophobicity of the surface, which allows rapid runoff of the impinging droplets before they turn to ice at air temperatures close to 0^{o}C. Theoretically heat conductivity of the surface material affects the icing intensity in the wet growth regime (see chapter 3.2.2.), but this effect is mostly small and is also restricted to the initial stage of the icing process. Black paints can be used in order to promote absorbtion of solar radiation, but this is of little use in the arctic areas in winter time. The effect of black paints is weak during the icing process since it is foggy or cloudy, and also it is weak when thick ice layer has already developed.

The use of low adhesion surface coatings is a de-icing measure, but not very effective one if used alone. This is because none of the presently available surface materials have adhesion strength low enough to promote a spontanious break out of ice, i.e., a break out due to ice weight alone. However, when combined with mechanical and thermal methods, the coatings and paints can be very effective in making de-icing easy. For example, it has been found that the time needed for de-icing a surface by heating is reduced considerabl when the surface is coated with a suitable material (Hanamoto, 1980) Also, the easiness of manual and automatic mechanical ice removal is very sensitive to the adhesion strength of the material to ice (see Eq. (33)). Especially polymer coatings have proved their usefulness in routine service when de-icing meteorological instruments (Gerger, 1974, Strangeways and Curran, 1978) and navigation lock walls (Frankenstein et al., 1976). Therefore the the adhesive properties of different surface materials and coatings are discussed in more detail in this chapter. For the effect of meteorological conditions during icing on ice adhesion, see chapter 5.4.

There are several theories suggested to explain the adhesion phenomenon such as electostatic, diffusion, mechanical, chemical, and mechanical-deformation theories (for references see Phan et al., 1978), but none of these theories seem to give completely satisfactory description of the nature of ice adhesion. Therefore, investigations of the adhesive strength of ice to different substances have been made purely empirically using laboratory instrumentation (e.g., Panyushkin et al., 1974c, Phan et al., 1978, Jellinek and Chodak, 1982). The lack of satisfactory theory of ice adhesion has resulted in considerably different views in the literature on the usefulness and ecpectable progress of de-icing coatings. Generally, the Soviet views are more optimistic (e.g., Borisenkov and Panov, 1974, Panyushkin et al., 1974 a,b) than those found in the western literature (e.g., Borte and Napier, 1963, Lock, 1972, Minsk, 1977) These somewhat contradicty views are probably due to the experimental results being partly confusing as well. There are considerable difficulties in making reliable and comparable adhesive strength measurements, and repeatable results are difficult to obtain even in laboratory conditions (see Phan et al., 1978). Moreover, the environmental conditions during ice accretion and after it as well as the time of contact affect the results (see chapter 5.4.).

When developing synthetic coatings with low adhesion to ice, connections with the adhesive strength and other more easily measureable properties have been searched for. Quantitative indicators of adhesive strength have not been revealed, but qualitatively it has been observed that low adhesion to ice is generally connected with low permeability, and absorption capacity as well as high hydrophobicity. Substances that fill these requirements, such as different kinds of synthetic polymer surfaces, have proved effective in reducing ice adhesion. An example of the effect of a Soviet product organosilicone epoxy "G" can be seen in Table 7 . From Tables 7 , and 4 it may be noticed that polymer coatings have a decisive effect on the adhesion strength. More than an order of magnitude decrease in adhesive strength is achieved with polymer coatings compared to the non-coated surfaces. In the actual full scale tests on a ship the best coatings were found to be teflon-4, organosilicone epoxy "G" and a vinyl polymer sheet with perfluorinated film (Panyushkin et al., 1974 b,c). Laboratory tests with ice accreted in a wind tunnel (Phan et al., 1978) showed that, taking

into account the durability of the tested products, silicone rubber proved most promising surface caoting for wires such as electrical conductors and guy ropes of masts (see Table 4). Reports of the effect of a poly-bisphenol-A-polycarbonate block copolymer have also been engouraging (Jellinek, 1978, Jellinek and Chodak, 1982).

Interpretation of the results in Tables 4 and 7 should be made with care, since they may not be entirely representative in the quantitative sense. As mentioned, differences in ambient conditions and technical difficulties in making the experiments may deteriorate the results. Also, it has been shown by Panyushkin et al. (1974d) that adhesive strength of ice depends markedly on the roughness of the icing surface as shown in Fig. 46 . Inpurities in the water from which the ice is formed is not meaningless either; as an example, salinity in the water leads to weaker bonding, see Panyushkin, 1974d). Moreover, there are indicators that the results obtained for bulk-formed ice are different from those obtained for the ice formed by droplet accretion. This is of great interest regarding problems caused by atmosperic ice accretion, and more adhesion measurements with real glaze and rime deposits should therefore be made. The importance of this aspect is demonstrated by the fact that Phan et al. (1978) found teflon to be quite ineffective regarding ice adhesion on conductor wires (see Table 4), whereas the adhesion strength on teflon has been shown to be very low in many other studies (see Aksiutin, 1979, p. 104). These differences are probably due to that the impinging droplets in droplet accretion penetrate more effectively to the relatively porous surface of teflon creating a strong mechanical bond. It therefore seems that the size of surface roughness elements and of the impinging droplets may have an important effect on adhesion strength of ice formed by droplet accretion. Indications of the impact speed of the droplets having this kind of effect have already been experimentally found (see Table 4).

Flexible surface coating materials whose de-icing effect is not based on low adhesion strength but on the easiness of ice removal on impact, have also been tested on ships (e.g., Tabata, 1968, Stallabrass, 1970, Sewell, 1971). The surfaces tested were plastic foam mats alone, and covered with a sheet of neoprene rubber. This kind of coatings have not been found to be very successful,

although they make it somewhat more easy to remove the ice manualy. However, a spontanious detachement of ice from a rubber mat has been observed on the outer side of ship's bulwark. High costs, relatively poor durability and problems in attaching the rubber mats firmly are the main reasons for the limited use of the flexible coatings.

10. DISCUSSION

Estimation of the probabilities of atmospheric icing and its expected intensity on sea structures is a difficult task because of the large number of environmental factors involved, and because of the lack of representative data. In this paper attempts have been made to approach the problem by theoretical considerations, by statistical relationships between icing and meteorological conditions and by data from continental locations, but it should be stressed that interpretation of these results should be made with care due to ucertainties in the theory and in the representativeness of the available data.

As to verification of the theoretical approach it may be pointed out that the dry growth theory (chapter 3.2.1.) has been found to give accurate results of the icing intensity $\dot{I}$ in the laboratory experiments (e.g., Lozowski et al., 1979). Also, the change from dry growth to wet growth is well predicted by the theory when compared to the results from laboratory experiments (e.g., Ludlam, 1951, Macklin, 1961). Comparisons of the wet growth theory with laboratory conditions have shown satisfactory agreement, as well (e.g., Stallabrass and Lozowski, 1978, Lozowski et al., 1979). There are, however, some discrepancies in the results from different experiments, probably due to effects of wind tunnel blockage, turbulence and inaccuracy in determining liquid water content w and droplet diameter d. Generally speaking the theoretical predictions of I in wet growth have slightly underestimated the growth rate, which may be due to underestimation of the heat exchange coefficient h for ice deposits with somewhat uneven shape and rough surface. Regarding atmospheric icing on sea structures it is problematic that practically all the laboratory experiments in order to confirm the validity of the wet growth theory have been made in much higher values of w and v than those typical for atmospheric icing. Fortunately, it seems that the agreement between the theory and the experimental results is better for low than for high values of w and v (see Lozowski et al., 1979). Stallabrass and Hearthy (1967) found in the laboratory experiments that the resulting ice thickness does not depend on the cylinder diameter D, which is in contradiction with the theory (see Eq. (17). The reason for this may be that for the blockage ratio of more than 6% there is considerabl

distortion of the flow due to blockage effect (West and Apelt, 1982) and in the wind tunnel experiments by Stallabrass and Hearthy (1967) this ratio varied from 3% to 26%, depending on D.

The decisive verification of the theoretical results should, of course, be made in the real outdoor environment. This is, however, extremely difficult, mainly due to difficulties in accurately determining the atmospheric conditions involved - especially liquid water content w and droplet size distribution. Moreover, the variability of the conditions in the real nature is not easy to take into account in the theoretical simulations. For these reasons, there are not many experimental results from outdoor environment, which could be used in quantitative verification of the theory, but by fixing some parameters in theoretical calculations it is possible to acchieve qualitative results for the effect of the other parameters that can be compared to observations. As an example, the dependence of ship icing severity on wind speed and air temperature in Fig. 47 can be compared to Fig. 13. Verifications of the heat balance theory in estimating ship icing intensity have also been made by e.g., Iwata (1973) and Kachurin et al.(1974) with satisfactory results. The dependence of icing efficiency E_i on wind speed according to the data of Glukhov (1971) in Fig. 48 is comparable to the theoretical prediction in Fig. 12.

An attempt to make a quantitative comparison of the theoretical icing intensity I with observations from real nature is shown in Fig. 49, in which the near-linear dependence of I on v, on the average, is demonstrated. The scatter of the points in Fig. 49 is considerable, although they represent mean values of the data for different wind speed intervals. The magnitude of the scatter of the individual observations can be seen in Fig. 50 showing that v explains only a small portion of the variance of the intensity of icing. The linear correlation coefficient between I and v is about 0.5 for glaze and hard rime, but very small for soft rime. The formula

$$I = 10^{-2} v \quad , \qquad (34)$$

where I is in g cm^{-2} h^{-1} and v in ms^{-1} roughly describes the mean behaviour of I in Figs. 49 and 50, but the relationship between I and v is somewhat different for each ice type as seen in Fig. 50. This is probably due to that the mean values of w and d are different for each ice types, as indicated by the theory. The theoretical result

that I is independent of air temperature in dry growth is in agreement with Fig. 51, which shows the intensity of icing scaled with the wind speed as a function of t_a. For glaze the dependence of $E_i w$ on t_a is opposite to the theoretical prediction with constant w and d indicating that w decreases with decreasing t_a, on the average. As can be seen in Fig. 7 this may not be the case at sea, however. This demonstrates that the results from continental locations - such as those in Figs. 49-51 -may not be used without great care when making predictions for the marine environment. The statistical relationship between I and wind speed is not determined by the mechanisms of icing and by the mean values of the relevant parameters only, but also by the cross-correlations of these parameters. These correlations may be different over the sea and in continental locations. If, however, attempts to estimate I at sea are made based on data such as in Figs. 49-51, it can be seen that the scatter of the values of I in relation to v, for example, is considerable, which is not engouraging. However, the maximum icing intensity seems to be closely related to v in Fig. 50. Also, it has been shown by Makkonen and Ahti (1982) that, at least in a continental region, fair estimates of the ice loads can be obtained using the wind speed and duration of icing only (see Fig. 52). If some estimates of the liquid water content can be made (see Eq. (20), Figs. 1 and 7 and Table 6), then useful predictions of the ice loads on sea structures should be within reach.

In the connection of theoretical estimation of the rate of ice accretion on sea structures the formula by Borisenkov (1969) should be mentioned, since it has been widely cited and suggested for use (e.g., Panov and Schmidt, 1971, Borisenkov and Panov, 1974, McLeod, 1977, Minsk, 1977, Lundqvist and Udin, 1978, Aksiutin, 1979), although a more correct theoretical description of ship icing intensity - corresponding to the treatment of the problem in chapter 3.2.2. - has been presented already in 1969 by Kaschurin and Gashi (1969) and in a more sophisticated form by Kaschurin et al. (1974). The formula by Borisenkov (1969) for atmospheric icing ($t_{drop} = t_{air}$) reads

$$I = \frac{t_s - t_a + 2.6\, L_e\, p_a^{-1} (e_a - e_s)}{L_f + c_i\,(t_a - t_s) + c_w\,(t_s - t_a)} \quad , \qquad (35)$$

where t_s is the temperature of the icing surface, e_s the water vapour pressure at t_s and c_i the specific heat of ice.

According to Eq. (35) I increases with increasing e_a, which seems illogical since evaporation decreases with increasing e_a (see Eq. (19), p. 18). Also, the effect of the term q_w in Eq. (19) is reversed in (35). Finally, the term $c_i (t_a - t_s)$ in (35) represents the heat releases in cooling of the ice after it has turned into ice, but this heat flux must be directed inwards since the icing surface is warmer than the underlying ice (see Fig. 9) and should, therefore, not be involved with the surface heat balance controlling icing intensity in wet growth. In dry growth, on the other hand, the heat balance does not restrict I at all (see chapter 3.2.1.). Because of these inconsistencies Eq. (35) should not be used, and in fact it gives more than an order of magnitude smaller values for I than Eq. (19) and what has been obtained experimentally (compare Fig. 13 to Fig. B2 in Minsk, 1977) for atmospheric icing intensity.

There are some uncertainties in the estimation of icing intensity in practice, but the boundary conditions where icing occurs are fairly well known (chapter 4.1.). Estimation of the probabilities of atmospheric icing are, therefore, limited mainly by our expertise in determining and forecasting the properties of the boundary layer over the sea. The future possibilities in this respect are closely related to the progress in marine meteorology in general.

Development of succesful anti-icing and de-icing measures requires much experimental work to be done. It seems probable that more effective mechanical devices for ice removal, and coatings with lower ice adhesion high durability shall be available in near future, but a complete solution of ice prevention is far from sight. Only a dramatic progress in solving the energy requirement problems involved with thermal anti-icing and de-icing methods would substantially improve our chances in combatting icing on sea structures.in an economical way.

REFERENCES

Achenbach, E., 1977: The effect of surface roughness on the heat transfer from circular cylinder to the cross flow of air. Int. J. Heat Mass Transfer, 20, 359-369.

Ackley, S.F. & Itagaki, K., 1974: Thr crystal structure of a natural freezing rain accretion. Weather, 29, 189-192.

- " - & Templeton, M.K., 1979: Computer modeling of atmospheric ice accretion. CRREL, Rep. 79-4, 36 pp.

- " - , Itagaki, K. & Frank, M., 1973: An evaluation of passive deicing, mechanical deicing and ice detection. CRREL int. rep. 351, 50 pp.

- " - , Itagaki, K. & Frank, M., 1977: De-icing of radomes and lock walls using pneumatic devices. J. Glaciol., 19, 467-478.

Ahti, K., 1978: [On factors affecting rime formation in Finland]. M.Sc. thesis, Univ. Helsinki, Dept. Meteorol., 31 pp. (in Finnish).

- " - & Makkonen, L., 1982: Observations on rime formation in relation to routinely measured meteorological parameters. Geophysica, 19. (in press).

Aksiutin, L.R., 1979: [Ship icing]. Sudostronie, Leningrad, 128 pp. (in Russian).

Alexeiev, Ju.K., 1974: Protecting sensors and masts of automatic meteorological stations against icing. WMO tech. note, 135, 7-16.

Anon, 1881: A singular case of shipwreck. Nature, 24, 106.

- " - , 1958: Oceanographic atlas of polar seas, Part II. U.S. Navy Hydrograph. Office, 705, Whasington D.C.

- " - , 1959: Climatological and oceanographic atlas for mariners, Vol. I. U.S. Dept. Commerce, Weather Bureau, Whasington D.C

- " - , 1962: Precipitation measurements at sea. WMO tech. note, 47

- " - , 1963: Marine climatic atlas of the world, Vol. VI. U.S. Government Printing Office, Whasington D.C.

- " - , 1981: First ship with practical de-icing system. Zosen, 26 (7), 26.

Austin, J.M. & Hensel, S.L., 1956: analysis of freezing precipitation along the eastern North American coastline. MIT, tech. rep., 112, 46 pp.

Ashworth, T. & Knight, C.A., 1978: Cylindrical ice accretions as simulations of hail growth: I. Effects of rotation and mixed clouds. J. Atmos. Sci., 35, 1987-1996.

Bain, M. & Gayet, J.F., 1982: Contribution to the modelling of the ice accretion process: Ice density variation with the impacted surface angle. Proc. 1. International Workshop on Atmos. Icing on structures, CRREL.

Baranowski,S & Liebersbach, J., 1977: The intensity of different kinds of rime on the upper tree line in the Sudety mountains. J. Glaciol., 19, 489-497.

Bashkirova, G.M. & Krasikov, P.N., 1958, Leningrad Glavnya Geofiz. Observ., Trudy, 73, 37-49. (in Russian, ref. Saunders, 1964

Bates, C.C., 1973: Navigation of ice covered waters. Rep. 23. International Congress of Navigation, Brussels.

Bauer, D., 1973: Snow accretion on power lines. Atmosphere, 11, 88-96.

Beard, K.V. & Pruppacher, H.R., 1969: A determination of the terminal velocity and drag of small water drops by means of a wind tunnel. J. Atmos. Sci., 26, 1066-1072.

Bennett, I., 1959: Glaze, its meteorology and climatology, geographical distribution and economic effects. Quartermaster Res. & Eng. Center, tech. rep., EP-105, 217 pp.

Best, A.C., 1950: The size distribution of raindrops. Quart. J. R. Met. Soc., 76, 16-36.

Borisenkov, E.P., 1969: [Physical justification of combinations of hydrometeorological conditions that produce ship icing]. Izd. Arkt. i Antarkt. Inst., Leningrad. (in Russian).

- " - & Panov, V.V., 1974: Basic result and perspectives on the investigation of hydrometeorological conditions related to ship icing. CRREL draft transl., 411, AD A003215, 1-31.

- " - & Pčelko, I.G., 1972: [Instructions for forecasting the hazard of ship icing]. Arkt. i Antarkt. Inst., Leningrad, 81 pp. (in Russian).

Brower, W.A.Jr., Searby, H.V., Wise, J.L., Diaz, H.F. & Prechtel, A.S., 1977: Climatic atlas of the outer continental shelf waters and coastal regions of Alaska, Vols. I-III, NCC, AEIDC, Alaska.

Brownscombe, J. & Hallet, J., 1967: Experimental and field studies of precipitation particles formed by the freezing of super cooled water. Quart. J. R. Met. Soc., 93, 455-474.

Bugayev, V.A. & Peskov, B.E., 1972: [The state and perspectives of operative forecasting of especially dangerous hydrometeorolgical phenomena]. Meteor. i Gidrol., 6, 106-115. (in Russian).

Buser, O. & Aufdermaur, A.N., 1972: The density of rime on cylinders. Quart. J. R. Met. Soc., 98, 388-391.

Cansdale, J.T. & McNaughtan, I.I., 1977: Calculation of surface temperature and ice accretion rate in mixed water droplet/ice crystal cloud. Farnborough, Roy. Aircraft. Establ., tech. rep., 77090, 29 pp.

Chaîné, P.M., 1974: In-cloud icing. Industrial Meteor., Study V, Environ. Canada, 17 pp.

Church, P.E., 1945: Steam-fog over Lake Michigan in winter. Trans. Amer. Geophys. Union, 26, 353-357.

Colbeck, S.C., 1979: Grain clusters in wet snow. J. Colloid Interface Sci., 72, 371-384.

- " - , Ackley, S.F., 1982: Mechanisms for ice bonding in wet snow accretions on power lines. Proc. 1. International Workshop on Atmospheric icing of structures, CRREL.

Čurakov, L.Ja., Savinih, V.K. & Bobrov, R.N., 1976: [Snow and ice removal methods used for steamships in Siberia]. Inst. Eng. Water Transport., Trudy, 94, 3-8, Novosibirsk. (in Russian).

Currier, E.L., Knox, J.B. & Crawford, T.V., 1974: Cooling pond steam fog. J. Air Poll. Control Assoc., 24, 860-864.

DeAngelis, R.M., 1974: Superstructure icing. Mariner's Weather Log, 18, 1-7.

Dickey, T.A., 1952: Variables determining the form of an ice accretion. Aeronautical Eng. Lab., rep. AEL-1206, 12 pp.

Drannevič, E.P., 1971: [Glaze and rime]. Gidromet. Izd., Leningrad, 227 pp. (in Russian).

Dunbar, M., 1964: Geographical distribution of superstructure icing in the northern hemisphere. Rep. Misc G-15, Defence Res. Board, Canada, 5 pp.

Fitzgerald, J.W., 1978: A numrical model of the formation of droplet spectra in advection fogs off Nova Scotia. J. Atmos. Sci. 35, 1522-1535.

Frankenstein, G., Wuebben, J., Jellinek, H.H.G. & Yokota, R., 1976: Ice removal from the walls of navigation locks. Proc. Symp. Inland Waters for Navigation, Flood Control and Water Division, 10-12, Colorado.

Fraser, D., Rush, C.K. & Baxter, D., 1953: Thermodynamic limitation of ice accretion instruments. Bull. Amer. Meteor. Soc., 34, 146-154.

Gaponov, B.S., 1939: [Temperature limits for glaze and rime formation]. Akadem. Nauk., SSSR, Izv., Ser. Geogr. i Geofiz., 3, 205-216. (in Russian).

Gavrilova, M.K., 1966: Radiation climate of the arctic. Israel progr. sci. transl., 178 pp., Jerusalem.

Gerger, H., 1974: Methods used to minimize, prevent and remove ice accretion on meteorological surface instruments. WMO tech. note, 135, 1-6.

Glukhov, V.G., 1971: Evaluation of ice loads on high structures from upper-air observations. Sov. Hydrol., Selec. Pap., 3, 223-228.

- " - , 1974: Distribution of glaze-rime deposits in the lower 300-meter layer of the atmosphere. U.S. Army foreign sci. tech. center transl., AD785965, 18 pp.

Godier, R., 1966: [Improvements in the measurements made by automatic weather stations under icing conditions]. WMO tech. note, 82, 63-66. (in French).

Golubev, V.N., 1974: On the structure of ice formed during icing of ships. CRREL draft transl., 411, AD003215, 108-116.

Goodman, J., 1977: The microstructure of California coastal fog and stratus. J. Appl. Meteor., 16, 1056-1067.

Grunow, J. & Tollner, H., 1969: Fog deposition in high mountains. Arch. Met. Geoph. Biokl., Ser. B, 17, 201-228 (in German).

Guttman, N.B., 1971: Study of worldwide occurence of fog, thunderstorms, supercooled low clouds and freezing temperatures. Naval Weather Serv. Command, NAVAIR 50-1c-60.

Hallett, J., 1964: Experimental studies of the crystallization of supercooled water. J. Atmos. Sci., 21, 671-682.

Hartranft, G.J., 1972: Evaluation of polyurethane shroud designed to prevent TACAN weather outages. Rep. FAA-RD-72-78, 39 pp

Hay, R.F.M., 1953: Frost smoke and unusually low air temperature at Ocean Weather Station India. Marine Observer, 23, 218-225.

Heath, E.D. & Cantrell, L.M., 1972: Aircraft icing climatology for the northern hemisphere. USAF tech. rep., 220.

Herman, G.F., 1980: Thermal radiation in Arctic stratus clouds. Quart. J. R. Met. Soc., 106, 771-780.

Hicks, B.B., 1977: The prediction of fog over cooling ponds. J. Air. Poll. Control Assoc., 27, 140-142.

Houghton, H.G. & Radford, W.H., 1938: On the measurement of drop size and liquid water content in fogs and clouds. MIT, Pap. phys. oceanogr. meteor. (ref. Minsk, 1977).

Imai, I., 1953: Studies of ice accretion. Res. snow and ice, 1, 35-44. (in Japanese).

Itagaki, K., 1977: Icing on ships and stationary structures under maritime conditions. CRREL special rep., 77-27, 22 pp.

Iwata, S., 1973: Ice accumulation on ships. J. Soc. Naval Archit. Japan, Selec. pap., 11, 60-86.

Jaakkola, Y., Laiho, J. & Vuorenvirta, M., 1982: Ice accumulation on tall radio and tv towers in Finland. Proc 1. International Workshop on Atmospheric Icing of Structures, CRREL.

Jacobs, L., 1954: Frost smoke. Marine Observer, 24, 113-114.

Jellinek, H.H.G. & Chodak, I., 1982: Abhesion of ice from helicopter rotor blades (preliminary work). Proc. 1. International Workshop on Atmospheric Icing of Structures, CRREL.

Jellinek, H.H.G., Kachi, H., Kittaka, S., Lee, M. & Yokota, R., 1978 Ice releasing block-copolymer coatings. Colloid and Polymer Sci., 256, 544-551.

Johnson, D.A. & Hallett, J., 1968: Freezing and shattering of supercooled water drops. Quart. J. R. Met. Soc., 94, 468-482.

Kamenitskiy, I.A., Cergacheva, N.A., Panyushkin, A.V. & Shvaysteyn, Z.I., 1971: Ice adhesion to anti-icing deck coatings . Gidrometeoizdat, Leningrad. (in Russian).

Kaplina, T.G. & Chukanin, K.I., 1971: Results of studies of synopti conditions of ship icing. Gidrometeoizdat, Leningrad. (in Russian).

Kachurin, L.G. & Gashin, L.I., 1969: Calculation of icing of sructures in a flow of supercooled aerosol in application to ship icing . Gidromet. Usloviya Obledeniya Sudov, 21-30, Leningrad. (in Russian).

- " - , Gashin, L.I. & Smirnov, I.A., 1974: Icing rate of small-capacity fishing vessels under various hydrometeorological conditions. Meteor. i Gidrol., 3, 50-60. (in Russian).

King, R.D., 1973: Hyviz-A new high light transmission and electrically conducting film for heating ships' bridge windows. Marine Eng. Rew., 1973, 37-38.

Klinov, F. Ya. & Boikov, V.P., 1974: Glaze/rime deposition in the lower 500-meter layer of the atmosphere as determined from interruptions in the operation of tv-towers . Gidrometeoizdat, Trudy, 333, 22-29, Leningrad. (in Russian).

Kolbig, J., 1973: Ice accretions on objects . Abhandl. Meteor. Dienst, DDR, 107, 36-40. (in German).

Kolosova, N.V., 1974: Regions of possible ship icing in Chukotsk Sea during summer-autumn period. CRREL draft transl., 411, AD A003215, 161-171.

Kornyushin, O.G. & Tyurin, A.P., 1979: Experince with regime advisories to the fishing fleet on particulary hazardous and hazardous hydrometeorological phenomena. Meteor.i Gidrol., 2, 114-117. (in Russian).

Kowalski, G.J. & Mitchell, J.W., 1976: Heat transfer from spheres in the naturally turbulent, outdoor environment. J. Heat Transfer, Trans ASME, 98, 649-653.

Kreutz, W., 1941. A contribution to ice accretion studies . Das Wetter, 58, 137-150. (in German).

Kumai, M, 1973: Arctic fog droplet size distribution and its effect on light attenuation. J. Atmos. Sci., 30, 635-643.

- " - & Francis, K.E., 1962: Size distribution and liquid water content of fog, Northwetern Greenland. CRREL res. rep., 100, 13 pp.

Kuroiwa, D., 1965: Icing and snow accretion on electric wires. CRREL res. rep., 123, 10 pp.

Laforte, J-L., Phan, C.L., Félin, B. & Martin, R., 1982a: Adhesion of ice on aluminium conductor and crystal size in the surface layer. Proc. 1. International Workshop on Atmospheric icing of structures, CRREL.

Laforte, J-L., Phan, C.L., Nguyen, D.D. & Félin, B., 1982b: Determining atmospheric parameters during ice accretion from the micro-structure of natural ice samples. Proc. 1. International Workshop on Atmospheric Icin on Structures, CRREL.

Langmuir, I. & Blodgett, K., 1946: A mathematical investigation of water droplet trajectories. U.S. Army Air Force tech. rep. 5418, 65 pp.

Larkin, B.S. & Dubuc, S., 1976: Self de-icing navigation byous using heat pipes. European Space Agency, ESA SP112, 1, 529-535.

Launiainen, J., Makkonen, L. & Lyyra, M., 1982: Wind tunnel experiments on ice accretion on sea structures. 13. Conf. of the Baltic Oceanographers, 6 pp. Helsinki.

Lee, A., 1958: Ice accumulation on trawlers in the Barents Sea. Marine Observer, 28, 138-142.

Lenhard, R.W., 1955: An indirect method for estimating the weight of glaze on wires. Bull. Amer. Meteor. Soc., 36, 1-5.

Lesins, G.B., List, R. & Joe, P.I., 1980: Ice accretions Part I: testing of new atmospheric icing concepts. J. Rech. Atmos. 14, 347-356.

Levi, L. & Prodi, F., 1978: Crystal size in ice grown by droplet accretion. J. Atmos. Sci., 35, 2181-2189.

List, R., 1977: Ice accretions on structures. J. Glaciol., 19, 451-465.

- " - , Joe, P.I., Lesins, G., Kry, P.R., de Quervain, M.R., McTaggart-Cowan, J.D., Stagg, P.W., Lozowski, E.P., Freire E., Stewart, R.E., List, C.G., Steiner, M.C. & Von Niederhäusern, J., 1976: On the variation of the collection efficiencies of icing cylinder. Proc. International Conf. of Cloud Physics, 233-239, Colorado.

Lock, G.S.H., 1972: Some aspects of ice formation with special reference to the marine environment. Trans. Northeast coas Inst. Eng. Shipbuild., 88, 175-186.

Lomilina, L.E., 1977; The effect of relief on glaze-ice and rime deposition. Sov. Meteor. Hydrol., 2, 39-43.

Lozowski, E.P., Stallabrass, J.R. & Hearthy, P.F., 1979: The icing of an unheated non-rotating cylinder in liquid water dropl -ice crystal clouds. National Res. Council Canada, rep., LTR-LT-96, 65 pp.

Ludlam, F.H., 1951: The heat economy of a rimed cylinder. Quart. J. R. Met. Soc., 77, 663-666.

Lundqvist, J-E. & Udin, I., 1977: Ice accretion on ships with a special emphasis on Baltic conditions. Winter Navig. Res. Board., res. rep., 23, 32 pp. Norrköping.

McComber, P. & Touzot, G., 1981: Calculation of the impingement of cloud droplets in a cylinder by the finite-element method. J. Atmos. Sci., 38, 1027-1036.

McKay, G.A. & Thompson, H.A., 1969: Estimating the hazard of ice accretion in Canada from climatological data. J. Appl. Meteor., 8, 927-935.

Macklin, W.C., 1961: Accretion in mixed clouds. Quart. J. R. Met. Soc., 87, 413-424.
- " - , 1962: The density and structure of ice formed by accretion. Quart. J. R. Met. Soc., 88, 30-50.
- " - & Payne, G.S., 1967: A theoretical investigation of the ice accretion process. Quart. J. R. Met. Soc., 93, 195-214.
- " - & Payne, G.S., 1968: Some aspects of the accretion process. Quart. J R. Met. Soc., 94, 167-175.
McLeod, W.R., 1977: Atmospheric ice accumulation measurements. Proc. Offshore Technology Conf., OTC 2950, 555-564.
- " - , 1981: Atmospheric superstructure ice accumulation measurements. Proc. Conf. Port and Ocean Eng. under Arctic Conditions, 1067-1093.
Makkonen, L., 1979: Ice accretion on structures at sea. M.Sc. thesis Univ. Helsinki, Dept. Meteor., 107 pp. (in Finnish).
- " - , 1980: Theoretical estimates of ice accretion intensity on structures. Proc. 12. Meeting of Nordic Meteorologists, 197-208, Helsinki.
- " - , 1981a: The heat balance of wet snow. Meteor. Mag., 110, 82.
- " - , 1981b: Estimating intensity of atmospheric ice accretion on stationary structures. J. Appl. Meteor., 20, 595-600.
- " - , 1982: Modeling of ice accretion on wires (summary). Annals of Glaciology (in press).
- " - & Ahti, K., 1982: The effect of meteorological parameters on rime formation in Finland. Proc. 1. International Workshop on Atmospheric Icing of Structures, CRREL.
Mason, B.J., 1971: The physics of clouds. Clarendon Press, 671 pp, Belfast.
Matveev, L.T., 1967: Physics of the atmosphere. Israel program for sci. transl., 699 pp., Jerusalem.
Melcher, D., 1951: Experimental investigation of icing phenomenon . Zeitsch. Angenwandte Math. Phys., 2, 421-443. (in German).
Milyutin, E.R. & Yaremenko, Yu.I., 1981: An experimental study of the correlation between meteorological visibility range and the height of the lower cloud boundary. Meteor. i Gidrol., 3, 32-38. (in Russian).
Minsk, L.D., 1977: Ice accumulation on ocean structures. CRREL rep. 77-17, 42 pp.
- " - , 1980: Icing on structures. CRREL rep. 80-31, 18 pp.
Mizuno, Y., 1981: Structure and orientation of frozen droplets on ice surfaces. Low Temp. Sci., Ser. A, 40, 11-23. (in Japanese).
Mook, R.H.G., 1965: Steam fog on rivers . Arch. Met. Geoph. Bioklim., Ser A, 14, 343-350.
Murray, W.A. & List, R., 1972: Freezing of water drops. J. Glaciol., 11, 415-429.
Nikiforov, Eu.P., 1982: Icing related problems, effect of line design and ice load mapping. Proc. 1. International Workshop on Atmospheric Icing of Structures, CRREL.
Nyberg, A., 1966: Evaporation at a snow surface. Arkiv. Geophys., 4, 577-590.
Okihara, T., Kanamori, M., Kamimura, A., Hamada, N., Matsuda, S., Buturlia, J. & Miskolczy, G., 1980: Design, testing, and shipboard evaluation of a heat pipe de-icing system. AIAA 15. Thermophysics Conf., Colorado.

Oleskiw, M.M., 1982: A computer simulation of time-dependent rime icing on airfoils. Ph.D. thesis, Univ. Alberta, Div. Meteor.
- " - & Lozowski, E.P., 1982: The design and testing of A Lagrangian computer model for simulating time-dependent rime-icing on two-dimensional structures. Proc. 1. International Workshop on Atmospheric Icing of Structures, CRREL.
Ono, N., 1967: Studies of ice accumulation on ships. Part II, conditions of icing and accreted ice weights. Defence Res. Board, Canada, transl., T 94 J., 9 pp.
Orlicz, M & Orliczowa, J., 1954: Ice deposits on the heigh Tatra . Przeglad Meteor. Hydrol., 7, 107-140. (in Polish).
Panov, V.V., 1976: Ship icing . Arkt. i Antarkt. Inst., Trudy, 334, 263 pp, Leningrad. (in Russian).
- " - , 1978: Icing of ships. Polar Geograph., 2, 166-186.
- " - & Shmidt, M.V., 1971: Gradiations of hydrometeorological complexes of icing considering their danger to ships. Problems of Arctic and Antarctic, 38, 150-156.
Panyushkin, V.B., Rozentsveyg, V.B., Petrov, Yu.B. Gurvich, L.Y. & Sergacheva, N.A., 1974a: Full-scale tests of coatings that reduce ice adhesion. CRREL draft trnsl., 411, 83-91.
- " - , Shvaysteyn, Z.I. & Sergacheva, H.A., 1974b: On certain thermodynamic criteria for the choise of materials for coatings that reduce ice adhesion to construction materials. CRREL draft transl., 411, 49-57.
- " - , Shvaysteyn, Z.I. & Sergacheva, H.A., 1974c: Method of determining adhesion of ice to construction materials and protective coatings by means of laboratory adhesiometer. CRREL draft transl., 411, 58-69.
- " - , Shvaysteyn, Z.I., Sergacheva, H.A. & Podokshik, V.S., 1974d Experimental investigations of ice adhesion to construction materials. CRREL draft transl., 411, 71-77.
- " - , Shvaysteyn, Z.I., Sergacheva, H.A., Rozetsveyg, V.B., Petrov A.P. & Petrov, Yu.B., 1974e: Test results of certain means of combatting ice under natural conditions. CRREL draft. transl., 411, 92-97.
Pflaum, J.C. & Pruppacher, H.R., 1979: A wind tunnel investigation of the growth of graupel initiated from frozen drops. J. Atmos. Sci., 36, 680-689.
Phan, C.L. & Laforte, J-L., 1981: The influence of electro-freezing on ice formation on high-voltage dc transmission lines. Cold Regions Sci. Tech., 4, 15-25.
- " - , McComber, P. & Mansiaux, A., 1978: Adhesion of rime and glaze on conducters protected by various materials. Trans. CSME, 4, 204-208.
Pilié, R.J. & Kocmond, W.C., 1967: Project fog drops. Cornell Aeronautical Lab., NASA CR-675, Whasington D.C.
Pinnick, R.G., Hoihjelle, D.L., Fernandez, G., Stenmark, E.B., Lindberg, J.D., Hoidale, G.B. & Jennings, S.G., 1978: Vertical structure in atmospheric fog and haze and its effects on visible and infrared extinction. J. Atmos. Sci., 35, 2020-2032.
Popolanský, F. & Kružik, J., 1976: Rime formation on different materials with different properties of the surfaces. Zeitschr. Meteor., 5, 310-313. (in German).

Porte, H.A. & Napier, T.E., 1963: Coating material for prevention of ice and snow accumulations. A literature survey. U.S. Naval Civil Eng. Lab., TN-541, 12.

Preobrazhenskii, L.Yu., 1973: Estimate of the content of spray drops in the near-water layer of the atmosphere. Fluid Mech. Sov. Res., 2, 95-100.

Prodi, F. & Levi, L., 1980: Hyperfine bubble structures in ice grown by droplet accretion. J. Resch. Atmos., 14, 373-384.

Pruppacher, H.R. & Klett, J.D., 1978: Microphysics of clouds and precipitation. D. Reidel Publ., 714 pp., Dordrecht.

Reiquam, H. & Diamond, M., 1959: Investigation of fog white-out. CRREL res. rep., 52, 18 pp.

Rink, J., 1938: The melt water amount of rime deposits . Reichsamt Wetterdienst, Wiss. Abhandl., 5, 26 pp. (in German).

Roos, D.v.d.S. & Pum, H.D.R., 1974: Sponginess in ice grown by accretion. Quart. J. R. Met. Soc., 100, 640-657.

Röthig, H., 1973: A device for continuous measuring and recording of ice accretion . Abhandl. Meteor. Dienst. DDR, 107, 26-30. (in German).

Rush, C.K. & Wardlaw, R.L., 1957: Icing measurements with a single rotating cylinder. National Aeronaut. Establishment, Canada Lab. rep., LR-206., 8 pp., Ottawa.

Rye, P.J. & Macklin, W.C., 1975: Crystal size in accreted ice. Quart. J. R. Met. Soc., 101, 207-215.

Sadowski, M., 1965: Ice accretion on electric wires in Poland . Prace Państowowego Inst., Hydrol.-Meteor., 87, 65-79. (in Polish).

Sanderson, J.I., 1973: Occurence of ice in the form of glaze, rime and hoarfrost with respect to the operation and storage of V/STOL aircraft. Studies Army Aviat. Environm., rep., 5 AD A001460, NTIS, 47 pp.

Saunders, P.M., 1964: Sea smoke and steam fog. Quart. J. R. Met. Soc., 90, 156-165.

Sawada, T., 1970: Ice accretion on ships in the northern part of the Sea of Japan. Bull. Hakodate Marine Observ., 15, 29-35

Schlichting, H., 1979: Boundary-layer theory. McGraw-Hill, 817 pp.

Schneider, H.W., 1978: Equation of the growth rate of frost formin on cooled surfaces. Int. J. Heat Mass Transfer, 21, 1019-1024.

Seban, R.A., 1960: The influence of free stream turbulence on the local heat transfer from cylinders. J. Heat Transfer, Trans. ASME, 82, 101-107.

Semenova, Ye.P., 1974: Laboratory tests of chemical anti-icing agents in ANII cold chamber. CRREL draft transl., 411, 98-107.

Sewell, J.H., 1971: Electro-impulse de-icing system. Tech. Air, 27, 6-9.

Shannon, J.D. & Everett, R.G., 1978: Effect of severe winter upon a cooling pond study. Bull. Amer. Meteor. Soc., 59, 60-61.

Shektman, A.N., 1968: The probability and intensity of the icing of ocean-going vessels. Naucho-issledovatel'skiu Inst. Aeroklim., Trudy, 50, 50-65. (in Russian).

Shellard, H.C., 1974: The meteorological aspects of ice accretion on ships. Marine Sci. Affairs Rep., 10 (WMO, 397), 34 pp., Geneve.

Shoda, M., 1953: Studies on snow accretion. Res. Snow and Ice, 1, 50-72. (in Japanese).

Spinnangr, G., 1949: Fog and fog forecasting in northern Norway. Meteor. Annaler, 3, 75-136.

Stallabrass, J.R., 1970: Methods for the alleviation fo ship icing. National Res. Coucil, Canada, Mech. Eng. Rep., MD-51, 16 pp., Ottawa.

- " - , 1975: Icing of fishing vessels in Canadian waters. DME/NAE Quarterly Bulletin, 1, 25-43.

- " - , 1978: Airborne snow concentration and visibility. Proc. 2. International Symp. on Snow Removal and Ice Control Res., CRREL.

- " - , 1980: Trawler icing, a compilation of work done at N.R.C. National Res. Council, Canada, Mech. Eng. Rep., MD-56, 103 pp., Ottawa.

- " - , 1982: Aspects of freezing rain simulation and testing. Proc. 1. International Workshop on Atmospheric Icing of Structures, CRREL.

- " - & Hearty, P.F., 1967: The icing of cylinders in conditions of simulated freezing sea spray. National Res. Council, Canada, Mech. Eng. Rep. MD-50, 12 pp., Ottawa.

- " - & Hearty, P.F., 1979: Further icing experiments on an unheate non-rotating cylinder. National Res. Coucil, Canada, Lab. tech. rep., LTR-LT-105, 21 pp., Ottawa.

- " - & Lozowski, E.P., 1978: Ice shapes on cylinders and rotor blades. NATO Panel X Symp. on Helicopter icing, 11 pp., London.

Stanew, Sw.v., 1976: On ice accretion on mountains . Zeitschr. Meteor., 5, 314-316. (in German).

Strangeways, I.C. & Curran, J.C., 1977: Meteorological measurements under conditions of icing: Some new attempts to solve the problem. WMO Tech. Conf. (TECIMO), 7-12., Hamburg.

Sundén, B., 1979: A theoretical investigation of the effect of freestream turbulence on skin friction and heat transfer for a bluff body. Int. J. Heat Mass Transfer, 22, 1125-1135.

Tabata, T., 1968: Research on prevention of ship icing. Defence Res. Board, Canada, Transl., T 95 J, 12 pp., Ottawa.

- " - , Iwata, S. & Ono, N., 1967: Studies of ice accumulation on ships. Part I. Defence Res. Board, Canada, Transl., T 93 J, 42 pp., Ottawa.

Tattelman, P., 1982: An objective method for measuring surface ice accretion. J. Appl. Meteor., 21, 599-612.

Temkin, S. & Mehta, H.K., 1982: Droplet drag in an accelerating and decelerating flow. J. Fluid Mech., 116, 297-313.

Terziev, F.S., 1973: Experience of the hydrometeorological service of the USSR in providing services to mariners and fisherie in northern waters and the Atlantic Ocean. Marine Sci. Affairs Rep., 8 (WMO, 352), 28-42.

Utaaker, K., 1979: Frost smoke downstream of hydroelectric power plants. Univ. Munchen, Wiss. Mitteil., 35, 206-210.

Vasilieva, G.V., 1967: Hydrometeorological conditions causing ice accretion on ships. Defence Res. Board, Canada, Transl., T 486 R, Ottawa.

Volobueva, G.V., 1975: Classification of glaze-rime deposits according to their weight . Meteor. Nagruzki Razlistnye Soorucheniya, Trudy, 303, 34-40. (in Russian).

Waibel, K., 1956: The meteorological conditions of rime deposition on high voltage electrical lines in the mountains. Arch. Met. Geoph. Biokl., Ser. B, 7, 74-83. (in German).

Wakahama, G., 1979: Experimental studies of snow accretion on electrical lines developed in a strong wind. J. Nat. Disaster Sci., 1, 21-23.

- " - , Kuroiwa, D. & Goto, K., 1977: Snow accretion on electric wires and its prevention. J. Glaciol., 19, 479-487.

- " - , Kobayashi, S. & Tusima, K., 1979: In situ wind tunnel for snow accretion experiments using natural snow flakes. Low Temp. Sci., Ser. A, 38, 183-187. (in Japanese).

Wang, C.S. & Street, R.L., 1978: Measurement of spray at an air-water interface. Dynamics of Atmos. Oceans, 2, 141-152.

Wessels, H.R.A., 1979: Growth and disappereance of evaporation fog during the transformation of cold air mass., Quart. J. R. Met. Soc., 105, 963-977.

West, G.S. & Apelt, C.J., 1982: The effects of tunnel blockage ratio on the mean flow past a circular cylinder with Reynolds numbers between 10^4 and 10^5. J. Fluid Mech., 114, 361-377.

Woodcock, A.H., 1978: Marine fog droplets and salt nuclei. Part I. J. Atmos. Sci., 35, 657-664.

Wu, J., 1979: Spray in the atmospheric surface layer: Review and analysis of laboratory and oceanic results. J. Geoph. Res., 84 (C4), 1693-1704.

Table 1. Course of icing (in %) on Soviet trawlers in 1965-66 according to Shektman (1968).

Icing intensity	Cause of icing					Number of cases
	Spray	Spray and Fog	Fog	Spray and Precipitation	Precipitation	
Fast growth	82	12	2	4	0	52
Slow growth	90	5	2	1	2	303
No change	94	0	2	2	2	54
All cases	89	5	2	2	2	409

Table 2. Synoptic conditions at time of ship icing according to Borisenkov and Pchelko (1972).

Sea	*Rear of low-pressure area (%)*	*Forward part of low (%)*	*Other conditions (%)*	*No. of cases*
Bering Sea	57	32	11	442
Sea of Okhotsk	70	23	7	312
Sea of Japan, Tatarskiy Strait	93	3	4	140
Western Pacific Ocean	75	19	6	182
Barents and Norwegian Seas	40	50	10	596
Baltic Sea	4	66	30	44
Black Sea and Sea of Azov	79	16	5	18

Table 3. Average number of days with fog at the outer coast of northern Norway. Left: fogs associated with cold advection, in the middle: fogs associated with warm advection, Right: fogs associated with fronts; W.F., warm front; C.F., cold front; Oc., occlusion front. (from Spinnangr, 1949).

		Outer Districts I	II	III	IV	V	VI	VII
Jan.	1							
	2							
	3							
	Sum							
Febr.	1							
	2					0.2	0.2	
	3							
	Sum					0.2	0.2	
March	1							
	2		0.2		0.2	0.4	0.4	0.2
	3							
	Sum		0.2		0.2	0.4	0.4	0.2
Apr.	1					0.6		0.6
	2				0.2	0.2	0.2	0.6
	3					0.2		
	Sum				0.2	1.0	0.2	1.2
May	1				0.4			
	2	0.2		0.2	0.4	0.4	0.2	0.4
	3				0.2	0.4	0.2	1.0
	Sum	0.2		0.2	1.0	0.8	0.4	1.4
June	1				0.2			
	2		0.2	0.2	0.6	0.6	0.2	1.0
	3	0.4	0.6	0.4	0.2	0.6	0.4	0.6
	Sum	0.4	0.8	0.6	1.0	1.2	0.6	1.6
July	1							
	2		0.4	0.2		0.2	0.4	0.2
	3	0.2		0.2	0.2	0.6	0.6	0.4
	Sum	0.2	0.4	0.4	0.2	0.8	1.0	0.6
Aug.	1		0.4	0.4	0.6	0.2	0.2	0.2
	2	0.8		0.4	1.4	0.6	1.2	0.8
	3					0.4	0.2	0.6
	Sum	0.8	0.4	0.8	2.0	1.2	1.6	1.6
Sept.	1			0.4				0.6
	2							
	3					0.2		0.4
	Sum			0.4		0.2		1.0
Oct.	1							
	2							
	3				0.2	0.2		
	Sum				0.2	0.2		
Nov.	1							
	2							
	3							
	Sum							
Dec.	1							
	2							
	3			0.2				
	Sum			0.2				
Total		1.6	1.8	2.6	4.8	6.0	4.4	7.6

		Outer Districts I	II	III	IV	V	VI	VII
Jan.	4				0.4		0.6	
	5	0.4						
	r. f.					0.2		0.2
	Sum	0.4		0.4	0.2	0.6	0.2	
Febr.	4	0.6	1.0	0.8	1.0	1.4	1.0	1.4
	5	0.2	0.2	0.4	0.4	0.2		
	r. f.	0.4				0.2	0.2	
	Sum	1.2	1.2	1.2	1.4	1.8	1.2	1.4
March	4				0.2	0.2	0.2	0.6
	5	0.6	0.2			0.2		0.2
	r. f.	2.4	1.4	1.6	1.6	1.8	0.6	1.2
	Sum	3.0	1.6	1.6	1.8	2.2	0.8	2.0
Apr.	4							0.2
	5	4.2	1.8	1.6	1.0	2.2	0.8	1.2
	r. f.	3.6	0.8	1.0	1.4	0.8	0.4	1.6
	Sum	7.8	2.6	2.6	2.4	3.0	1.2	3.0
May	4	1.0	0.2	1.0	1.6	2.0	1.4	1.8
	5	2.4	1.0	0.4	0.6	0.4	0.2	0.2
	r. f.	1.2		0.2	0.2	0.2	0.2	0.2
	Sum	4.6	1.2	1.6	2.4	2.6	1.8	2.2
June	4		0.2				0.2	
	5	1.4	0.2	0.2				
	r. f.	0.4	0.2		0.4	0.4		0.2
	Sum	1.8	0.6	0.2	0.4	0.4	0.2	0.2
July								
Aug.								
Sept.								
Oct.								
Nov.								
Dec.								
Total		18.8	7.2	7.6	8.6	10.6	5.4	8.8

		Outer Districts I	II	III	IV	V	VI	VII
Jan.	W. F.							
	C. F.							
	Oc.							0.4
	Sum							0.4
Febr.	W. F.						0.2	
	C. F.							
	Oc.							
	Sum						0.2	
March	W. F.					0.2		0.4
	C. F.				0.4			
	Oc.			0.2				0.2
	Sum			0.2	0.4	0.2		0.6
Apr.	W. F.					0.2		0.6
	C. F.							
	Oc.		0.2	0.2	0.2	0.2		0.2
	Sum		0.2	0.2	0.2	0.4		0.8
May	W. F.					0.2		
	C. F.	0.2			0.2			
	Oc.				0.6	0.2	0.2	
	Sum	0.2			0.8	0.4	0.2	
June	W. F.							
	C. F.			0.2	0.2			
	Oc.	0.4		0.2	0.2	0.8	0.2	1.2
	Sum	0.4		0.4	0.4	0.8	0.2	1.2
July	W. F.							
	C. F.							
	Oc.	0.2		0.2	0.2			0.4
	Sum	0.2		0.2	0.2			0.4
Aug.	W. F.	0.2						
	C. F.							
	Oc.	0.6	0.2		0.4	0.2		0.8
	Sum	0.8	0.2		0.4	0.2		0.8
Sept.	W. F.		0.2					
	C. F.							
	Oc.	0.2	0.2		0.4	0.2		
	Sum	0.2	0.4		0.4	0.2		
Oct.	W. F.							0.4
	C. F.							
	Oc.							0.2
	Sum							0.6
Nov.	W. F.							
	C. F.							
	Oc.				0.2			
	Sum				0.2			
Dec.	W. F.							
	C. F.							
	Co.							
	Sum							
Total		1.8	0.8	1.0	3.0	2.2	0.6	4.8

Table 4. Glaze and rime adhesion on different substances (Phan et al., 1978).

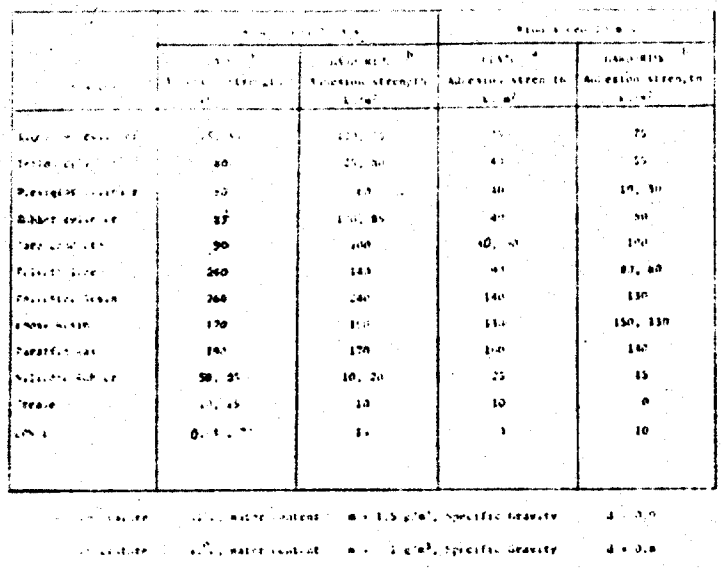

Table 5. Period of ship icing according to Borisenkov and Pchelko (1972).

Seas & Oceans	No.of Cases	Period of possible Icing
Western Seas.....	584	1 Jan -- 31 Mar
Eastern Seas	931	15 Dec -- 15 Mar
Northwest Atlantic	85	15 Dec -- 15 Mar
Norway & Greenland Seas	109	15 Dec -- 31 Mar
North Atlantic	63	15 Dec -- 15 Apr
Barents Sea	390	1 Jan -- 15 Mar
Baltic Sea	21	15 Dec -- 29 Feb
Baffin Sea & Hudson Bay	7	1 Dec -- 31 Mar
Newfoundland Region	15	1 Jan -- 15 Mar
Bering Sea	185	1 Dec -- 31 Mar
Okhotsk Sea	337	1 Dec -- 31 Mar
Sea of Japan	226	1 Dec -- 29 Feb
Northwest Pacific	185	15 Dec -- 31 Mar
Arctic Sea (Kara, Laptev, Eastern Siberia & Chukotsk	71	15 Jun -- 15 Nov

Table 6. Example of the properties of the adiabatic layer as functions of the downwind distance from the shore, with a lifted inversion as initial profile, according to the model by Wessels (1979).

x (km)		0	1	2	3	5	10	20	30	50	100
α		1	0·991	0·982	0·974	0·957	0·917	0·846	0·780	0·687	0·522
β		1	0·994	0·988	0·982	0·971	0·946	0·902	0·864	0·813	0·728
h (m)		250	252	254	256	260	270	292	316	358	459
max	cloud			<0·01	0·01	0·03	0·05	0·09	0·12	0·15	0·17
l.w.c. ($g m^{-3}$)	fog	0·29	0·28	0·27	0·26	0·25	0·23	0·18	0·13	0·08	
p_r		0·19	0·19	0·19	0·19	0·19	0·21	0·23	0·28	0·41	
z_r (m)		6*	6	6	6	6	4	3	1		

Table 7. Ice adhesion on different coatings according to Panyushkin et al., (1974 a).

Type of coating	Adhesion of ice (kg/cm^2)
Type "G" coating	0.1
Perfluorinated	0.1
Standard coating (oil-base)	4.67
Standard with perfluorinated surface	0.84
Standard with organosilicon surface	0.98

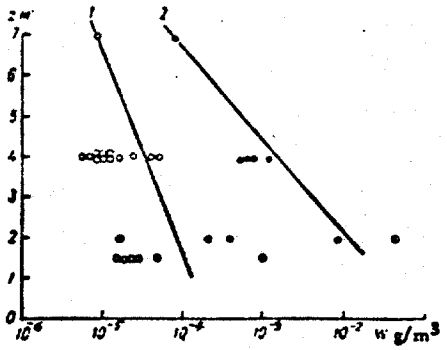

Vertical distribution of water content in the lower layer of the atmosphere at moderate (1) and strong (2) winds.

Fig.1. (from Preobrazhenskii, 1973)

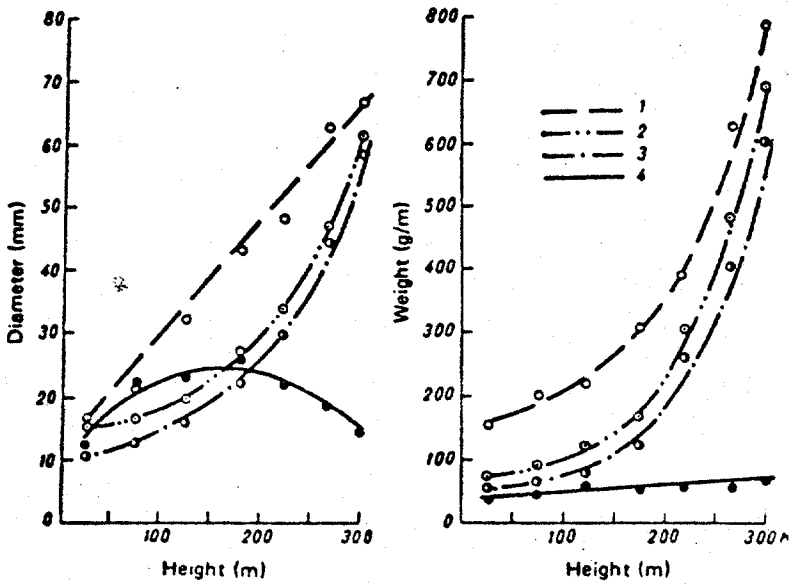

a. Average diameter vs height. *b. Average weight vs height.*

Variation of average diameter and weight of ice accumulation (1—mixture, 2—hard rime, 3—glaze ice, 4—soft rime) with height on meteorological tower at Obninsk, U.S.S.R. (Glukhov 1972).

Fig.2. (from Minsk, 1977)

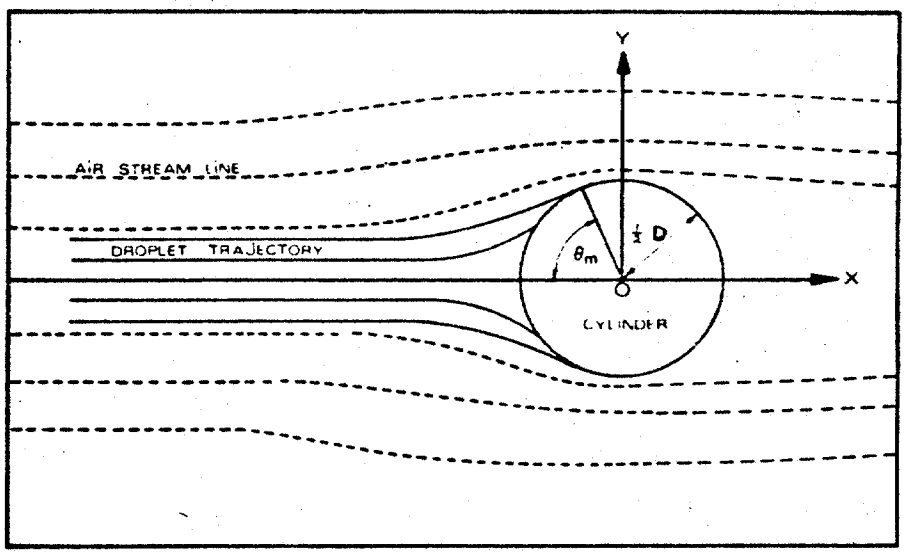

Description of droplet trajectories in front of a cylinder in an airstream.

Fig.3. (from McComber and Toutzot, 1981)

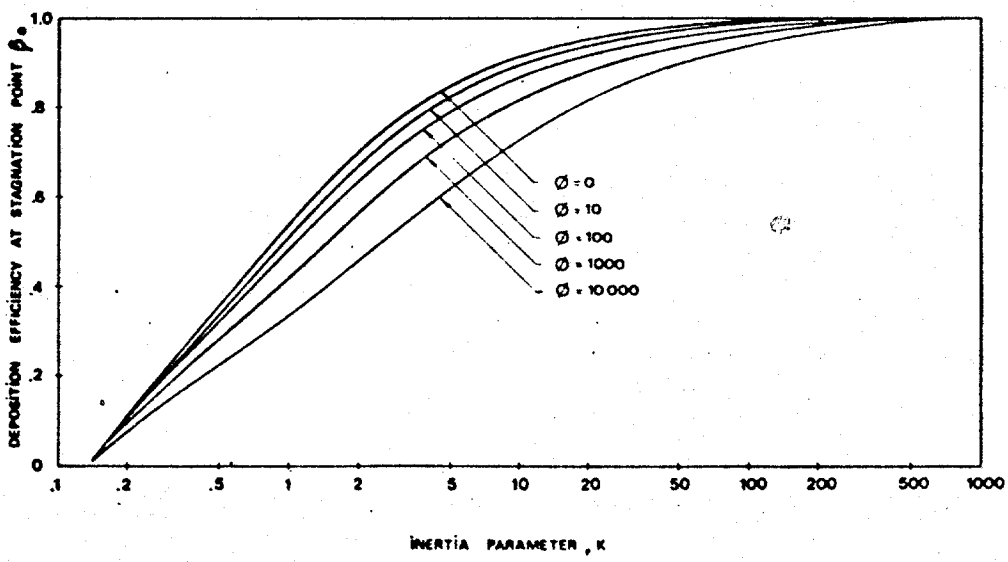

Local impingement efficiency at the stagnation point β_0 as a function of the inertia parameter K and parameter ϕ.

Fig.4. (from McComber and Toutzot, 1981)

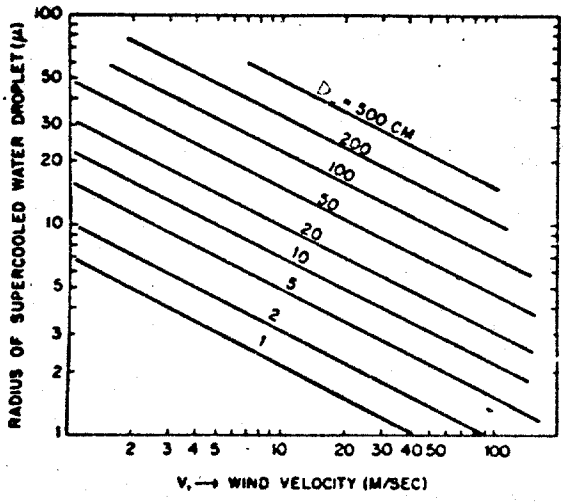

Fig. 5. Critical diameter of cylinder above which icing theoretically does not occur (from Kuroiwa, 1965).

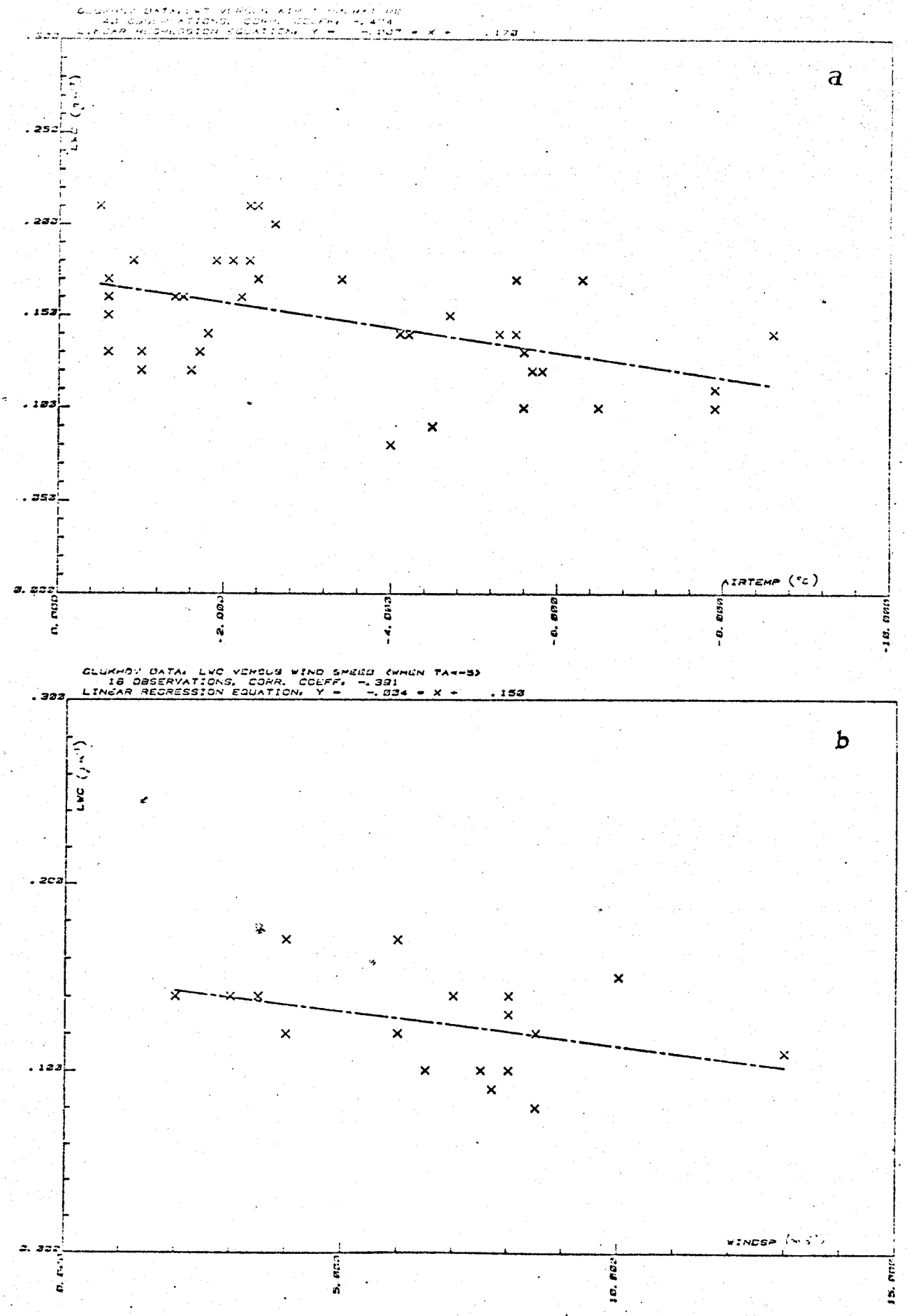

Fig.6. Liquid water content in air versus air temperature (a) and wind speed (b) on a high mast (data from Glukhov, 1971).

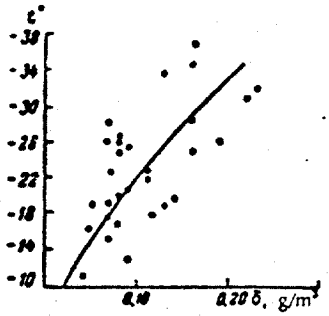

Liquid-water content of evaporation fogs (Angara) at various temperatures (after G. M. Bashkirova and P. N. Krasikov).

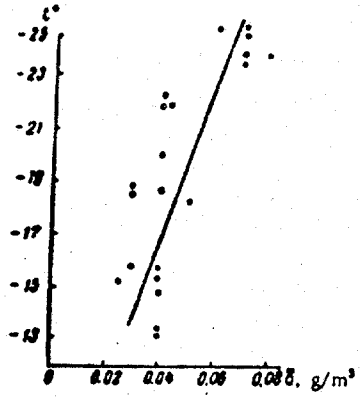

Liquid-water content of evaporation fogs (Kola Bay) at various temperatures (after G. M. Bashkirova and P. N. Krasikov).

Fig.7. (from Matveev, 1967)

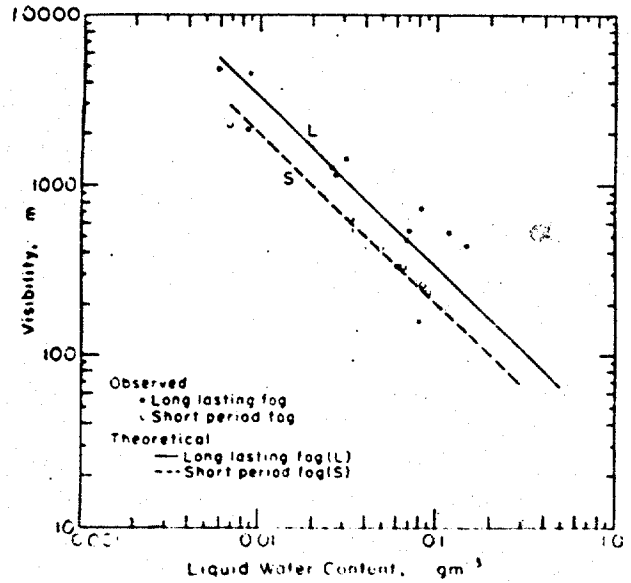

Liquid water content as a function of visibility in Barrow fogs. The lines L and S are calculated by Mie theory for the mean size distributions of long-lasting and short-period fogs, respectively.

Fig.8. (from Kumai, 1973)

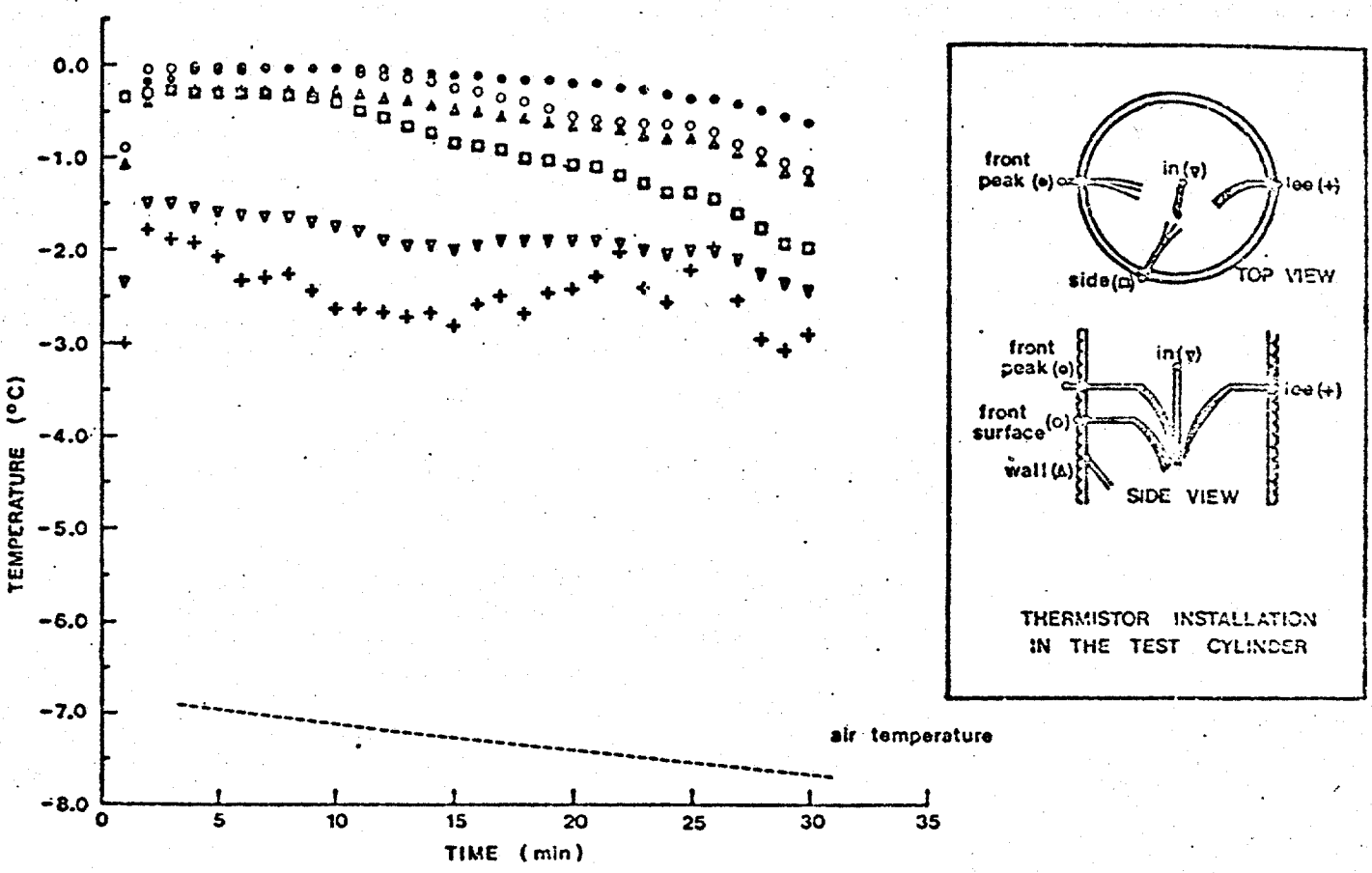

Fig.9. TIME SERIES OF TEMPERATURES IN A TEST CYLINDER. THE TEMPERATURE AT THE FRONT SURFACE ON THE STAGNATION LINE STAYS NEAR THE FREEZING TEMPERATURE UNTIL THE ICE LAYER IS A FEW MILLIMETERS THICK, AFTER WHICH IT SINKS GRADUALLY. THE FRONT PEAK TEMPERATURE INCREASES TO THE FREEZING TEMPERATURE WHEN THE ICE LAYER REACHES THE TERMISTOR AND DECREASES AFTERWARDS GRADUALLY. THE WALL AND INSIDE TEMPERATURES CHARACTERIZE THE HEAT FLOWS THROUGH THE CYLINDER AND AIR INSIDE. ALL THE TEMPERATURES CONVERGE WHEN THE ICE LAYER GROWS VERY THICK. (from Launiainen et al., 1982)

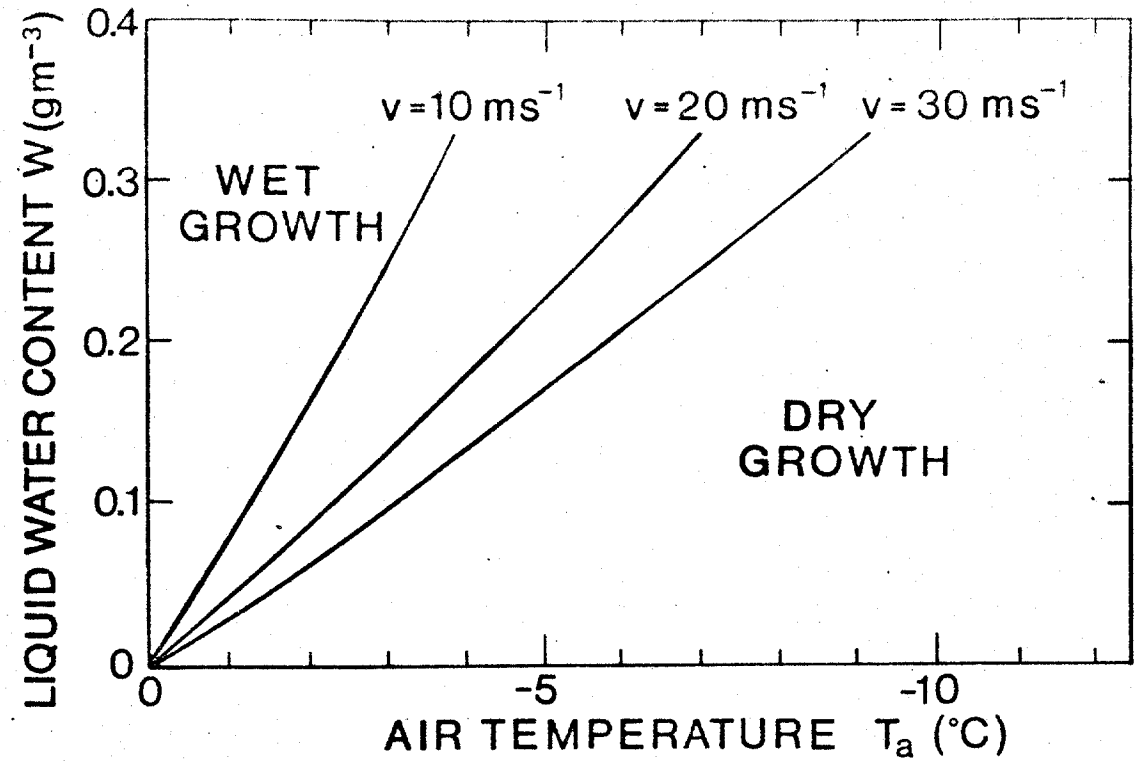

Fig.10. The lines separating the dry-growth and wet-growth processes on a 5cm diameter cylinder (stagnation line). The droplet diameter is 30 μm. (from Makkonen, 1981)

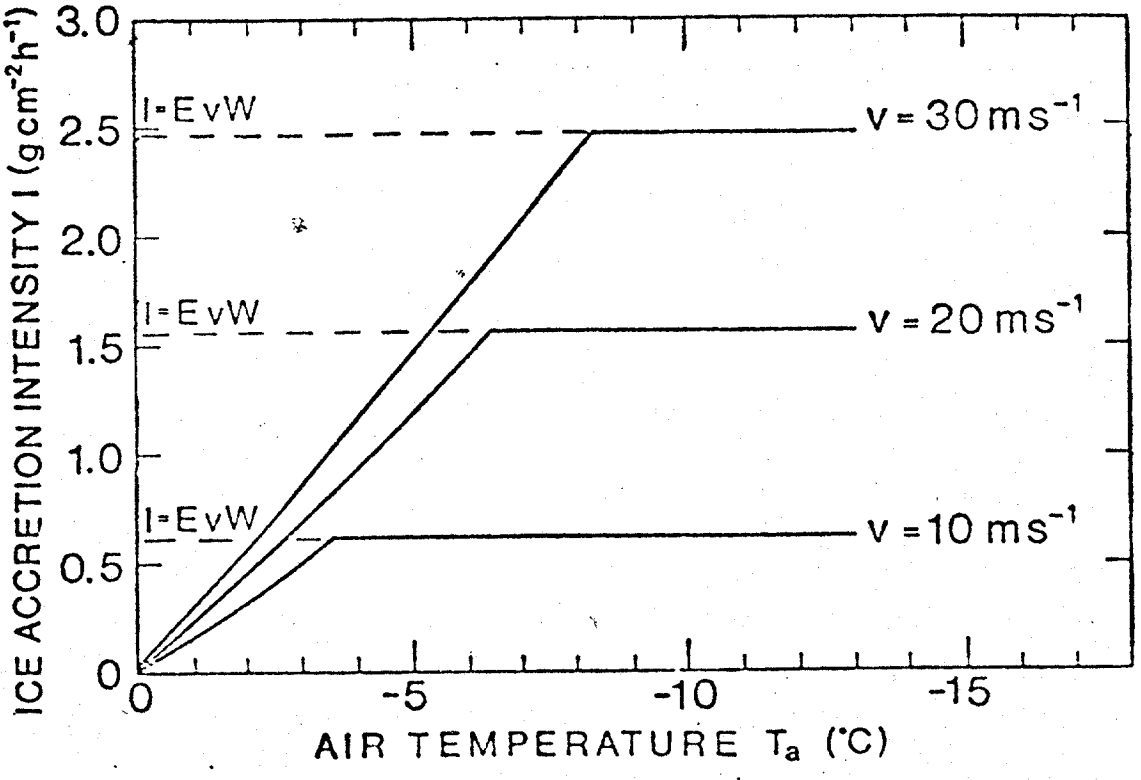

Fig.11. Ice accretion intensity in the stagnation region of a 5 cm diameter cylinder as a function of the air temperature. w = 0.3 g m^{-3} and d = 30 μm.

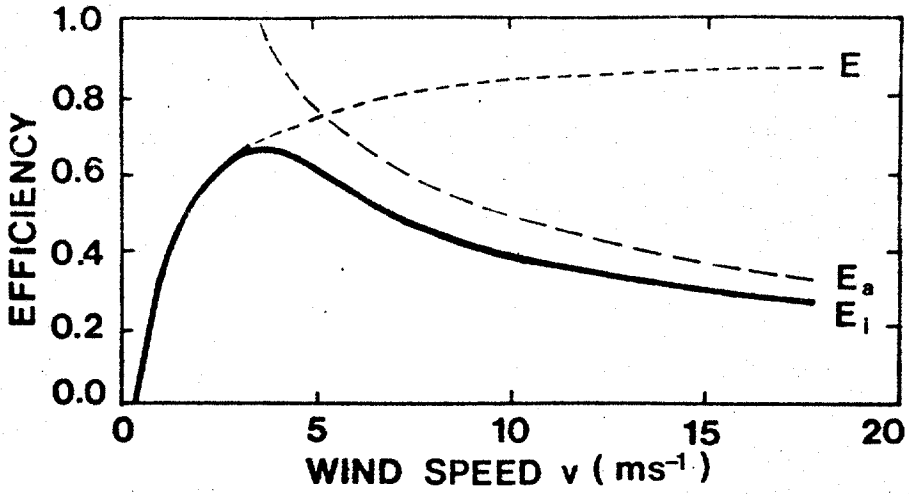

Fig.12. Icing efficiency E_i, accretion efficiency E_a and collection efficiency E on the stagnation line of a 15 mm diameter cylinder as a function of the wind speed. $t_a = -1^{\circ}C$, $w = 0.2\ g\ m^{-3}$ and d = 30 m. (from Makkonen, 1981)

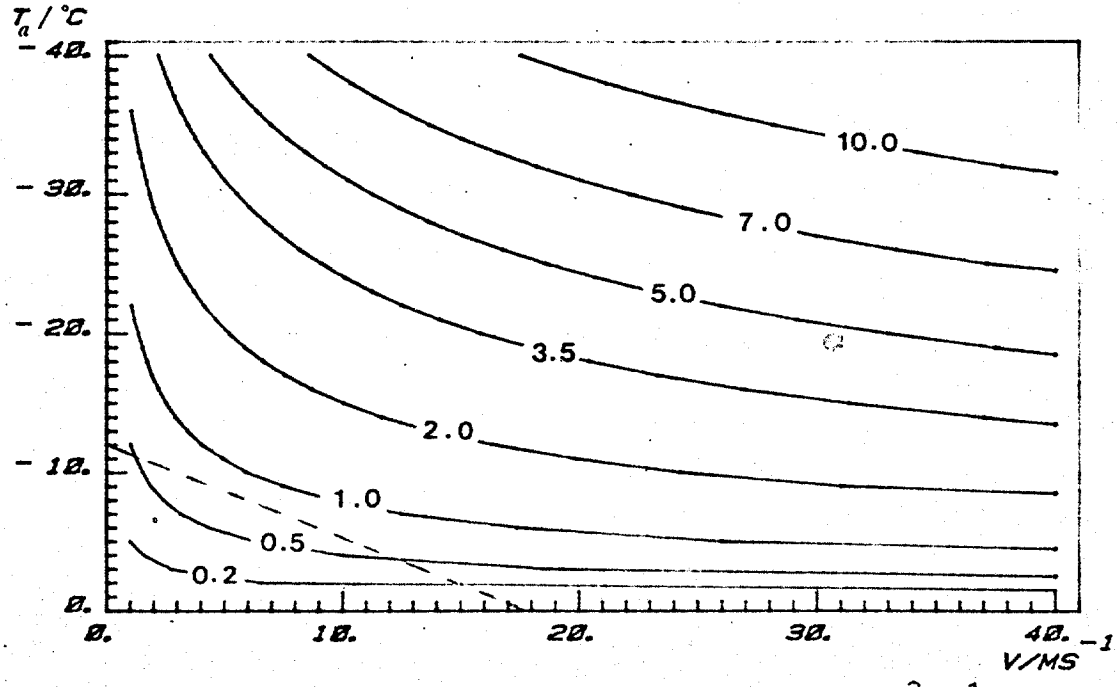

Fig.13. Theoretical icing intensity in g $cm^{-2}h^{-1}$ as as a function of the wind speed and air temperature. The calculation is made for a 5 cm diameter cylinder supposing unlimited liquid water content (wet growth for all combinations of v and t_a), but neglecting the effect of run-off water on the heat balance. (from Makkonen, 1980). The dotted line represents Eq.(21),

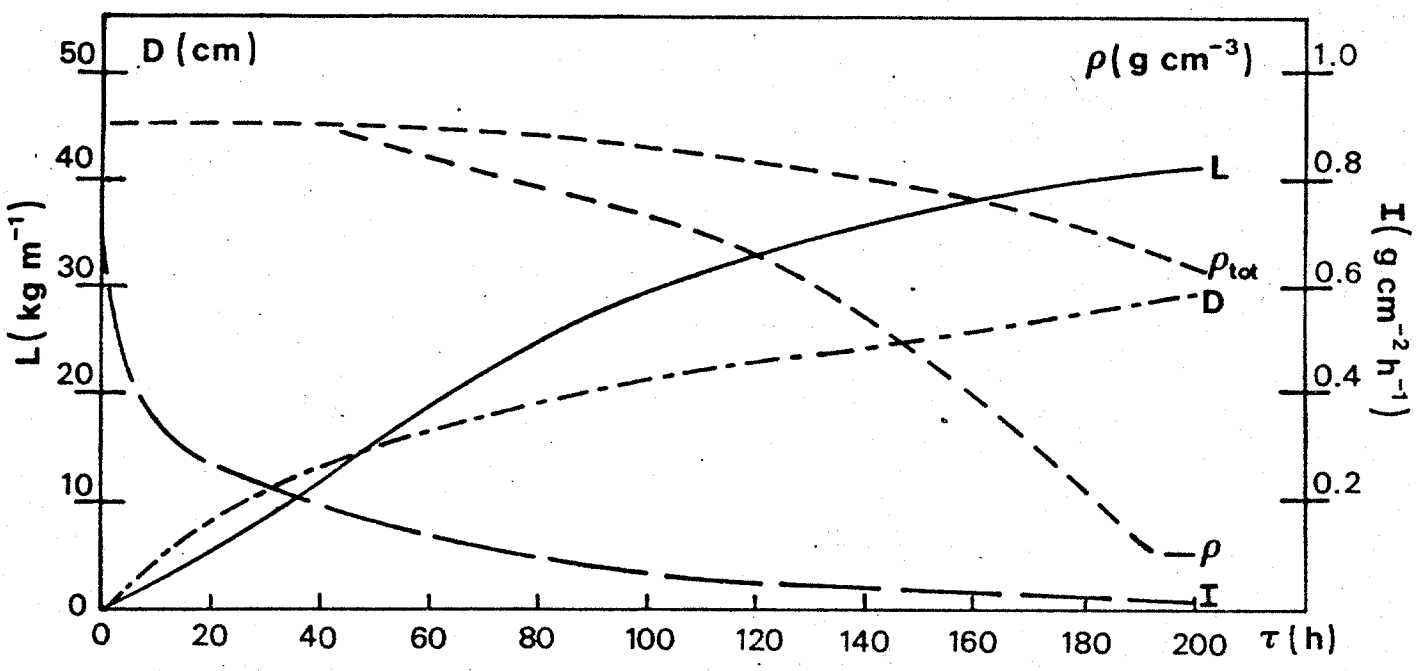

Fig.14. Numerical simulation of ice accretion on a 1 cm diameter wire. The simulated quantities are ice load L, ice deposit diameter D, icing intensity I, density of the accreting ice ρ and the total deposit density ρ_{tot}. Wind speed is 15 ms^{-1}, air temperature -2 ^{o}C, liquid water content 0.3 gm^{-3} and droplet diameter 30 μm. (from Makkonen, 1982).

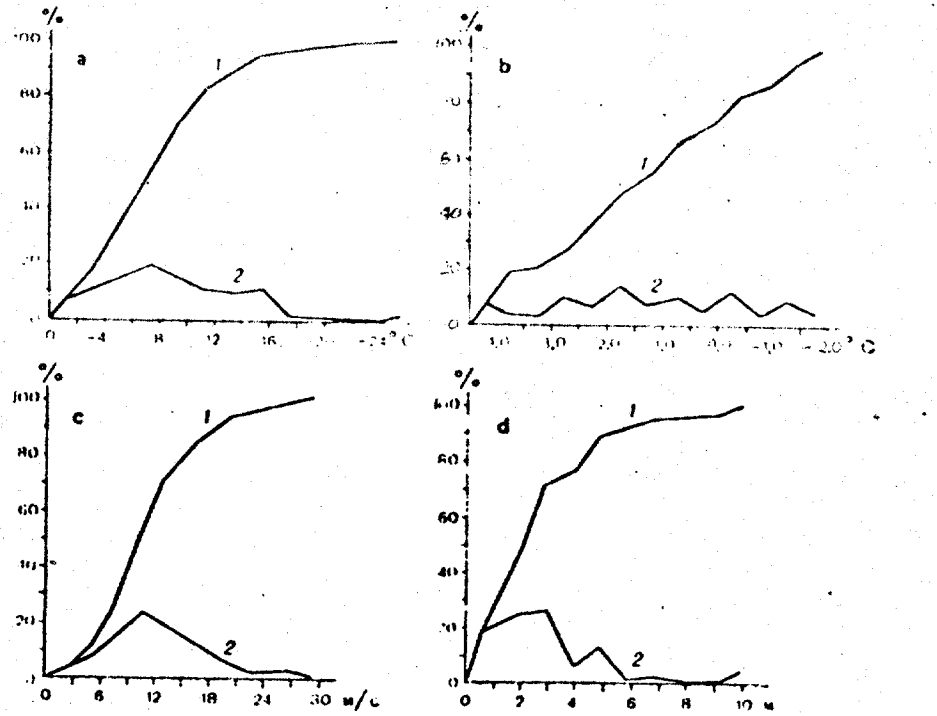

Total (1) and differential (2) frequency of hydrometeorological elements during the icing of ships.

Legend: a–air temperature
b–water temperature
c–wind speed
d–wave height

Fig.15. (from Panov, 1978)

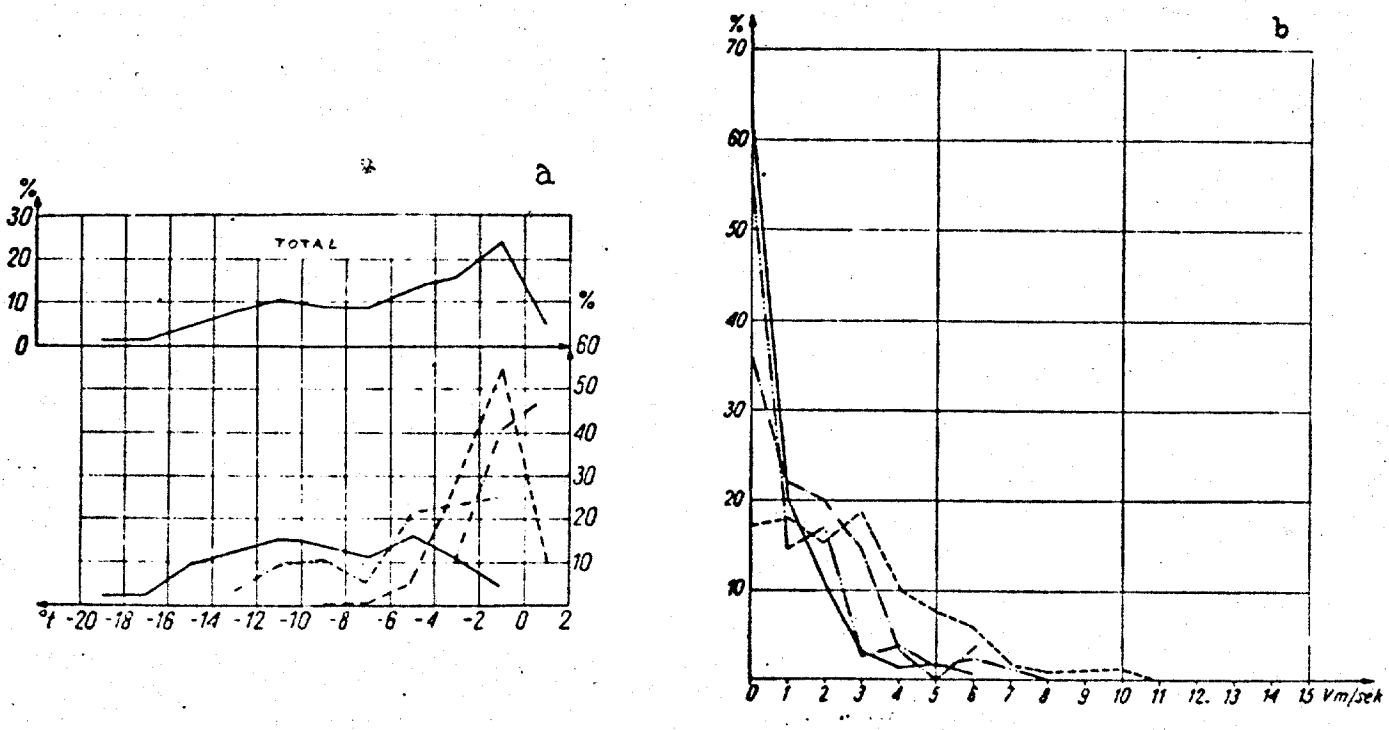

Fig.16. Frequency of atmospheric ice accretion related to the air temperature (a) and wind speed (b). —— soft rime, -·-·- hard rime, --- glaze, -···-·- wet snow. (from Sadowski, 1965)

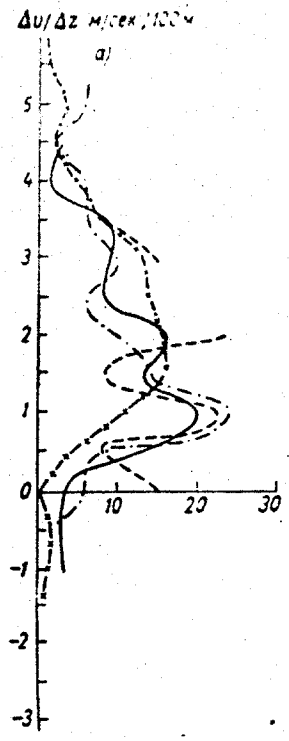

Fig.17. Frequency (%) of atmospheric ice accretion related to the wind shear in the lowest 300 m layer of the boundary layer. -x-x- glaze, —— crystalline rime, --- grain rime, -·-·- mixture. (from Dranevič, 1971)

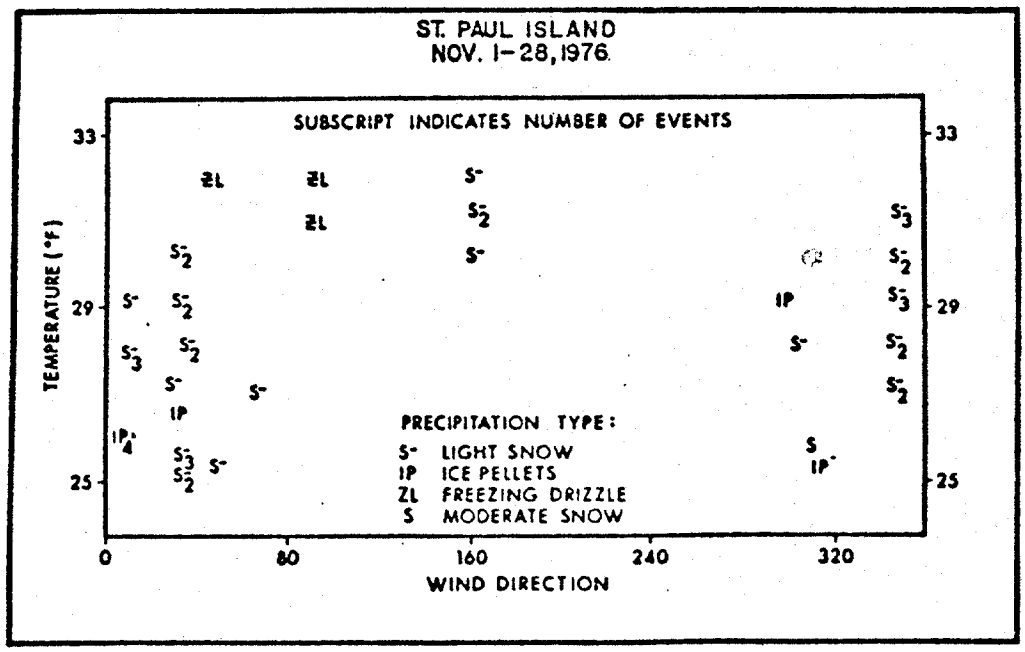

Fig.18. St. Paul Island icing events related to wind direction. (from McLeod, 1981)

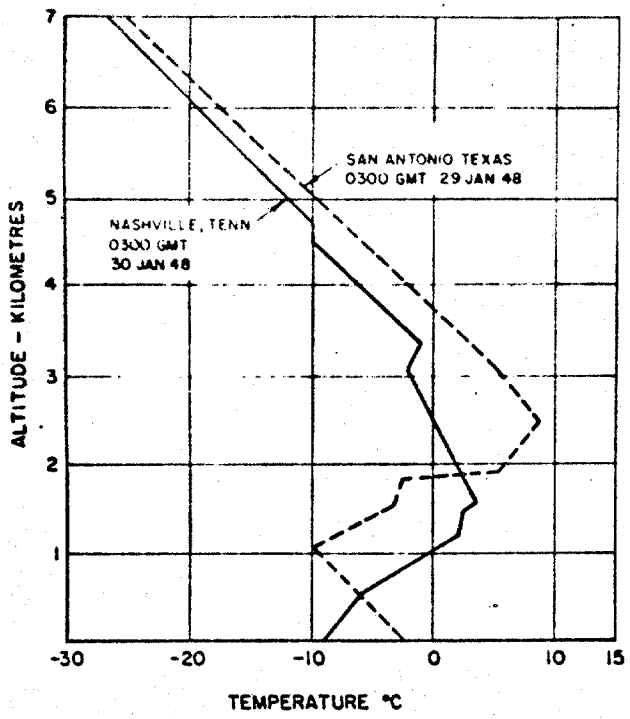

Typical temperature profiles during the occurrence of supercooled precipitation at the ground.

Fig. 19. (from Stallabrass, 1982)

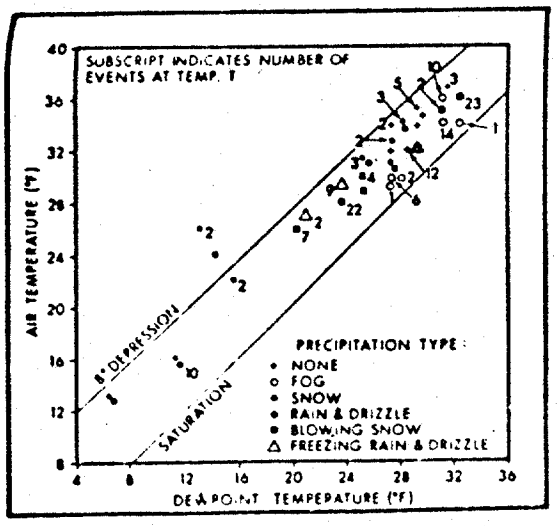

- Rosemount events, Dec. 1, 1976 - Jan. 15, 1977.

Fig.20. Icing events related to air temperature and dew-point spread (^{o}F). (from McLeod, 1977)

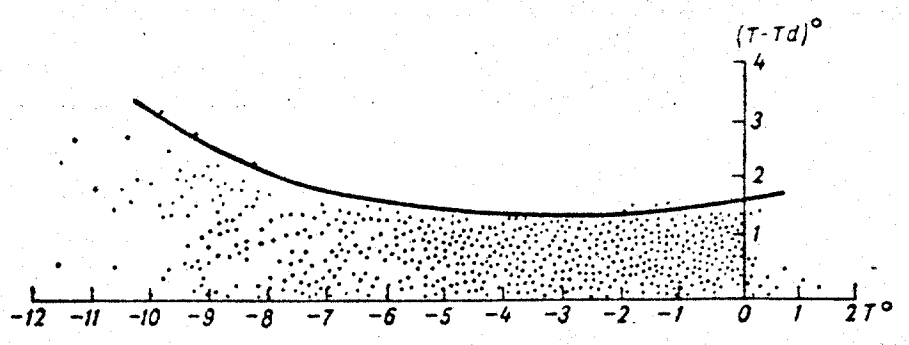

Fig.21. Glaze events related to air temperature and dew-point spread (°C). (from Dranevič, 1971)

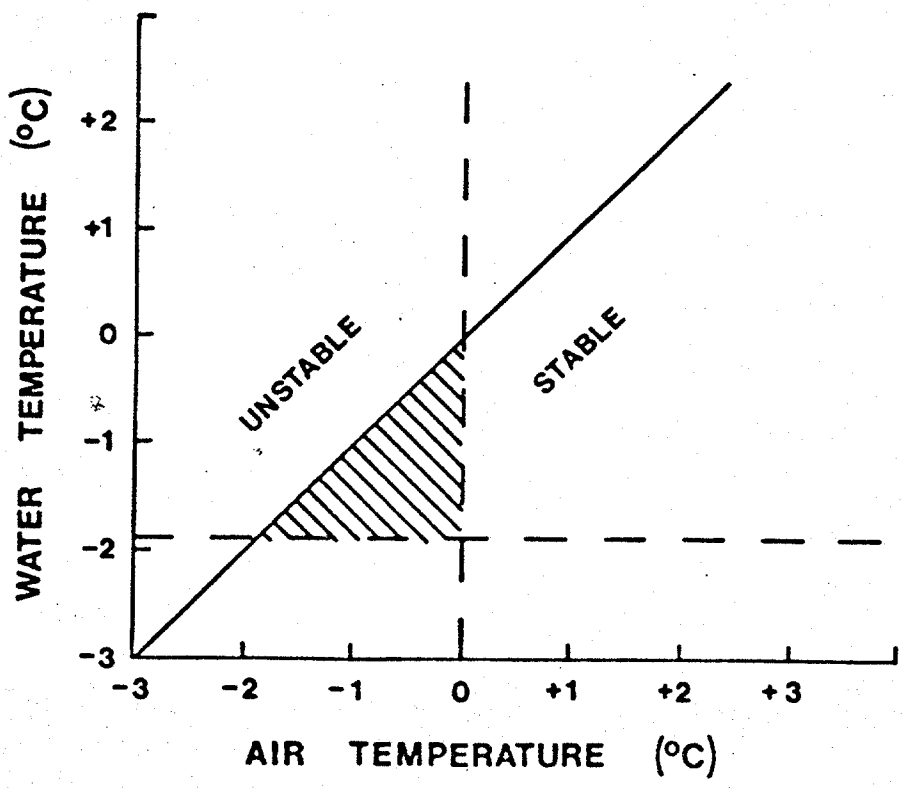

Fig.22. The regime of the existece of supercooled advection fog over the sea (dashed area). The solid line represents thermally neutral conditions, the horizontal dotted line the limiting water temperature and the vertical dotted line the limiting air temperature.

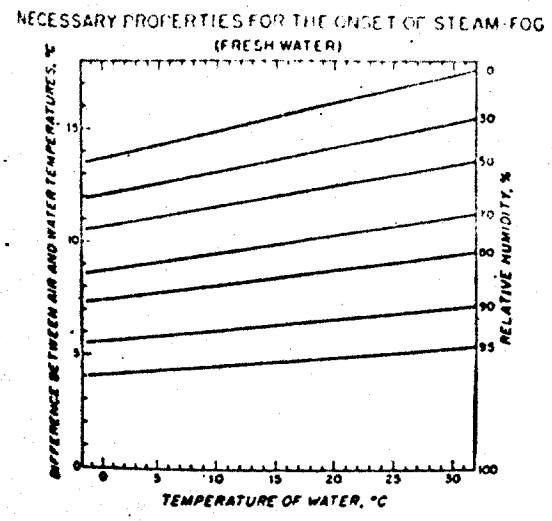

Necessary properties of air for the steaming of fresh water. The relative humidity is measured near the surface in the cold air.

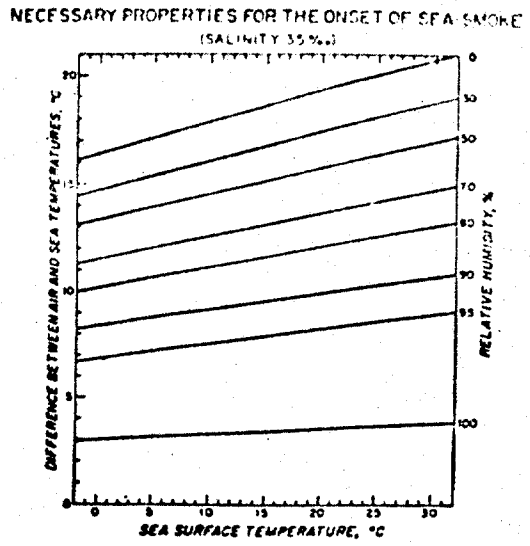

Necessary properties of air for the steaming of saline water (salinity 35‰). The relative humidity is measured near the surface in the cold air.

Fig.23. (from Saunders, 1964)

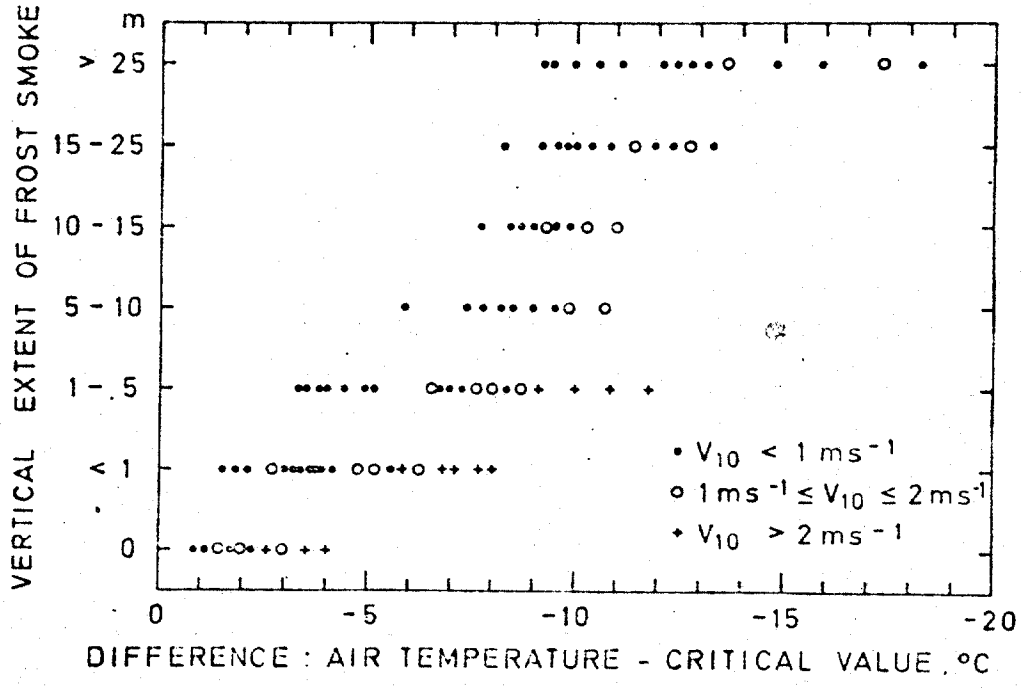

Fig.24. Vertical extent of evaporation fog in relation to the difference between air temperature at 2 m height and the critical temperature given by the theory by Saunders (1964). (from Utaaker, 1979)

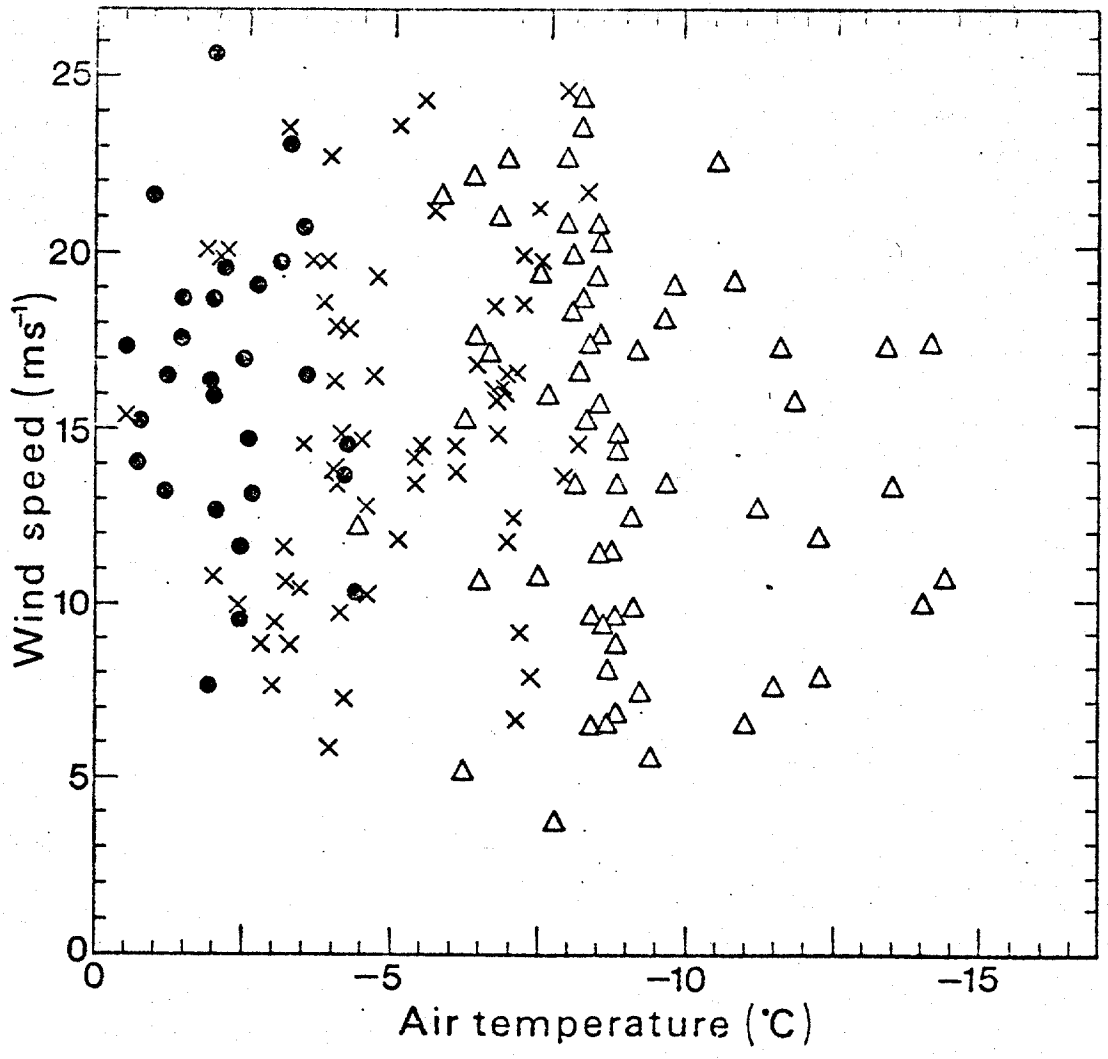

Fig.25. Atmospheric icing events in relation to air temperature and wind speed. o : glaze; x : hard rime; Δ : soft rime. (data from Rink, 1938)

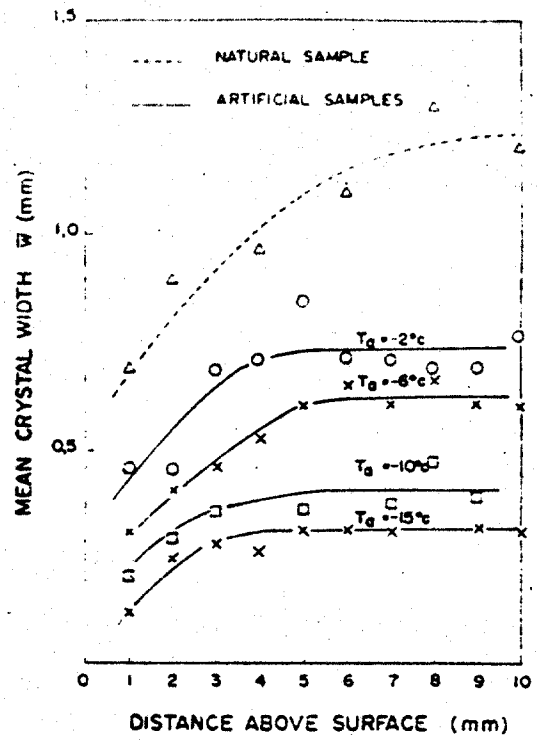

VARIATION OF MEAN WIDTH OF ICE CRYSTAL WITH THE AMBIENT TEMPERATURE AND THE RADIAL DISTANCE ABOVE THE CONDUCTOR SURFACE

Fig.26. (from Laforte et al., 1982 a)

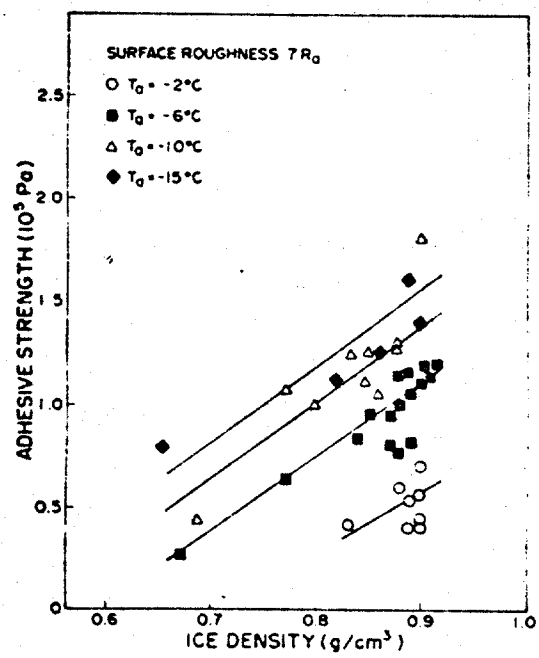

ADHESIVE STRENGTH OF ICE VERSUS DENSITY AND AIR TEMPERATURE

Fig.27. (from Laforte et al., 1982 a)

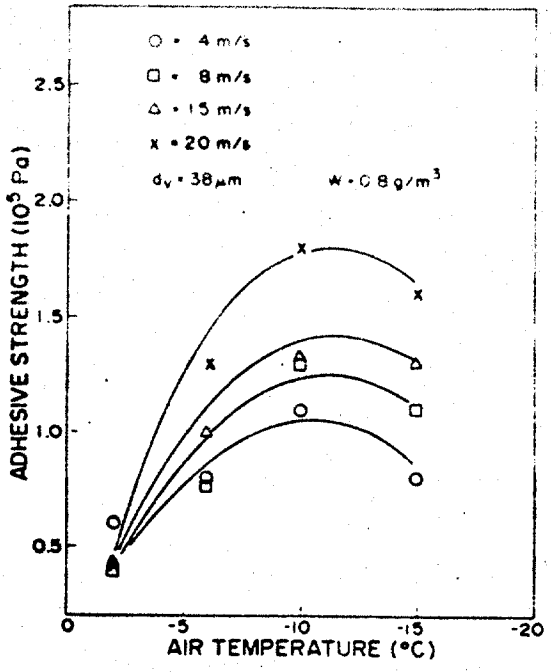

ADHESIVE STRENGTH OF ICE ACCRETION GROWN AT DIFFERENT AMBIENT TEMPERATURE AND AIR VELOCITIES

Fig.28. (from Laforte et al., 1982 a)

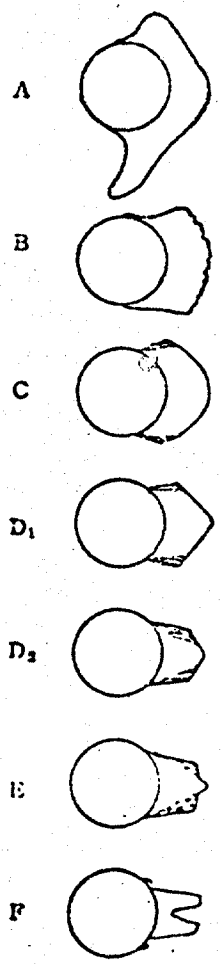

Fig.29. Typical ice profiles on cylinders (from Imai, 1953)

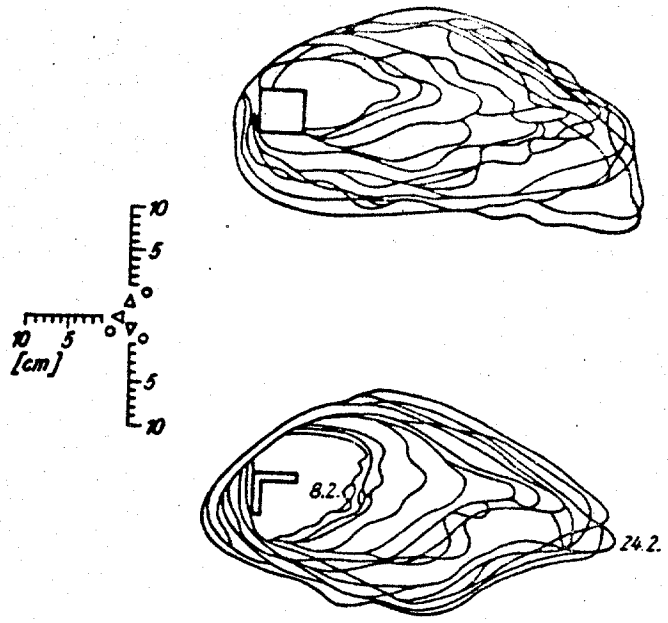

Fig.30. Horizontal (above) and vertical (below) cross section of an ice deposit formed by droplet accretion. (from Kolbig, 1967)

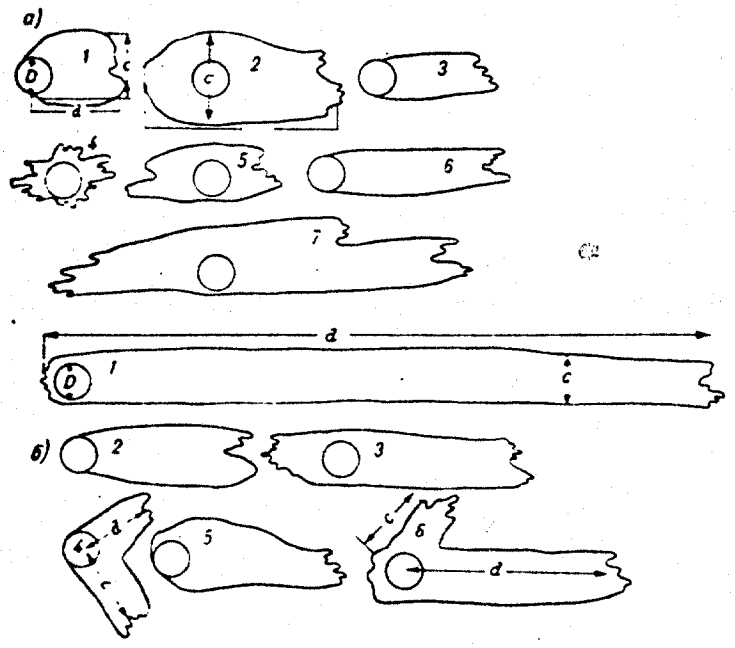

Fig.31. Observed ice profiles (from Klinov and Boikov, 1974)

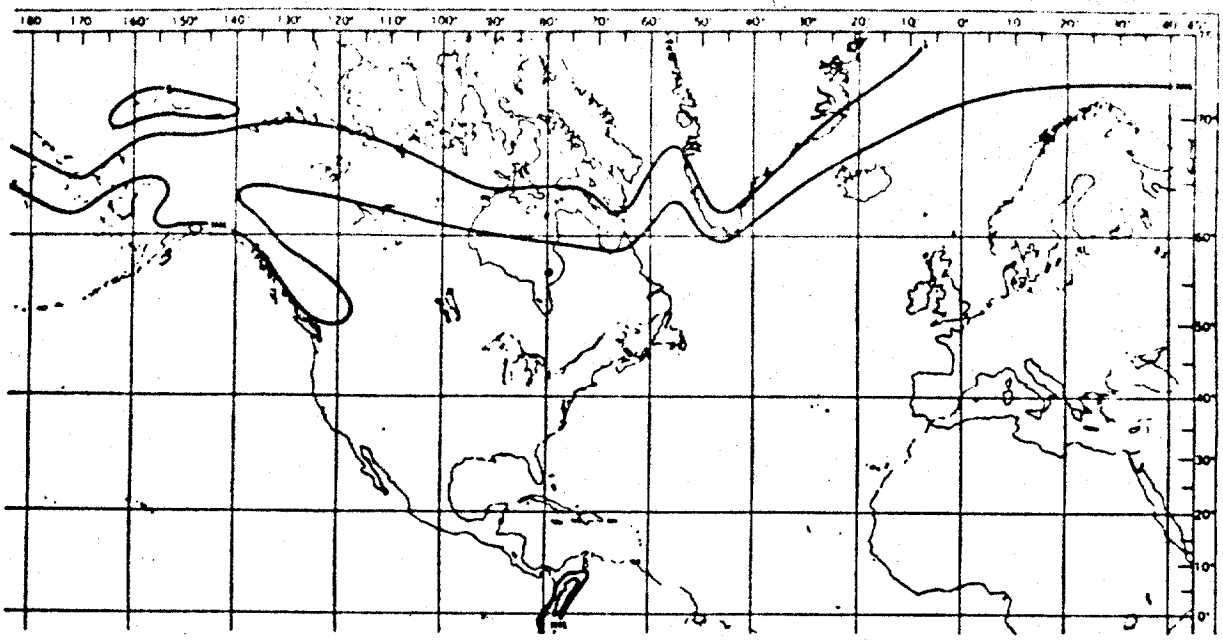

a. September.

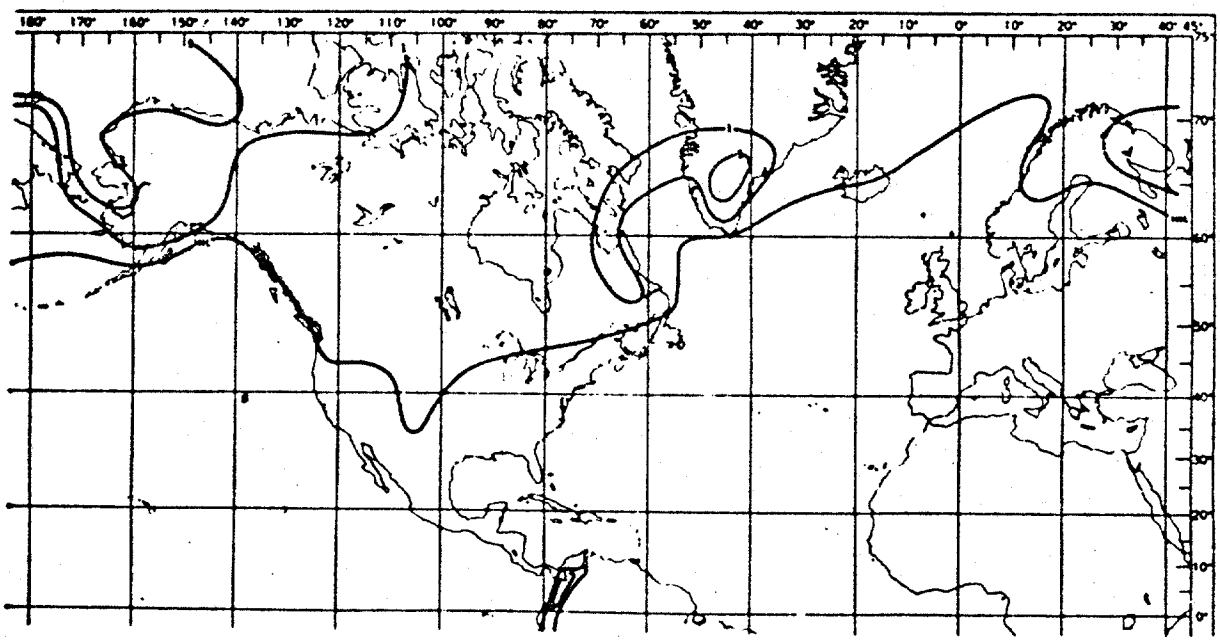

b. October.

Fig. 32. Probability of occurence of supercooled fog (%) by month according to Guttman (1971). (from Minsk, 1977)

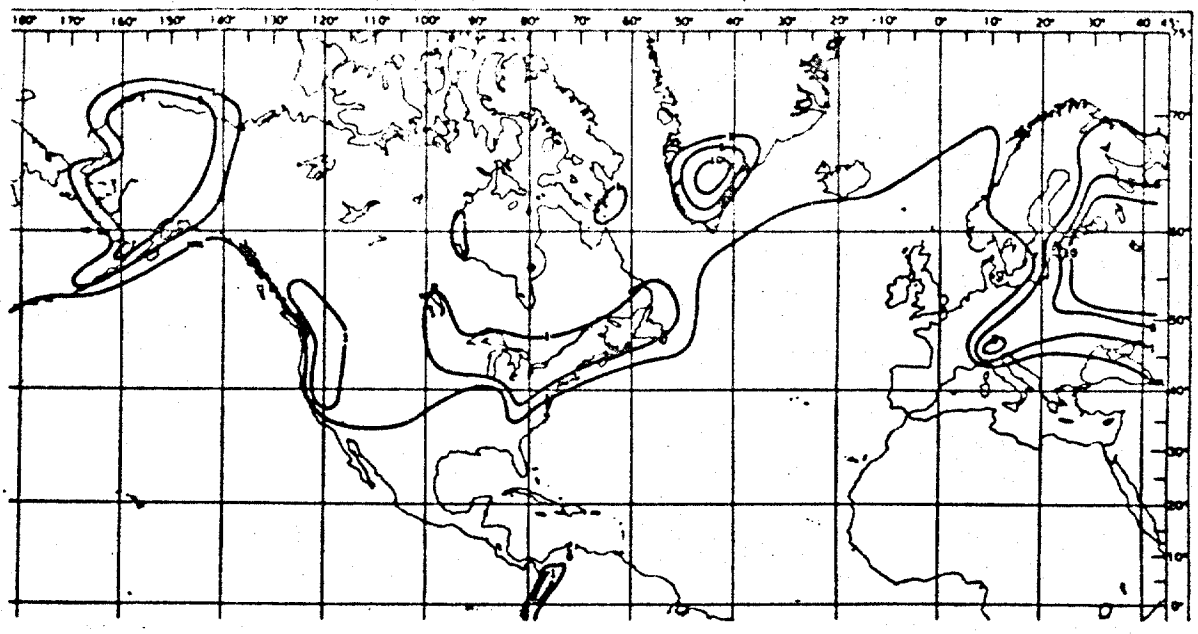

c. November.

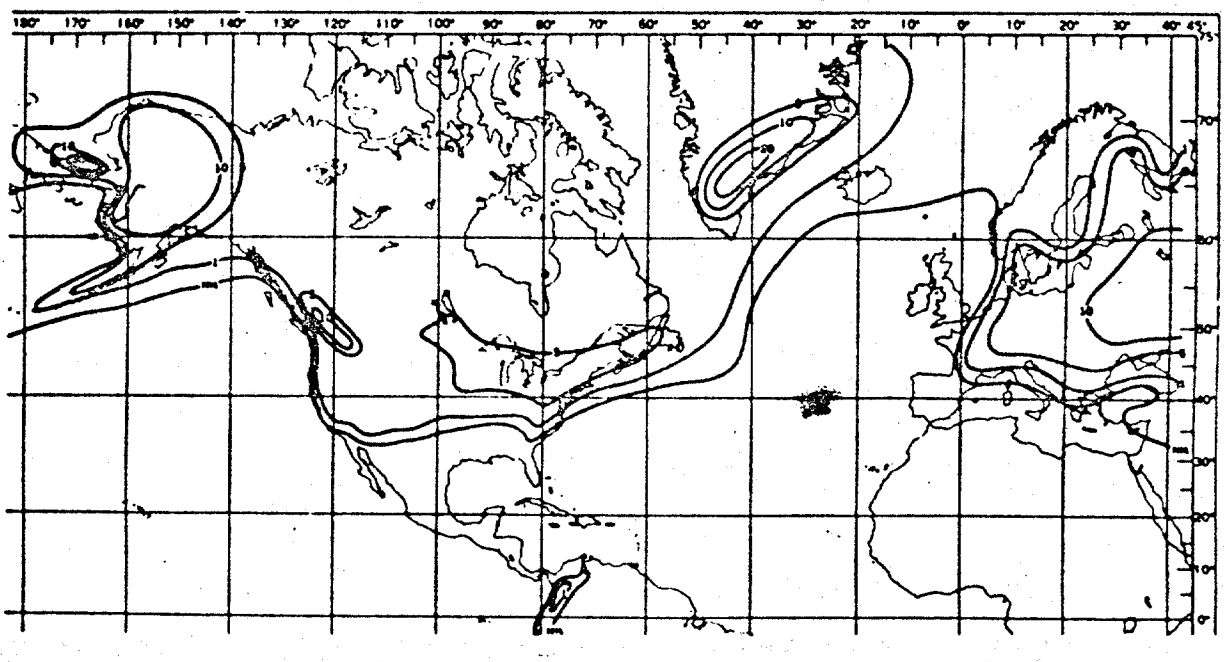

d. December.

Fig. 32. (continued)

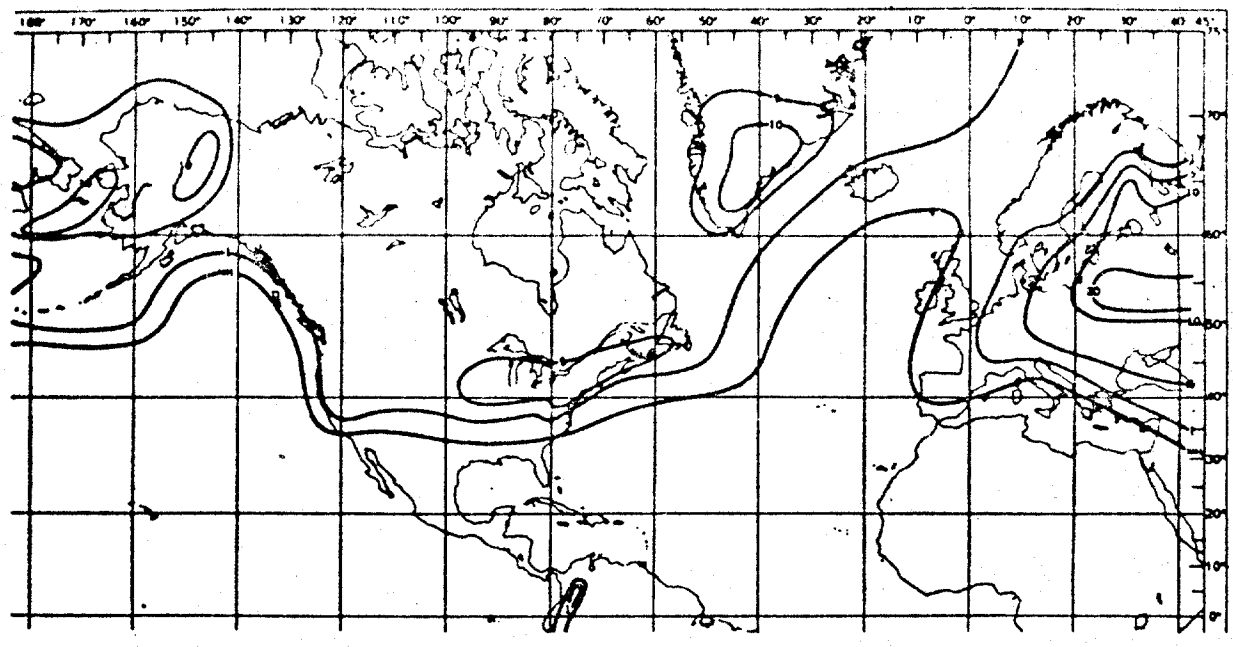

e. January.

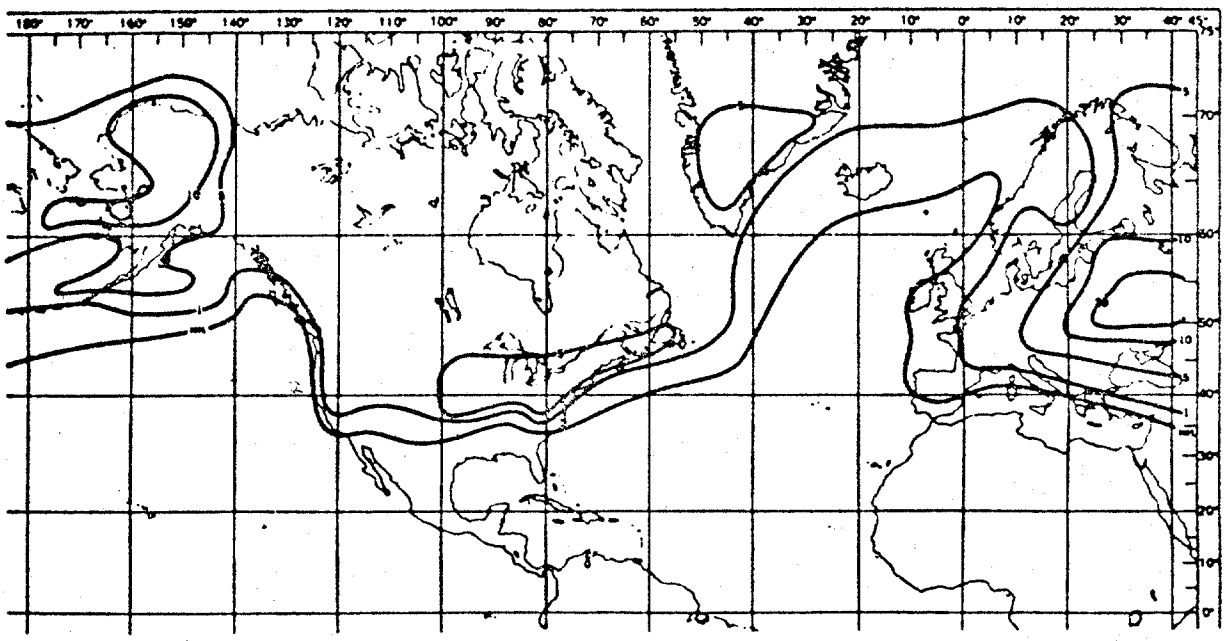

f. February.

Fig. 32. (continued)

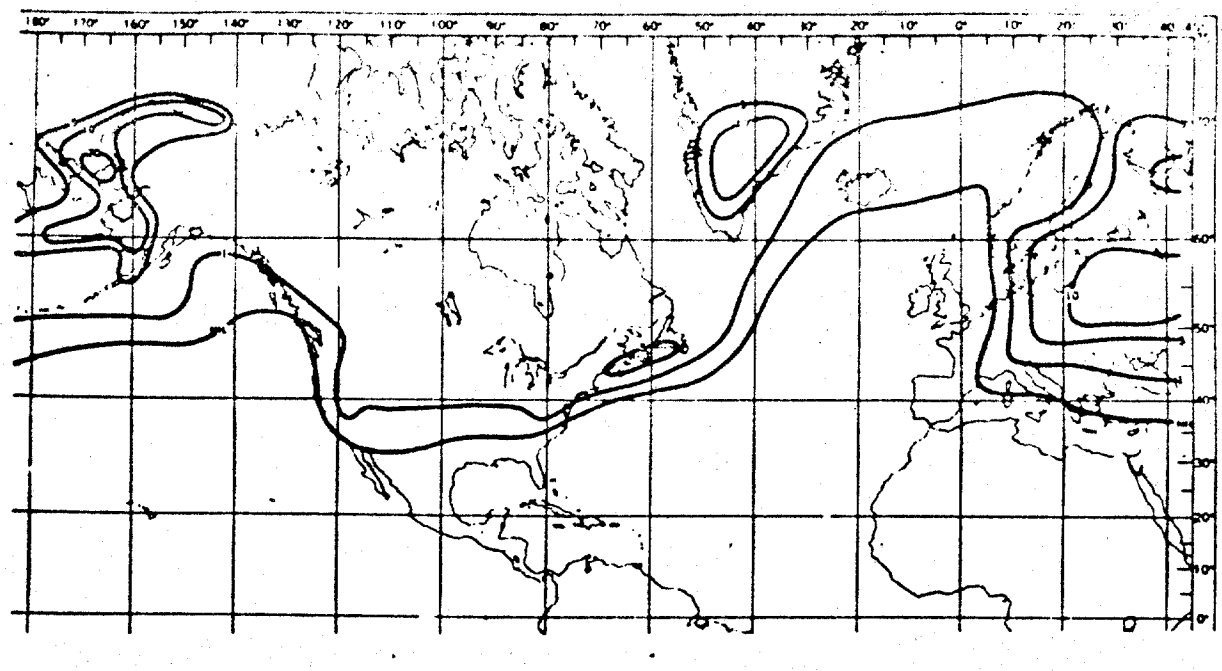

g. March.

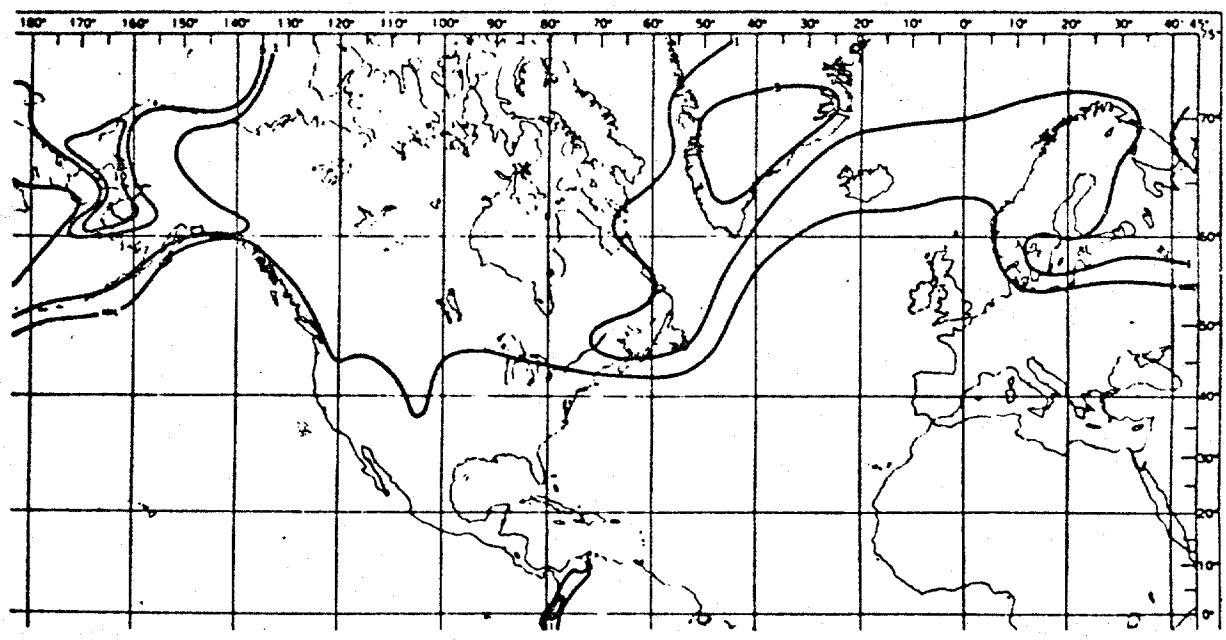

h. April.

Fig. 32. (continued)

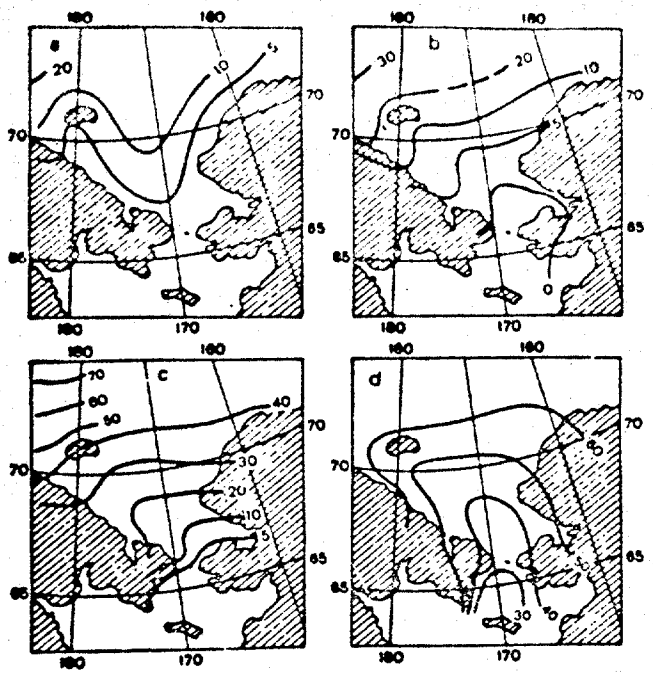

Fig.33. Probablity (%) of the conditions $t_a \leq 0^{o}C$ and $v \leq 7\ ms^{-1}$ in the Chukchki Sea according to Kolosova (1972). (from Minsk, 1977). a-July, b-August, c- September, d-October.

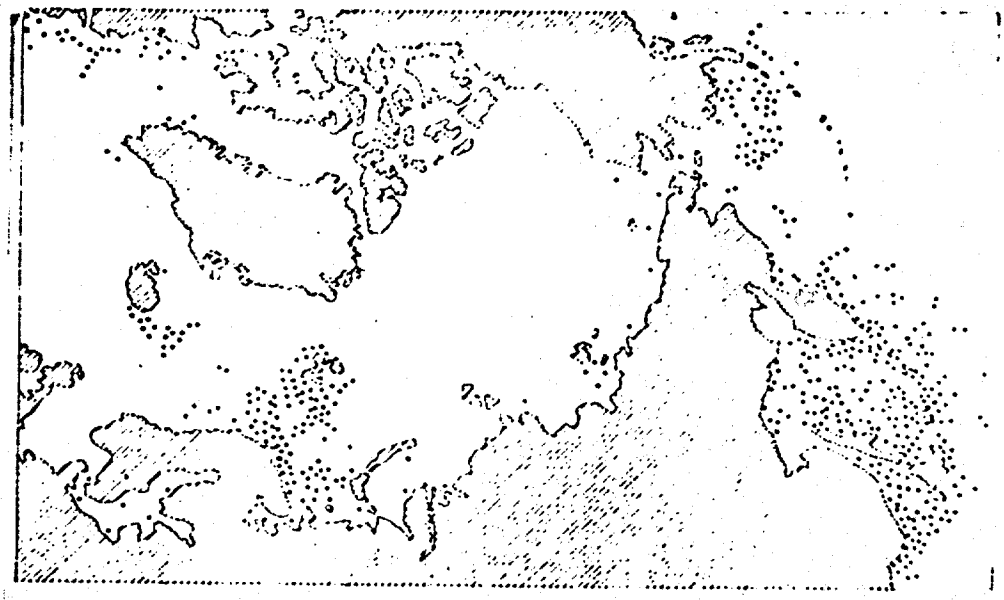

Fig.34. Regions where ship icing was observed in the Soviet data according to Panov (1978).

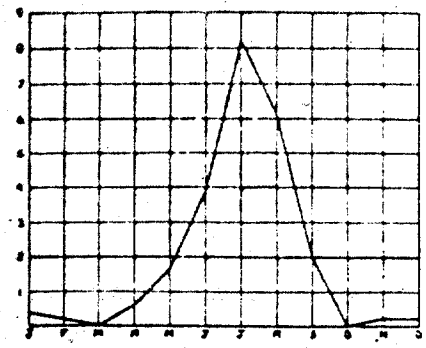

Average number of days with fog in the different months on the coast Nordkapp—Vardø.

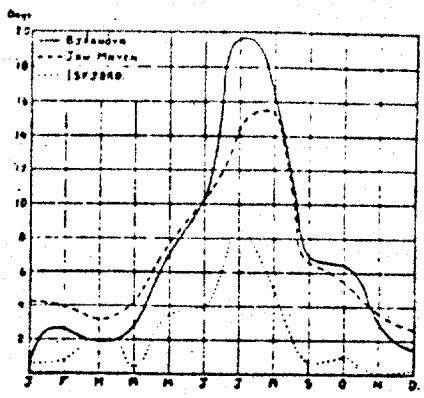

Average number of days with fog in the different months at 3 Norwegian Arctic stations.

Fig.35. (from Spinnangr, 1949)

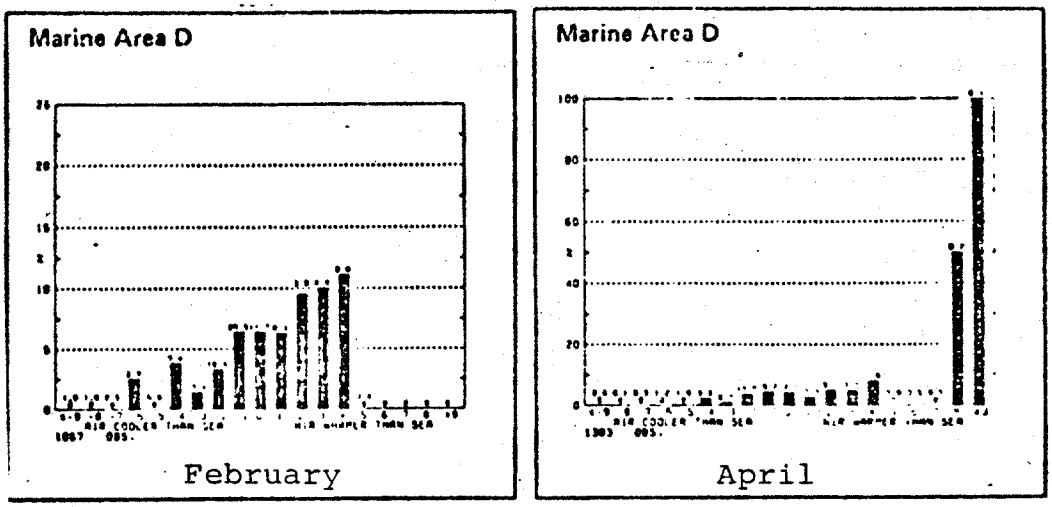

Middleton Island, Gulf of Alaska

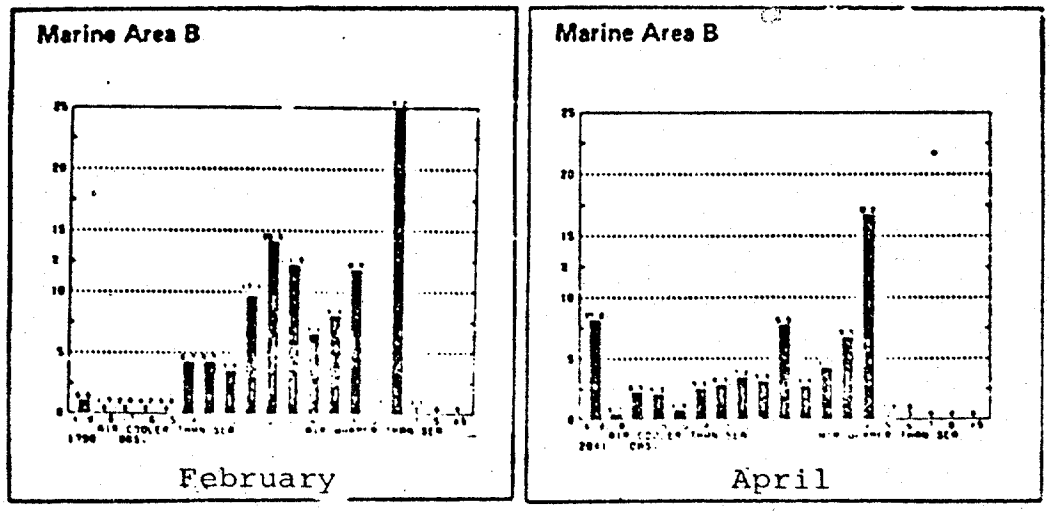

St. Paul Island, The Bering Sea

Fig.36. Distribution of fog events in relation to air-sea temperature difference in arctic marine weather

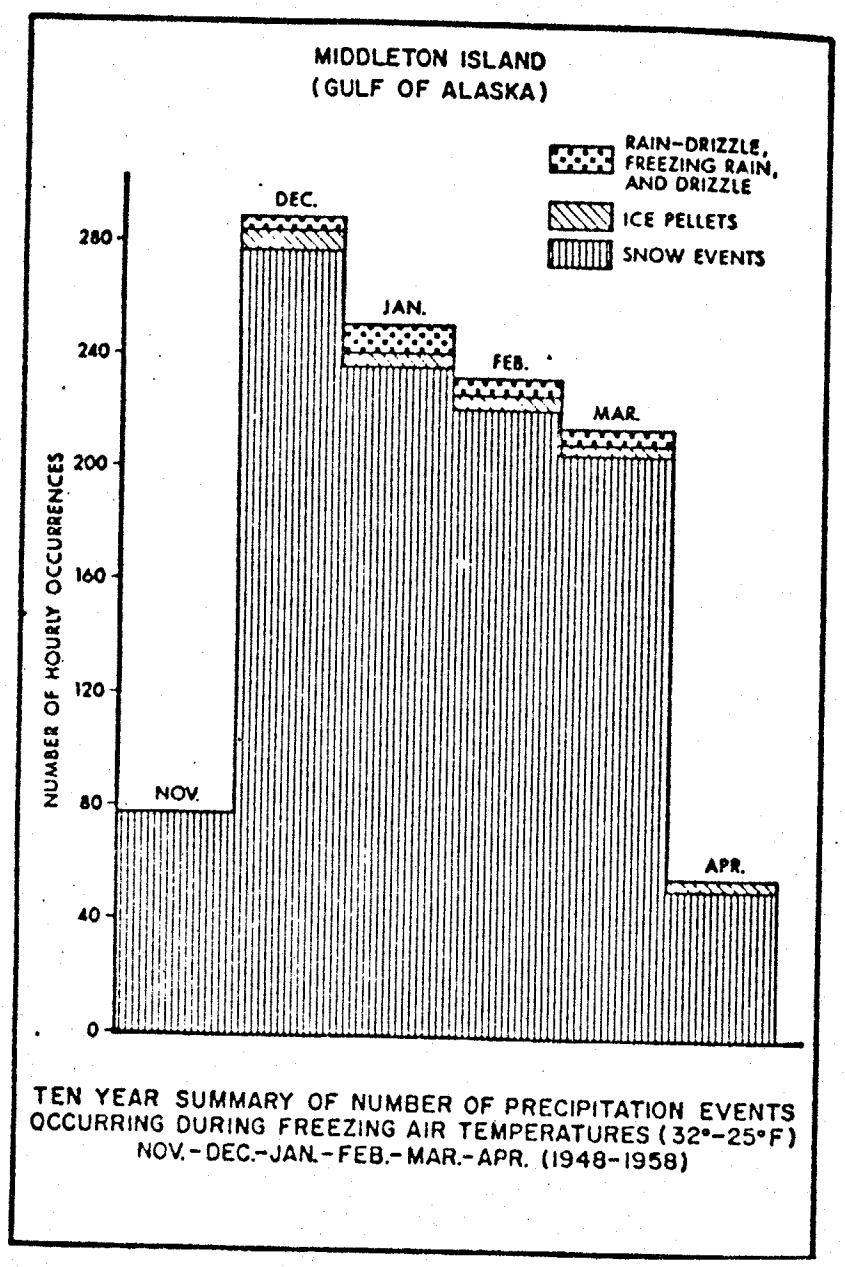

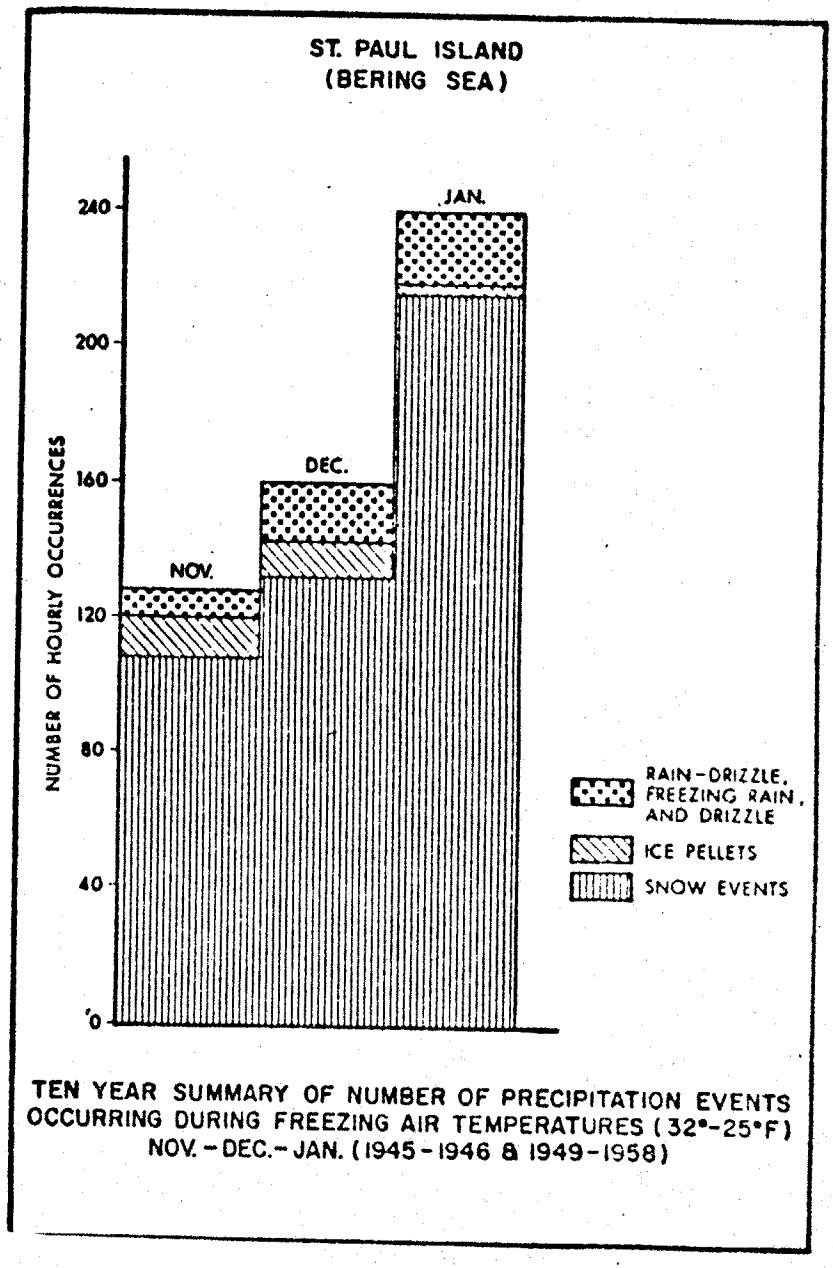

Fig. 37. (from McLeod, 1981)

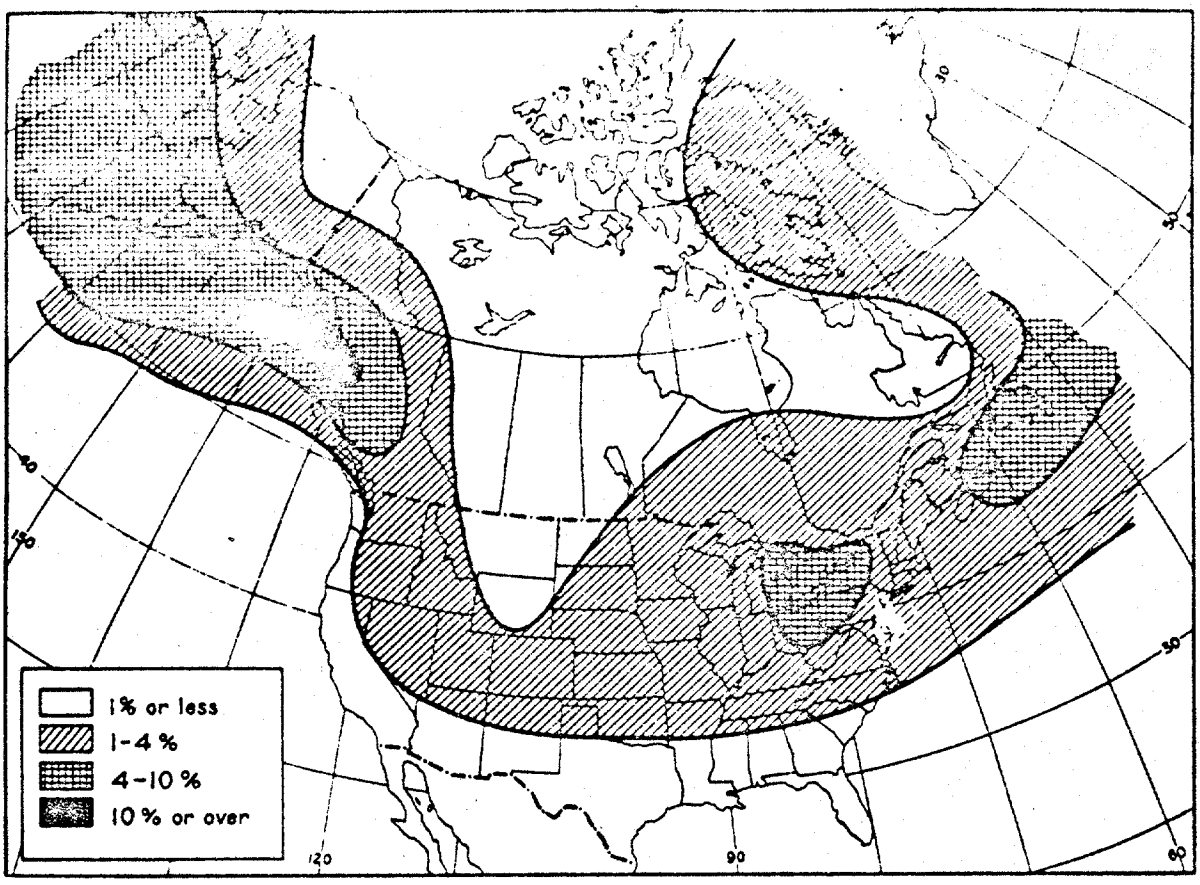

Mean annual percentage of hourly weather observations with freezing rain, North America. Based on a map prepared in 1943 by the Weather Information Service of the U.S. Army Air Forces (Bennett 1959).

Fig.38. (from Minsk, 1980)

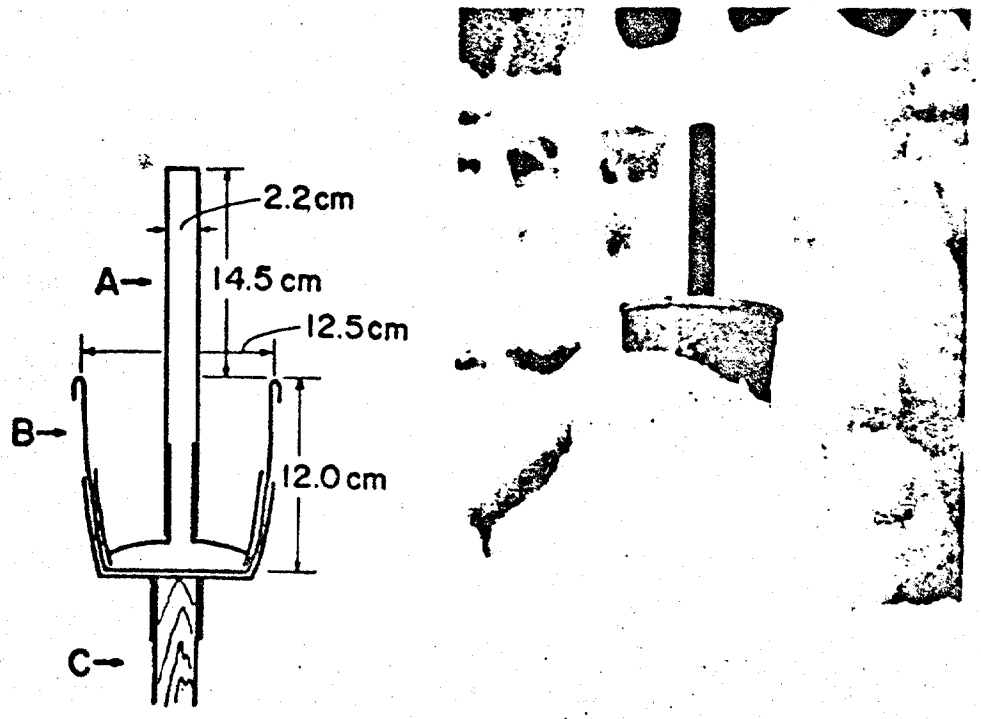

Fig.39. Icing gauge of Tabata et al. (1967)

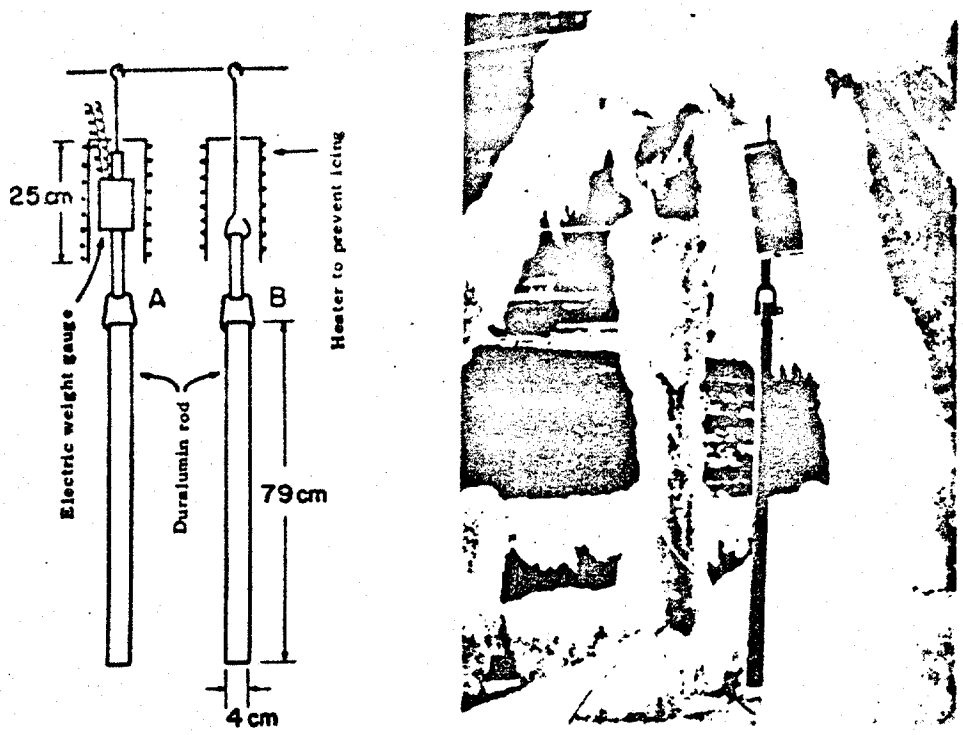

Fig.40. Icing rod of Tabata et al. (1967).

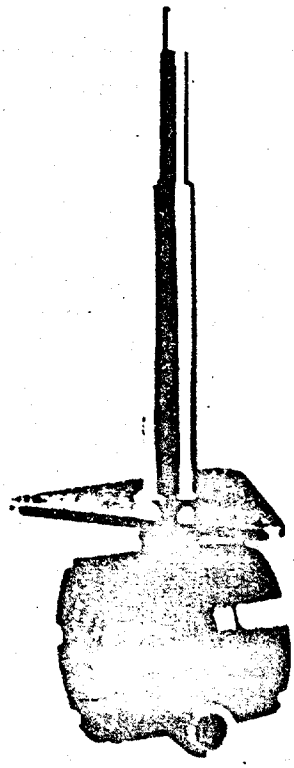

The Rosemount Model 872DC Ice Detector. The sensing probe sits atop the 25.4 cm (10 in.) strut. During de-icing, the sensor and the top 7.6 cm (3 in.) of the strut are heated.

Fig.41. (from Tattelman, 1982)

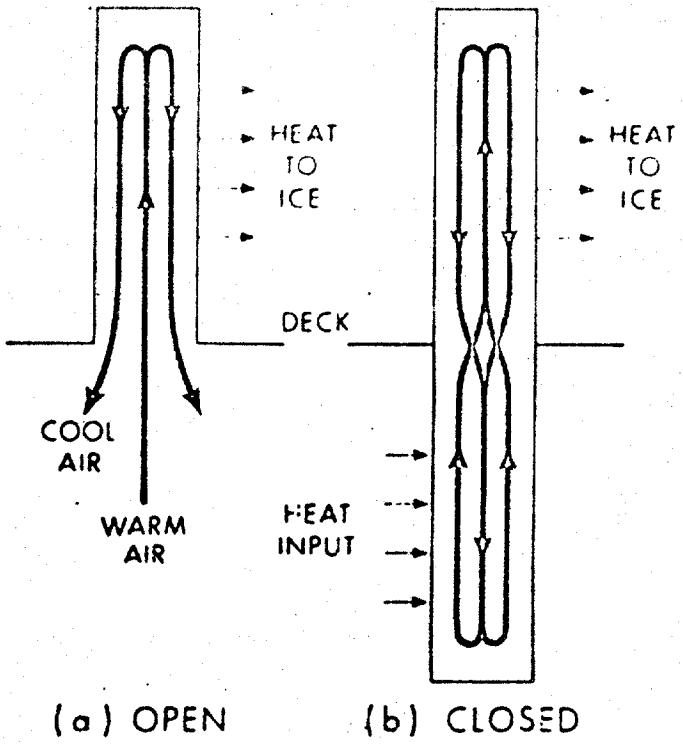

Fig.42. The working principle of an open (a) and a closed (b) termsyphon. (from Lock, 1972)

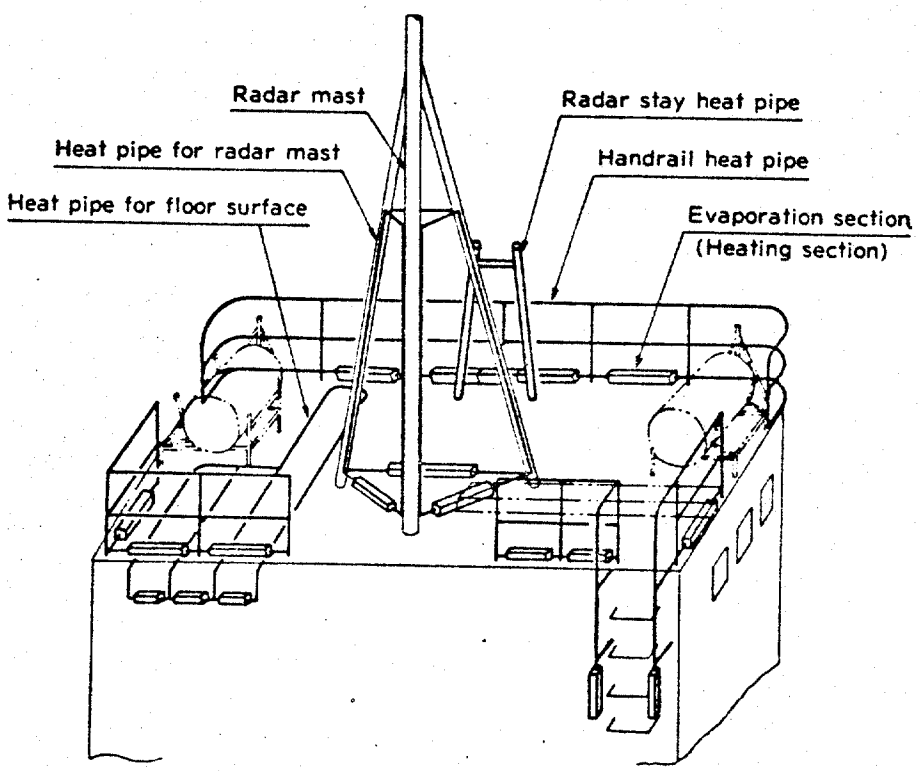

Fig.43. Schematic presentation of a heat pipe de-icing system installed on a ship. (from Anon, 1981)

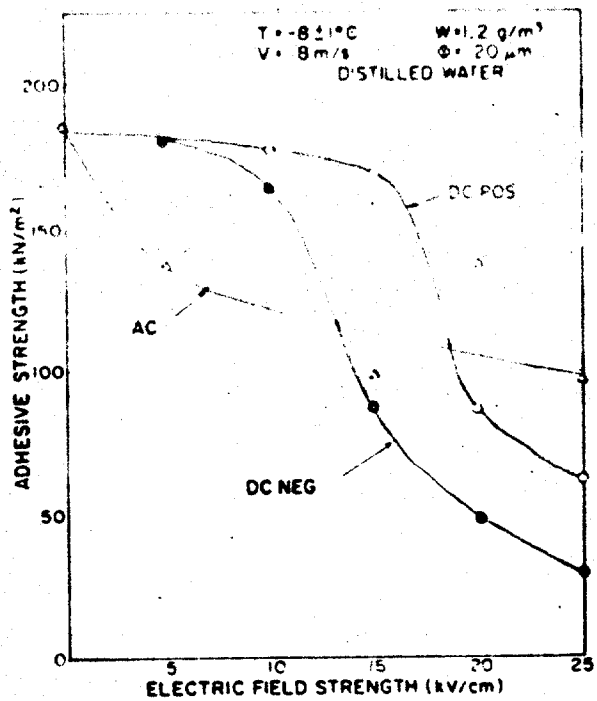

. Adhesive strength of ice versus electric field strength.

Fig.44. (from Phan and Laforte, 1981)

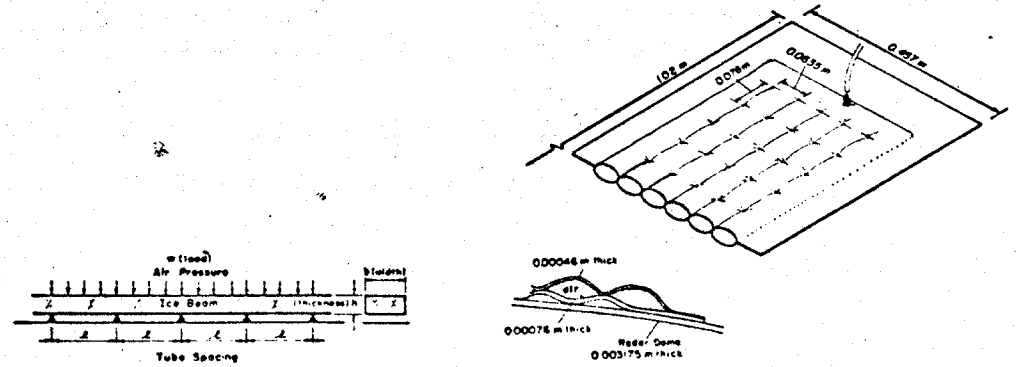

left : A model for ice fracture by a pneumatic boot as a simply-supported beam under a uniform load. The supports on the beam are approximated by the immovable area between inflatable tubes and the uniform loading is approximated by the pressure in the boot.

right : The structure of the boot used in the radome covering.

Fig.45. (from Ackley et al., 1977)

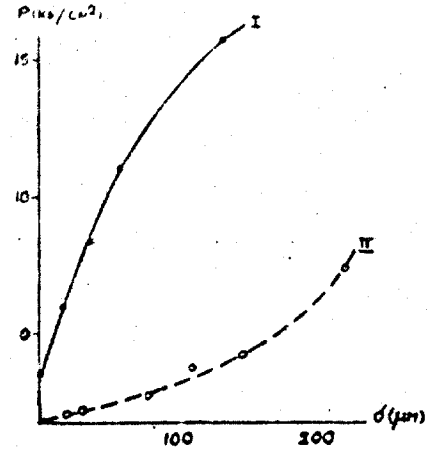

Dependence of adhesion of ice on size of irregularities: I -- for clean steel; II -- for steel with sorbed toluene film;

Fig.46. (from Panyushkin et al., 1974 d)

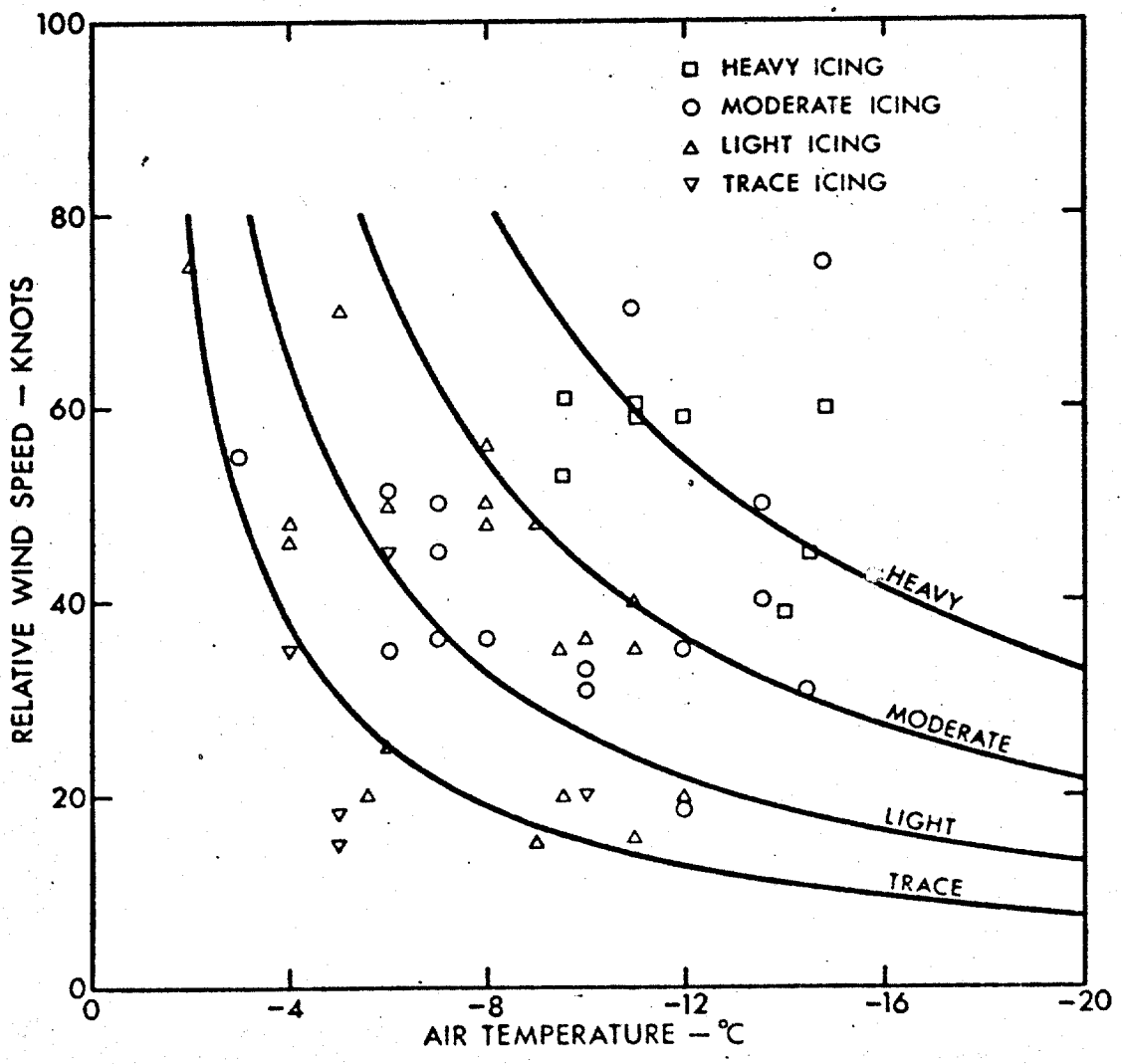

Fig.47. Effect of air temperature and relative wind speed on reported icing severity for fishing vessels at low speeds (4 knots and below) according to Stallabrass (1980).

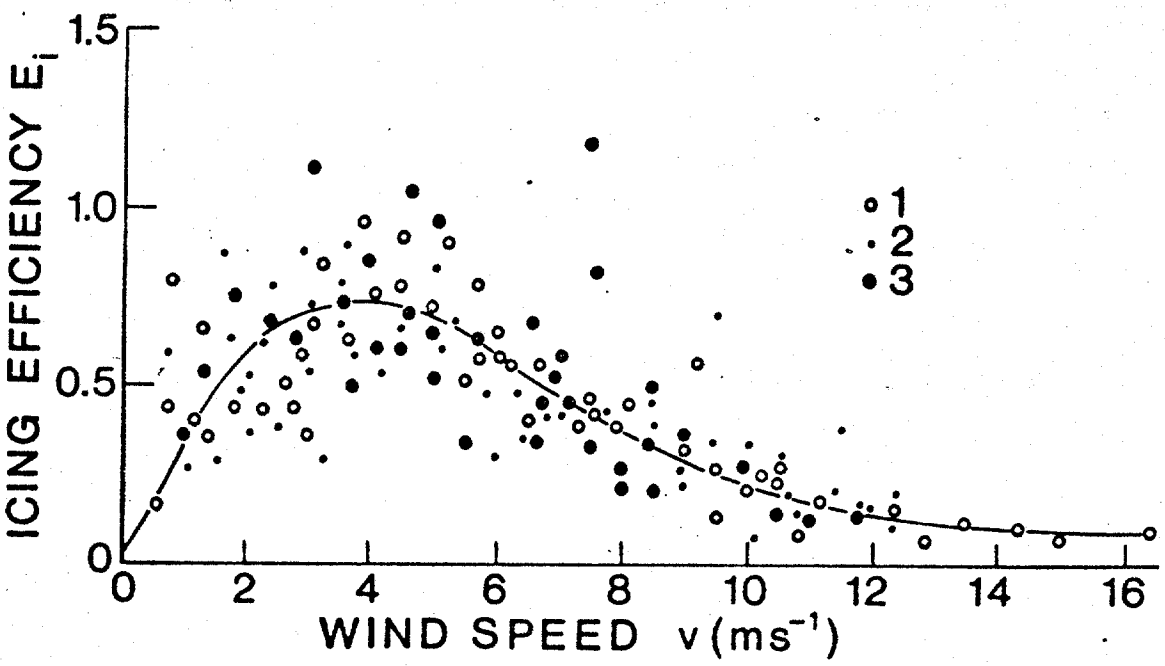

Fig.48. Dependence of the overall icing efficiency on the wind speed for various liquid water contents w according to Glukhov (1971), where 1) w=0.12-0.16 gm^{-3}, 2) w= 0.17-0.21 gm^{-3}, 3) w=0.22-0.26 gm^{-3}. (from Makkonen, 1981)

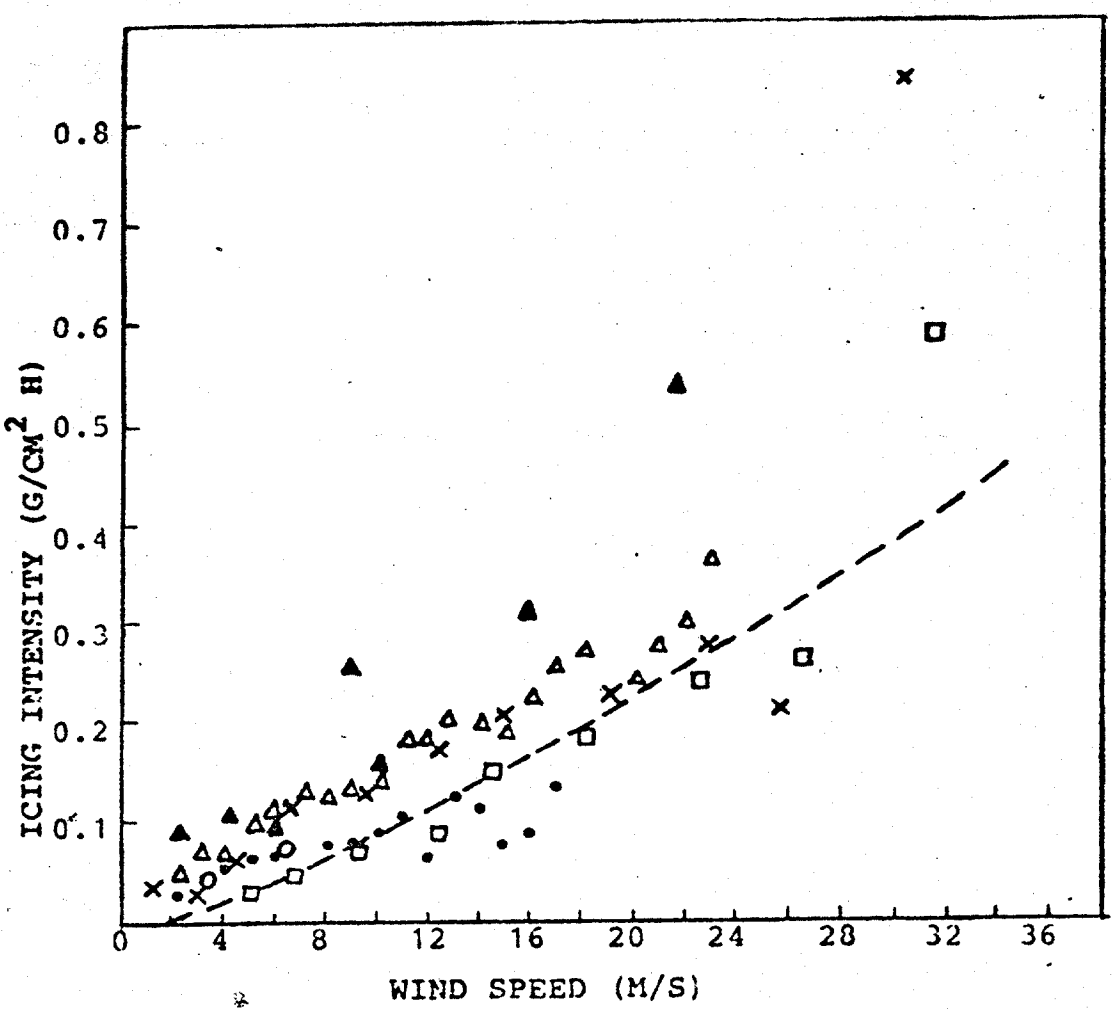

Fig.49. Dependence of icing intensity on wind speed according to observations in natural outdoor environment, and according to the theory with arbitrary constant parameters (dotted curve). x) Waibel (1956), □) Rink (1938), o) Ahti and Makkonen (1982), •) Baranowski and Liebersbach (1977), soft rime, △) B&L, hard rime, ▲) B&L, glaze. The points, except those by B&L represent a mean value for a wind speed interval. The theoretical curve is calculated for dry growth using the values D= 5 cm, d= 25 μm and w= 0.05 g m^{-3}.

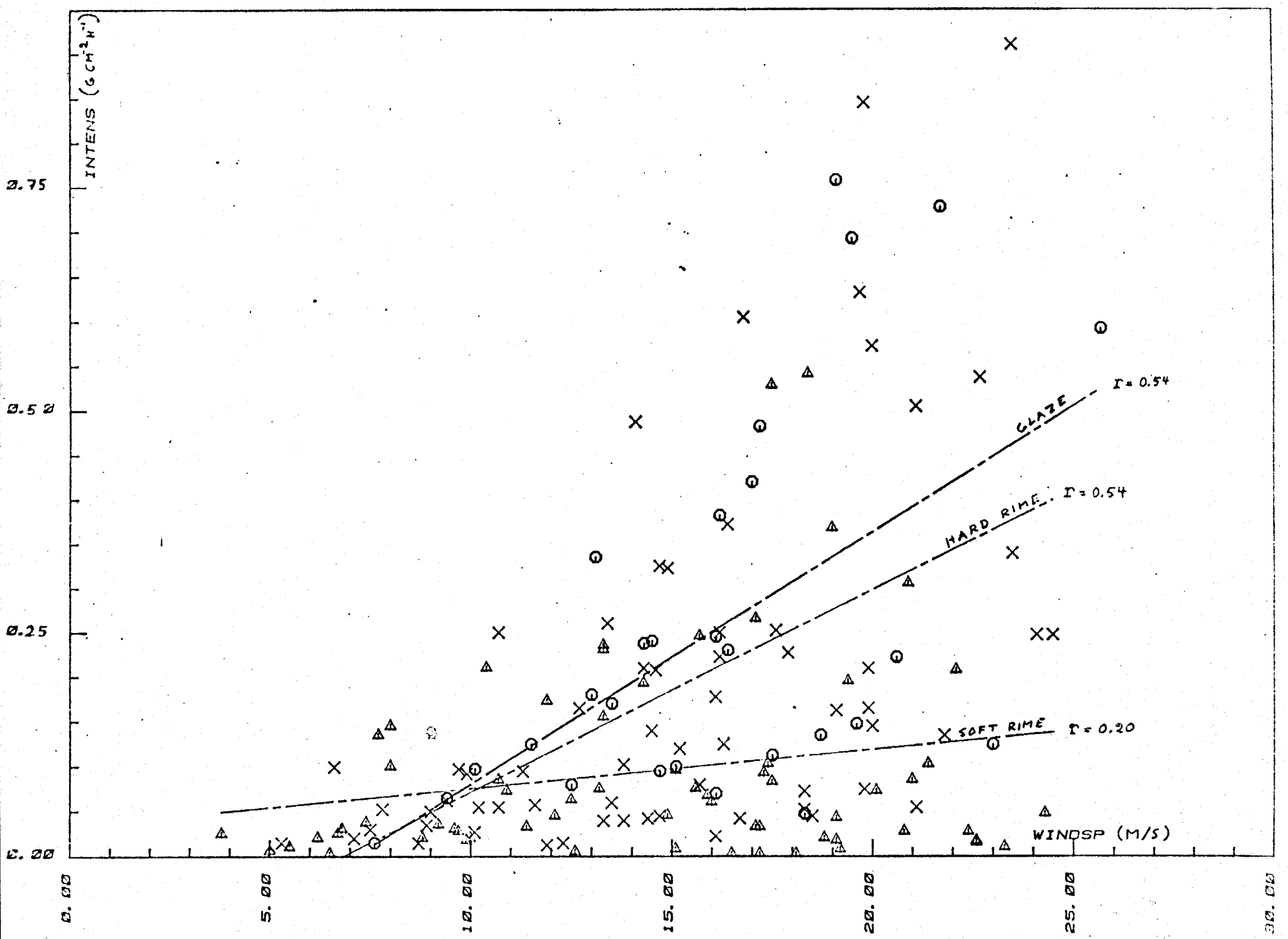

Fig.50. Icing intensity versus wind speed (data from Rink, 1938). ⊙)glaze, △)hard rime, ×)soft rime

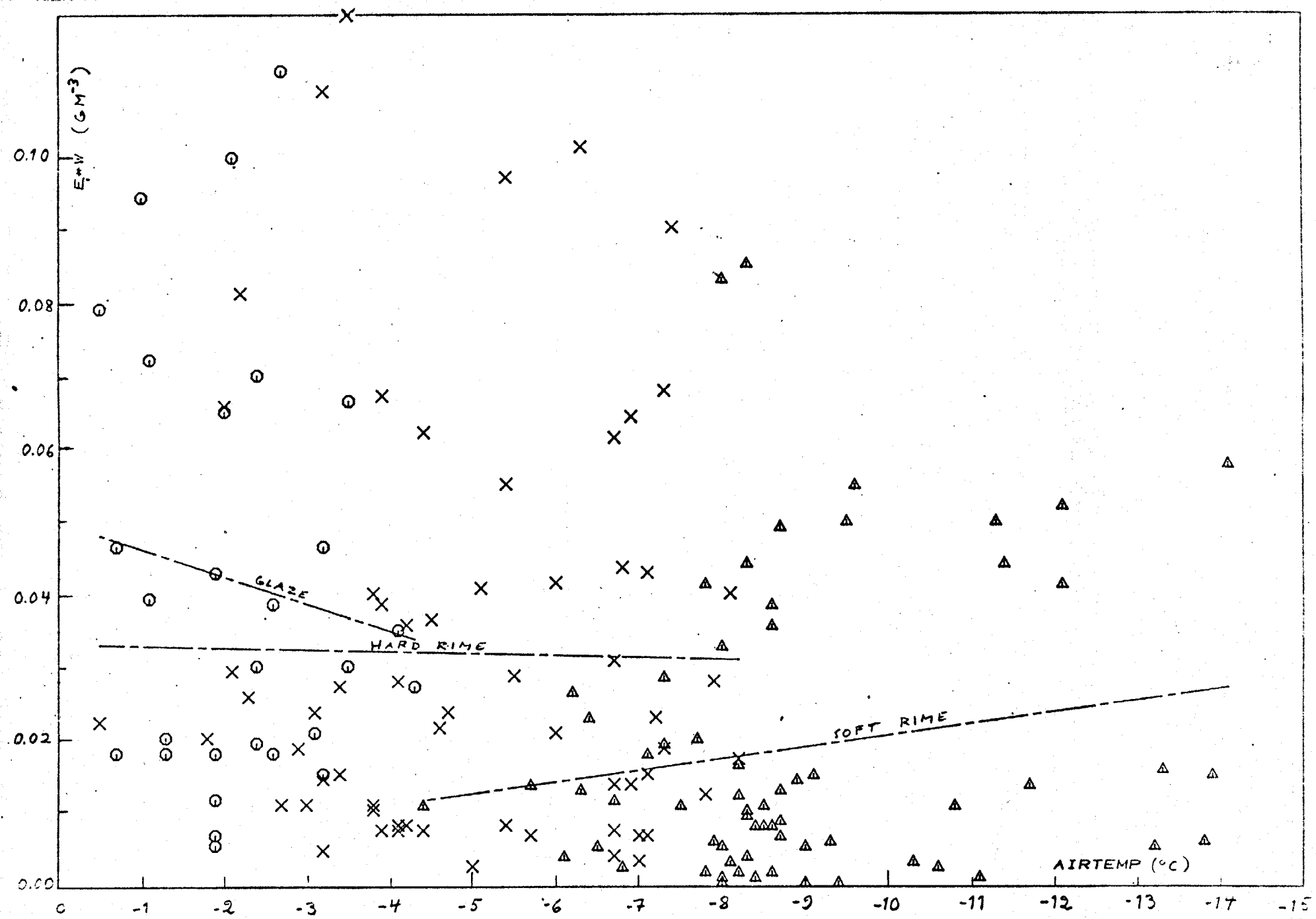

Fig.51. Icing intensity devided by wind speed versus air temperature (data from Rink, 1938). code: Fig.50

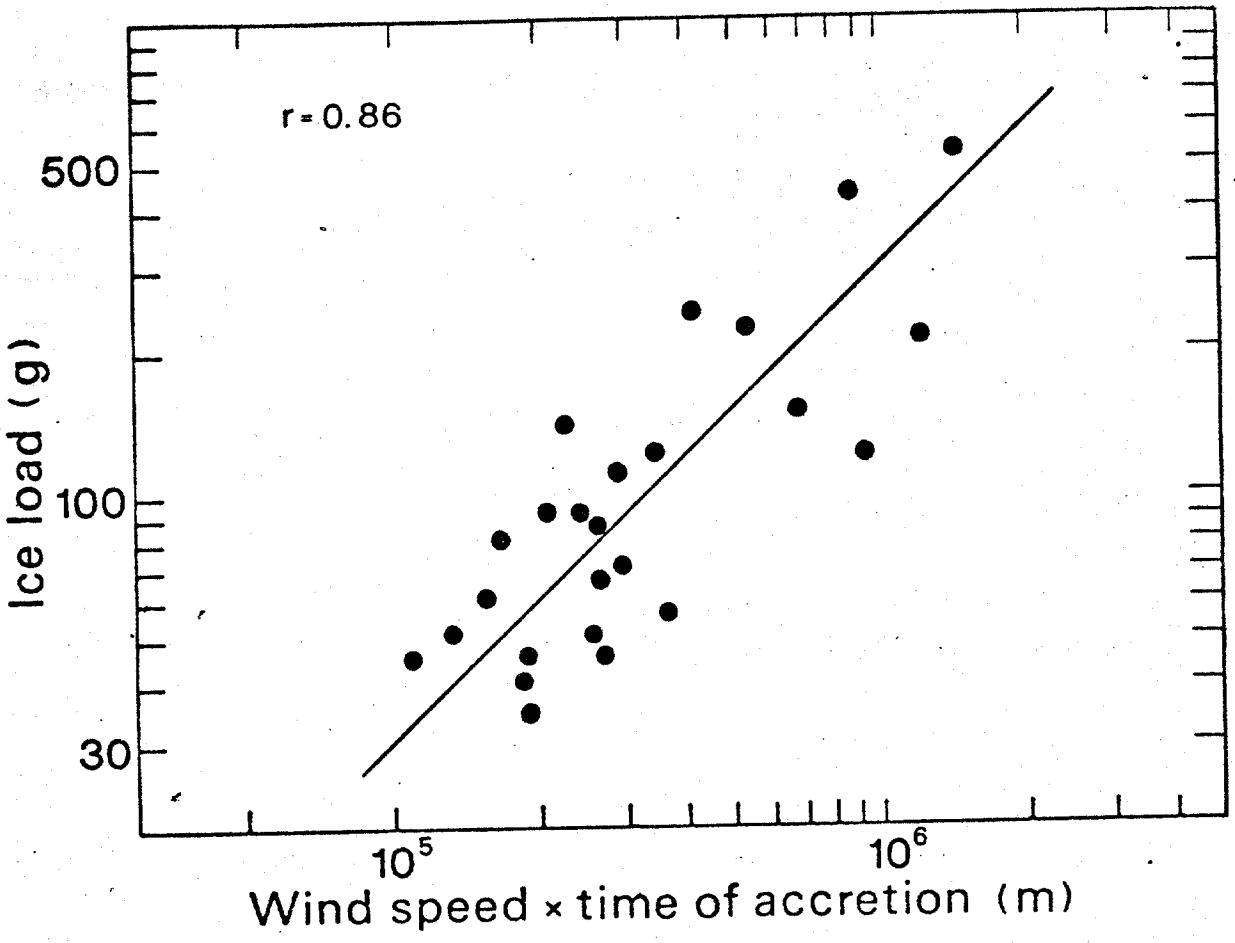

Fig.52. Ice load versus wind speed multiplied by the estimated time of in-cloud conditions according to Makkonen and Ahti (1982).

Characteristics of icing sources in the atmospheric surface layer

source	droplet diameter range (m)	mean(^{x}:median volume) diameter (m)	liquid water content	reference
sea spray on a moving ship	1000 - 3500	2400	0 - 219	Borisenkov and Panov (1974)
sea spray in the first 10cm layer	10 - 1000	200	..	Wu (1979)
sea spray on a stationary ship				
v > 15 m/s, h = 2m	3 - 2000	5 - 30	0.03	Preobrazhenskii(1973)
v > 15 m/s, h = 7m	3 - 90	5 - 30	0.00	Preobrazhenskii(1973)
marine advection fog	..	8 - 16	0.03 - 0.17	Fitzgerald (1978)
coastal fog	4 - 20	..	0.01 - 0.16	Goodman (1977)
evaporation fog	6 - 120	13 - 38 ^{x}	0.01 - 0.30	Houghton and Radford (1938)
evaporation fog	..	..	0.04 - 0.14	Bashkirova and Krasikov (1958)
evaporation fog	..	8 - 10	0.20	Curriér et al. (1974)
arctic fog	7 - 130	16	0.00 - 0.15	Kumai (1973)
arctic fog	2 - 75	18	0.02	Kumai and Francis (1962)
arctic fog	6 - 60	..	0.04 - 0.17	Reiquam and Diamond (1953)
continental winter fog	..	10	0.00 - 0.45	Pinnick et al. (1978)
mountain fog	..	7 - 23 ^{x}	0.05 - 0.30	Bain and Gayet (1982)
low stratus	2 - 43	5	0.05 - 0.25	Pilié and Kocmond (1967)

Photographes of accreted 100 μm diameter droplets in different values of air temperature T_a and deposit temperature t_d (from Macklin and Payne, 1968).

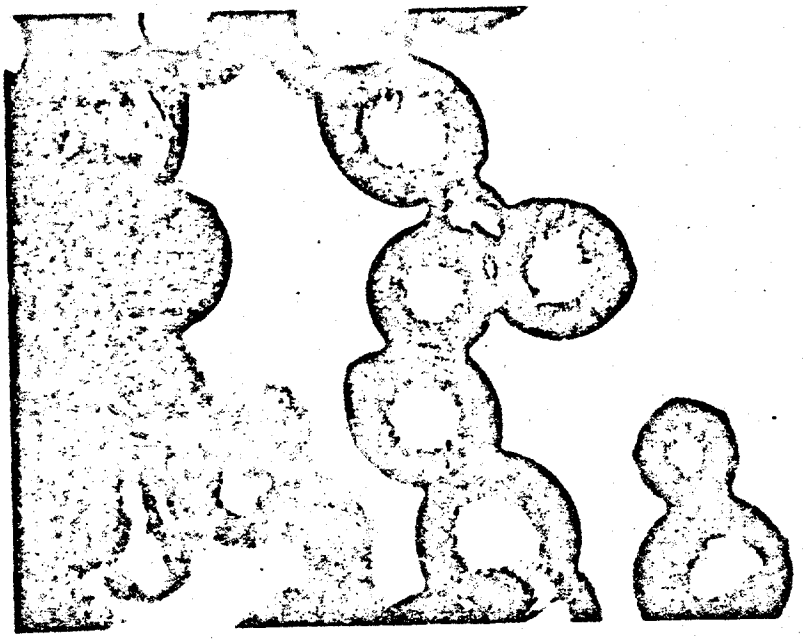

$T_a = -27°C$, $T_d = -15°C$, $r \simeq 50\,\mu$. Magnification: 200 ×

(a)

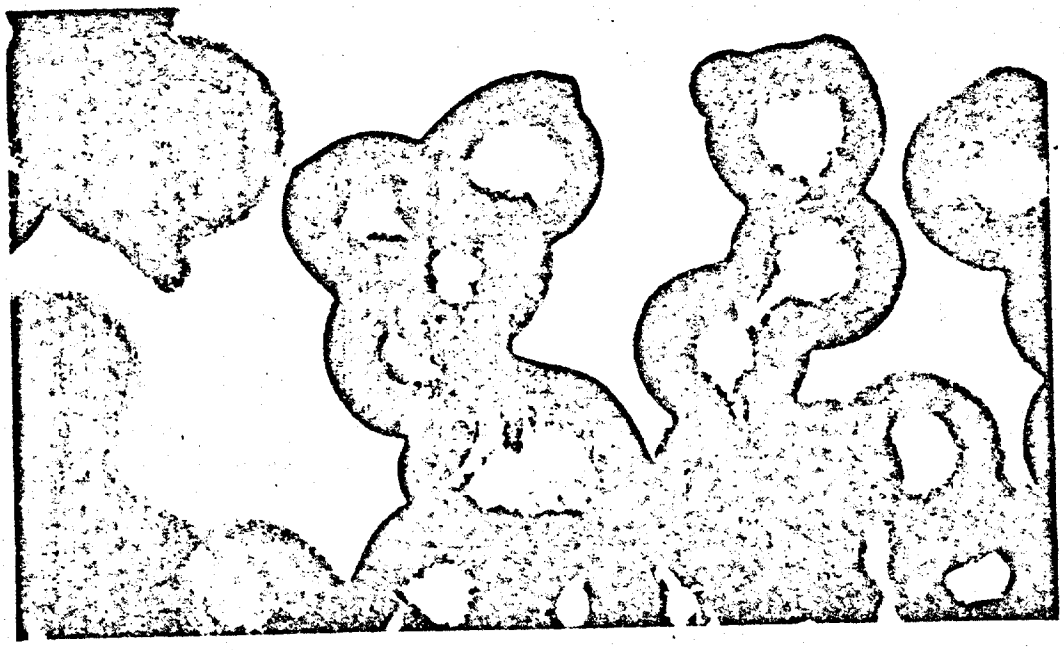

$T_a = -27$ C, $T_d = -10$ C, $r \simeq 50\,\mu$. Magnification: 200 ×

(b)

Figure 1 (a) and (b). Photographs of accreted droplets taken through a microscope normal to the direction of accretion. The direction of accretion was from the top of the photographs.

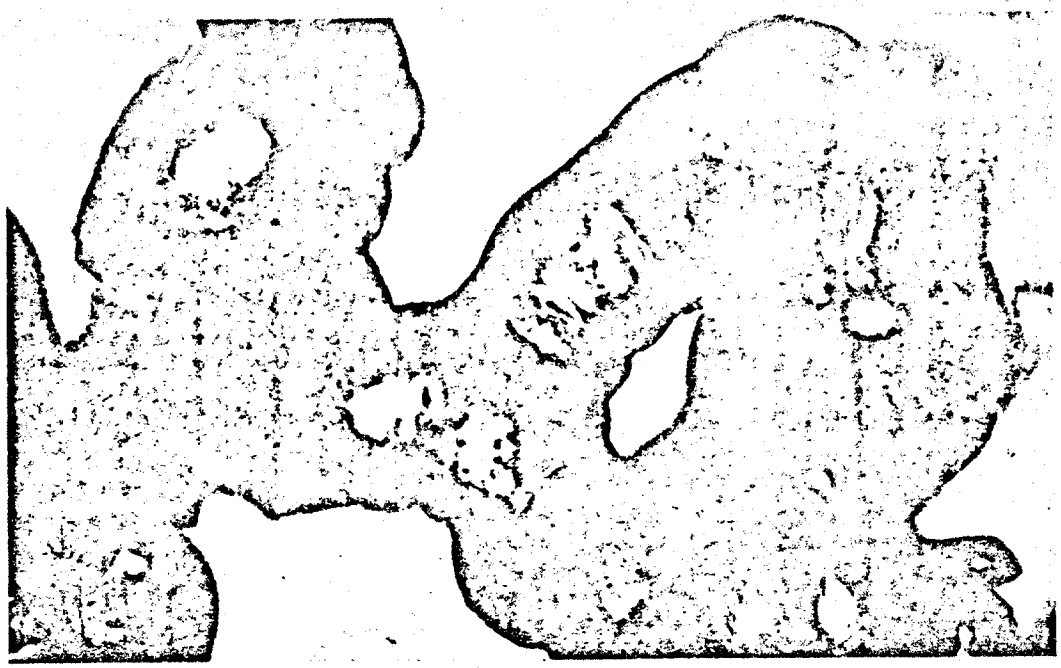

$T_a = -27°C$, $T_d = -5°C$, $r \simeq 50\,\mu$. Magnification: 200 ×

(c)

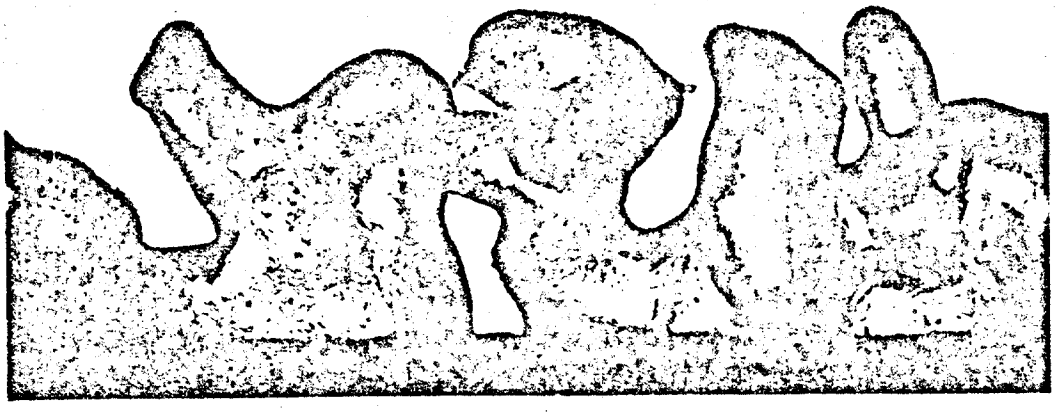

$T_a = -27°C$, $T_d = -1°C$, $r \simeq 50\,\mu$. Magnification: 80 ×

(d)

Figure 1 (c) and (d). Photographs of accreted droplets taken through a microscope normal to the direction of accretion. The direction of accretion was from the top of the photographs.